CORRECTION OF TEMPERATURE AND ACCELERATION EFFECTS ON MEMS GYRO OUTPUT SIGNALS

A THESIS SUBMITTED TO
THE GRADUATE SCHOOL OF NATURAL AND APPLIED SCIENCES
OF
MIDDLE EAST TECHNICAL UNIVERSITY

BY
MUHAMMAD ALI

IN PARTIAL FULFILLMENT OF THE REQUIREMENTS
FOR
THE DEGREE OF MASTER OF SCIENCE
IN
ELECTRICAL AND ELECTRONICS ENGINEERING

DECEMBER 2014

Approval of the thesis:

CORRECTION OF TEMPERATURE AND ACCELERATION EFFECTS ON MEMS GYRO OUTPUT SIGNALS

submitted by **MUHAMMAD ALI** in partial fulfillment of the requirements for the degree of **Master of Science in Electrical and Electronics Engineering Department, Middle East Technical University** by,

Prof. Dr. Gülbin Dural Ünver _____
Dean, Graduate School of **Natural and Applied Sciences**

Prof. Dr. Gönül Turhan Sayan _____
Head of Department, **Electrical and Electronics Engineering**

Prof. Dr. Tayfun Akın _____
Supervisor, **Electrical and Electronics Eng. Dept., METU**

Assist. Prof. Dr. Kıvanç Azgın _____
Co-Supervisor, **Mechanical Engineering Dept., METU**

Examining Committee Members

Prof. Dr. Haluk Külah _____
Electrical and Electronics Engineering Dept., METU

Prof. Dr. Tayfun Akın _____
Electrical and Electronics Engineering Dept., METU

Dr. Fatih Koçer _____
Electrical and Electronics Engineering Dept., METU

Assist. Prof. Dr. Kıvanç Azgın _____
Mechanical Engineering Dept., METU

Dr. Said Emre Alper _____
Technical Vocational School of Higher Education, METU

Date: December 08, 2014

I hereby declare that all information in this document has been obtained and presented in accordance with academic rules and ethical conduct. I also declare that, as required by these rules and conduct, I have fully cited and referenced all material and results that are not original to this work.

Name, Last Name : Muhammad Ali

Signature : _____

ABSTRACT

CORRECTION OF TEMPERATURE AND ACCELERATION EFFECTS ON MEMS GYRO OUTPUT SIGNALS

Ali, Muhammad

MS, Department of Electrical and Electronics Engineering

Supervisor : Prof. Dr. Tayfun Akın

Co-Supervisor : Assist. Prof. Dr. Kıvanç Azgın

December 2014, 133 pages

The scope of this thesis is to study the effects of temperature and acceleration on a MEMS gyroscope and present a workable solution to compensate these errors using various techniques. Compensation for errors is implemented considering the output bias data of the gyroscope. The study also provides comparison of these various techniques, namely Polynomial Curve fitting and Neural Networks. In addition, Moving Average Filtering is used as an auxiliary technique. The study provides novelty of compensating both the factors based on empirical data which is not done before this study. The thesis also discusses the hysteresis present in the gyroscope output data due to change in temperature slope (ascending and descending) and provides a solution to compensate this error. The relation between the magnitude of hysteresis and temperature range is formulated. The methodology adopted in this study is to use existing techniques with some modifications and to compensate different types of errors collectively. The techniques are implemented on data acquired from some commercial sensors, namely ADIS16488, ADXRS450, and XSENS MTi-10. In terms of bias instability temperature compensation can achieve up to 20% improvement (from 33.5°/hr to 26.5°/hr) in ADXRS450 and 50% improvement (from 12.24°/hr to 6.12°/hr) in XSENS MTi-10 sensors' data. By including hysteresis compensation, the improvement can be increased to 28% (from

34.2°/hr to 26°/hr) and 57% (from 10.8°/hr to 4.68°/hr) for ADXRS450 and XSENS MTi-10 respectively. Compensating temperature, acceleration and hysteresis at the same time can improve the bias instability of XSENS MTi-10 up to 70% (from 16.56°/hr to 5.04°/hr). The compensation of these factors also reduces the rate random walk significantly, which is evident from Allan variance plots. The integration times can be improved 4 times for ADIS16488 and ADXRS450 and 8 times for XSENS MTi-10. The offset in the gyroscope output can be reduced 50 times (from 0.05°/sec to 0.001°/sec) by integrated compensation as compared to 10 times (from 0.05°/sec to 0.005°/sec) by conventional temperature compensation in the XSENS gyroscope data. Integrated compensation of temperature, acceleration and hysteresis results in better performance as compared to the conventional method of compensating only for temperature, providing a more accurate and error free data.

Keywords: MEMS Gyroscope, Temperature Compensation, Acceleration compensation, Hysteresis

ÖZ

MEMS DÖNÜÖÇLER ÇİKİŞ SİNYALİ ÜZERİNDEKİ SICAKLIK VE İVME ETKİLERİ HATALARININ DÜZELTİLMESİ

Ali, Muhammad

Yüksek Lisans, Elektrik ve Elektronik Mühendisliği Bölümü

Tez Yöneticisi : Prof. Dr. Tayfun Akın

Ortak Tez Yöneticisi : Assist. Prof. Dr. Kıvanç Azgın

Aralık 2014, 133 sayfa

Bu tezde sıcaklık ve ivmenin MEMS dönüölçer üzerindeki etkileri çalışılmış ve bu etkilerin azaltılması için geliştirilen çeşitli telafi teknikleri sunulmuştur. Bu teknikler dönüölçer çıkışından toplanan ofset verileri kullanılarak uygulanmıştır. Ayrıca bu çalışmada, önerilen Çoklu Doğrusal Regresyon ve Neural Networks gibi tekniklerinin karşılaştırması yapılmıştır. Ek olarak, Kayan Ortalama Filtrelemesi de yardımcı bir teknik olarak kullanılmıştır. Bu tezde literatürde ilk defa, deneyler sonucunda elde edilmiş dönüölçer verisi üzerinden sıcaklık ve ivme etkilerinin azaltılması sunulmaktadır. Bu tezde ek olarak sıcaklık değişiminden dolayı (artan ve azalan) dönüölçerin çıkış verisindeki histeresis incelenmiş ve histeresis sorununu azaltmak için bir çözüm sunulmuştur. Ayrıca, histeresis büyüklüğü ve sıcaklık arasındaki ilişki formüle edilmiştir. Bu çalışmada kullanılan metodoloji, literatürde var olan tekniklerin değiştirilerek kullanımı ve farklı türdeki etkilerin aynı anda azaltılmasını hedeflemektedir. Bu teknikler, AIS16448, ADXRS450 ve XSENS MTi-10 gibi bazı ticari duyargalardan toplanan veriler üzerinde uygulanmıştır. Sıcaklık telafisi kullanımı, ofset kararsızlığında ADXRS450 duyargası için %20 (33.5 °/sa'den 26.5°/sa'te); XSENS MTi-10 duyargası için %50'ye (12.24 °/sa'den 6.12°/sa'te) kadar iyileştirme sağlayabilmektedir. Histeresis telafisi de eklendiğinde elde edilen iyileştirmeler ADXRS450 duyargası için %28'e (34.2 °/sa'den

26°/sa’te), XSENS MTi-10 duyargası için %57’ye (10.8°/sa’den 4.68°/sa’te) kadar arttırılabilir. Sıcaklık, ivme ve histerezis telafisi XSENS MTi-10 duyargası için ofset kararsızlık değerini %70’e (16.56 °/sa’den 5.04°/sa’te) kadar iyileştirebilmektedir. Aynı zamanda, bu etkilerin telafisiyle açı rastgele yürüyüş değeri Allan Variance grafiğinden de açıkça görüleceği üzere önemli miktarda azalmıştır. Allan Variance grafiğinde ofset kararsızlığına ulaşılan zaman ADIS16488 ve ADXRS450 için 4 kat; XSENS MTi-10 için 8 kat geliştirilmiştir. XSENS MTi-10 dönüölçer verisindeki ofset, sadece sıcaklık verisi kullanılarak yapılan bilindik telafi yöntemi ile 10 kata (0.05°/s’den 0.005°/s’ye) kadar; ivme, sıcaklık ve histeresis düzeltmesiyle 50 kata (0.05°/s’den 0.001°/s’ye) kadar azaltılmıştır. İvme, sıcaklık ve histeresis düzeltmesi ile yapılan telafi, yalnızca sıcaklık kullanılarak yapılan bilindik telafi yöntemine kıyasla daha iyi bir performans sergilemiş ve hatasız veri elde edilmesini sağlamıştır.

Anahatar Kelimeler: MEMS dönüölçer, Sıcaklık düzliltemesi, İvem düzliltemesi, Histeresis

To My Dear Parents

To My Sweet Wife

And

To My Life, Usman

ACKNOWLEDGEMENTS

First, I am very grateful to my thesis advisor Prof. Dr. Tayfun Akın for his support, guidance, encouragement, optimistic approach and his trust in me. He always accommodated my requirements and I am grateful for the patience he has shown towards me. It is a pleasure working with him.

I am also grateful to Dr. Said Emre Alper for his support, guidance and valuable technical discussions. He was always there to help me out and provided excellent ideas for data collection and analysis. I really benefited a lot from his experience and knowledge. I also appreciate the time and effort he has dedicated in the improvement of this thesis.

I am also thankful to my group mate Ulaş for his support as well. It was very kind enough of him to help me with initial testing and also helped me work with some of the equipment in the lab. I am also thankful to Yunus for his kind guidance.

Besides, I am very grateful to my parents for their invaluable efforts and their dedication throughout my life. Finally, memorable thanks to my wife for her understanding, endless patience, support, and love.

I am also thankful to Government of Pakistan for their funding throughout my study. I am also thankful to METU for providing such an opportunity to be part of this prestigious institute. It’s an honor being part of METU.

TABLE OF CONTENTS

LIST OF TABLES

TABLES

LIST OF FIGURES

FIGURES

CHAPTER 1

INTRODUCTION

Micro Electro Mechanical Systems (MEMS) have, without any doubt, revolutionized the modern electronic technology. MEMS technology has applications starting from daily consumer products like mobile cell phones to tactical grade products like navigation and space gadgets [1-12]. The benefits of MEMS technology are so lucrative that the MEMS industry has shown a lot of growth in the last decade and replaced other electronics [10]. In current era, absence of MEMS technology in any electronic device is not very common. The miniaturization of electronics together with cost effectiveness is such a big advantage that MEMS is used so widely. There are numerous applications of MEMS technology, and hence cannot be mentioned here in detail. The importance of MEMS is evident from the fact that so much research is being done in miniaturization of devices, and MEMS is used to replace the conventional bulkier devices. One of the devices where MEMS started to replace the conventional bulkier devices is gyroscopes.

Gyroscopes have been used for navigational applications since the time they are invented and still are used for the same purpose. Mechanical gyroscopes are bulkier devices as compared to MEMS gyroscopes, and more volume is occupied by them. Therefore, a device which can perform similar function and is lighter in weight and smaller in volume is much more preferred one. Different studies show that the market of MEMS gyroscopes has grown much in the last decade and it is still growing as the demand and consumers are increasing [6, 10]. The miniature size has opened new avenues for daily consumer products and thus has resulted in the growth of MEMS gyroscopes market.

It is imperative here to mention some applications and advantages of MEMS gyroscopes so that the motivation behind this work is understood completely. By understanding the importance of MEMS devices and their usage in so many applications, the much required improvement in the performance of these devices will become clear.

The motivation of this thesis is to improve the performance of a MEMS gyroscope by removing error from its output data. MEMS gyroscope output bias data is degraded adversely by environmental factors like temperature, acceleration, vibration etc. The aim of this study is to compensate drift in a MEMS gyroscope output data caused by temperature and acceleration. Different compensation methods are used in this study and their performance is also compared. Some background knowledge about MEMS gyroscope is presented first and then research objectives of this study are listed.

1.1. Applications of MEMS Gyroscopes

MEMS gyroscopes have been used in almost every field of modern life. The applications are from commercial users to military [1-5]. In 2011, the market price for MEMS gyroscope was estimated to be around USD 1.3 Billion [6], which show the importance of MEMS gyroscopes' applications. This section mentions some very important applications of MEMS gyroscopes.

The application of a MEMS gyroscope that is seen mostly in daily life is smart cell phones. Almost all smart phones are equipped with a MEMS gyroscope nowadays that is used to detect motion of the phone with support of other sensors. The miniaturization and cost effectiveness have made it possible for vendors to equip smart phones with such sensors. The penetration of MEMS accelerometers and MEMS gyroscopes in consumer electronics shows increasing trend from year 2009 to 2013 [10].

The second commercial application is the use of a MEMS gyroscope sensor in gaming consoles. Games with 3D effect are available currently, that include hand

held devices or large devices such as motion rides. Tennis can be played on screen while using a real racket or a first person shooting game can be played by holding a real gun, and all that is fruits of the MEMS technology.

There are industrial applications that require tactical grade MEMS gyroscopes which have better performance than the ones used for commercial use. The applications are platform stabilization for different applications like surveillance cameras. It is used for leveling of cranes or other mechanical machinery that do not require inertial grade accuracy. Automobile industry is using the MEMS technology to its fullest benefits [8].

The most serious application of MEMS gyroscopes is for inertial purposes. Gyroscopes with inertial grade properties (like bias instability of the order 0.01°/hour) can be used for inertial purposes [7]. The on-going research is trying to achieve this much accuracy for a MEMS gyroscope, so that it can be used in inertial applications. MEMS gyroscopes with accuracy of such magnitude can be used in strategic applications such as smart ammunitions, submarines, missiles, rockets, fighter jets etc [7].

1.2. Advantages of MEMS Gyroscopes

There are numerous advantages of MEMS gyroscopes that make it superior to other conventional gyroscopes. Literature shows the importance and advantages of the MEMS technology in detail [1-12]. The first advantage is the miniaturization that has attracted the development of MEMS gyroscopes. Space applications have so much volume constraints and the MEMS technology was a blessing in disguise. With smaller size and lighter weight, MEMS devices have taken over the market in many applications especially consumer electronics [10, 11].

The second biggest advantage is the cost effectiveness which has made it very attractive for vendors to introduce such sensors in daily consumer products. The growth of MEMS market is resulting from cost effectiveness of the sensor.

The most important advantage from designer's or manufacturer's point of view is the mass production of MEMS devices. This technology allows fabrication of hundreds of sensors from a single wafer, and thus is the cause for low cost of MEMS sensors. With the available modern technology repeatability is achieved, and consecutive processes can get sensors with same properties. The important point is to design and execute the fabrication very carefully, and once the design is verified repeated processes can get as many devices as required without changing the design.

Another important feature of a MEMS gyroscope is reduced power consumption. As the sensor is very small, so the power requirements are also very small for such sensors. The sensors can run using 5V, 3.3V or even 1.2V for operation, which is readily available on electronic circuit boards.

1.3. Drawbacks of MEMS Gyroscopes

MEMS gyroscopes have some drawbacks that restrict them for use in applications that require inertial grade accuracy. The most important drawback is the drift in the output of a MEMS gyroscope that does not allow it to be used for inertial applications. The drift in a MEMS gyroscope is due to many reasons which include internal (physical structure, alignment, material type etc) and external (temperature, atmospheric pressure, acceleration, time etc) factors. Some of these errors are related to the limitations of currently available technology, and other errors are environment dependent. The drifts in MEMS gyroscope output makes it difficult to be used in navigational applications because such errors accumulate over time.

1.4. Detailed Problem Review

The drift in a MEMS gyroscope results from many factors that include internal structure errors and external stimuli to a sensor. There are many designs of MEMS gyroscopes, and each one of them has different responses and performances depending upon their design [4]. For example a linear vibratory MEMS gyroscope is more susceptible to linear acceleration as compared to a tuning fork MEMS gyroscope.

This section discusses the sources of error but they are explained without the specific reference to any particular type of a MEMS gyroscope design. The examples of error sources are taken from literature. This study is based on the compensation for drift error based on empirical data rather than the theoretical nature of the error sources. The study is not concerned with the fact that certain type of error is dominant in any specific type of MEMS design. It is important to know the sources that cause error in MEMS gyroscopes. Also it is important to understand some working principles behind these errors and how exactly they cause the errors.

The error sources can be divided into two main categories namely structural and environmental [25]. The structural errors can be result of either mechanical error, damping effect or drive defects [25]. The environmental errors can result from change in temperature, pressure, linear acceleration, vibration or any other external stimulus that can affect the operation of a MEMS gyroscope.

1.4.1. Structural Error Sources

The structural error sources are inherent in a sensor due to its material properties or the fabrication technology. The level of detail in any fabrication process has some limitations, and beyond that the fabrication cannot do much for the sensor surface. The **critical dimension** of a fabrication process is the minimum feature size required by the design in some process and the **resolution** of a process is the minimum feature size that can be attained repeatedly by any process. If there is a clear margin between the critical dimension and the resolution of a process then the features of a device are very fine but if the margin is very small then the feature may not be well defined and there are errors in the operation of the device.

1.4.1.1. Mechanical Error

The vibratory MEMS gyroscope works on the principle of spring-mass equation. Equation 1.1 defines the relation between coriolis force and other parameters.

$$\vec{F} = 2 * m * \vec{\dot{x}} \; X \, \vec{\Omega} \tag{1.1}$$

Where **F** is the coriolis force, $\vec{\dot{x}}$ is the speed vector and $\vec{\Omega}$ is the rotation rate vector. It is known from the basics of working principle of a MEMS gyroscope that there are two modes; **drive** mode and **sense** mode. A MEMS gyroscope is actuated at a resonant frequency which is called drive mode. When a rotation is applied to the sensor it is sensed by the sense mode. Both the modes are comprised of springs which vibrate about their position corresponding to amount of applied rotation. The fabrication of these springs is never identical and they impart non-diagonal stiffness coefficient. When force is applied in on one axis some fraction of it is transferred to other orthogonal axis. The literature shows that careful designing of a MEMS gyroscope can result in reduced mechanical error in gyroscopes [25].

1.4.1.2. Damping Error

This error is associated with non-diagonal damping of the structure that makes MEMS gyroscopes prone to drift errors. This error is very much dependent on the shape of the spring used in a sensor, and it can be manipulated by changing the spring shape. Literature reports that this error is not very significant and does not add significant noise when compared to other factors [25].

1.4.1.3. Drive Defects

MEMS gyroscopes are actuated by electrostatic comb drive electrodes and their uniformity is very important. The uniformity has two meaning; one is that the width of the comb should be uniform, and second is that the gap between the combs should be consistent. These two types of errors can be reduced by careful designing and fabrication of a MEMS gyroscope sensor. The electrode width should be increased and the gap between them should be increased. Also the error can be reduced by increasing the number of electrodes [25].

1.4.2. External Noise Sources

Two environmental factors that affect the output of a MEMS gyroscope are temperature and linear acceleration. There are other factors like pressure and vibration etc. but only two factors are focus of this study. The temperature inside a

MEMS gyroscope changes either due to environmental change or due to friction caused by the moving parts of the sensor. Likewise, gyroscopes experience linear acceleration of some magnitude when in operation, and that also affects the output of a MEMS gyroscope. Then there are other random noises present in a gyroscope data due to high frequency components, which are normally Gaussian in nature and easier to deal with. To explain these error sources the classification of noise is used so that an overall understanding is achieved. The noise is classified in two main categories namely deterministic and random [26].

1.4.2.1. Deterministic Noise

This is the type of error that is associated with the system in a way that its state at any given point is known by calibrating the sensor, or by data provided by the manufacturer. The error is close to the mechanical sources as these calibration results due to misalignment in the structure of a sensor. It can be further divided into following categories.

Bias Offset

Bias offset is the difference between the expected output value and actual output obtained from a sensor. The bias offset is the in-built error of a MEMS gyroscope that exists due to inherent fabrication, mechanical misalignment, or design drawbacks.

Scale Factors

When the analog voltage of a sensor is converted to a digital value the scale factor is used for such a conversion. This results in the error due to quantization of the analog voltage.

1.4.2.2. Random Noise

As compared to deterministic or systematic noise the random noise is the one that cannot be predicted before hand, while collection of data from a sensor. The main problem that researchers face is modeling this random noise so that data can be separated from this noise. The theme of compensation is actually understanding this

noise and removing it from sensor data. The random noise can be divided in two categories called high frequency noise and low frequency noise [26].

High Frequency Noise

High Frequency Noise is also called ***short term noise*** as it is the spontaneous noise that is changing very quickly at high frequency. The most common methods to remove this type of noise is using low pass filter, wavelet decomposition, moving average filter, median filter or back propagation neural networks [26]. A simple averaging can be used to reduce this noise at crude level.

Low Frequency Noise

Low frequency noise is also known as ***long term noise*** because the effect of this noise appears gradually with time. This is a co-related noise which has relation with other parameters like change in temperature [26]. The type of compensation aimed in this study is to counter this noise caused by the temperature. Section 1.4.3 discusses this noise in detail where the factors that actually cause this error are explained mathematically.

1.4.3. Effects of Temperature on MEMS Gyroscope

It can be said without any doubt that the most important factor that affects the output of a MEMS gyroscope is the change in ambient temperature. The importance of this parameter arises from the observation that all MEMS sensors respond to change in temperature thus adding an error in their output.

It is very important to understand how the temperature causes degradation in the output of a MEMS gyroscope. Change in the temperature cause changes in the micro level physical properties of the material that constitutes the structure of a MEMS gyroscope. There may be more factors that are being affected by the temperature depending upon a specific design of a sensor. Some of the evident factors that can be considered common to working principle of all MEMS gyroscope sensors are discussed here.

1.4.3.1. Effect of Temperature on Resonant Frequency of a MEMS Gyroscope

The Young's Modulus (E) of a material is defined as the ratio of stress (σ) to strain (ε) and it tells about the stiffness of a materials. Equation 1.2 shows mathematical relation of Young's modulus.

$$E = {}^{\sigma}/_{\varepsilon} \tag{1.2}$$

Equation 1.3 gives the relationship between Young's modulus of a material and its temperature (T) [27].

$$E = K_E\, TE_0 \tag{1.3}$$

Where $\mathbf{K_E}$ is the temperature coefficient of silicon material and $\mathbf{E_0}$ is the temperature coefficient of monocrystalline silicon. Equations 1.2 and 1.3 show that when there is difference in beam and support material of a sensor, then residual stress and strain exist whose effects are more dominant when temperature is changing. Equation 1.4 gives the relation between the resonant frequency (ω) and the other parameters including Young's modulus, which in turn is dependent on the change in temperature [27]. **W** is the stability index, **h** and **L** are dimensions of the beam, **A** is the area and **m** is the mass of the structure.

$$\omega = \sqrt{(4\, EhW^3 + \pi AL^2\, \sigma/4)/(mL^3)} \tag{1.4}$$

This equation shows the dependence of resonant frequency on the Young's Modulus of the material, which itself is dependent on the temperature of the material.

1.4.3.2. Effect of Temperature on Q-Factor of a MEMS Gyroscope

Quality factor of a resonator is a parameter that is used to determine the quality of a resonator. The accuracy and good quality of a resonator is very important as it later determines the output of a MEMS gyroscope. Equation 1.5 defines quality factor (Q) mathematically.

$$Q = \frac{Total\ Energy}{Energy\ Lost\ in\ One\ Cycle} \tag{1.5}$$

The loss in the energy is attributed to three factors.

1. ***Gas Damping***

   The damping is caused by the air present inside a sensor package and results in loss of energy in a resonator [28].

2. ***Anchor Loses***

   This loss is caused due to coupling of resonators with surrounding materials like packaging or substrate [28].

3. ***Intrinsic Loses***

   Energy is lost due to material properties such as viscosity [28].

For a system where the dominant factor for loss of energy in micro resonators is gas damping, Equation 1.6 shows the relation for quality factor [27].

$$Q = \frac{h\rho\omega_0}{4}\sqrt{\frac{\pi}{2}}\sqrt{\frac{R\,C}{M\,T}} \tag{1.6}$$

Q is the quality factor, **ω** is the resonant frequency, **ρ** is the density of electrode, **h** is the thickness of electrode, **R** is molar constant, **M** is mass of gas in moles and **T** is the temperature of a sensor. The equation indicates the dependency of quality factor of resonators used in a MEMS vibratory gyroscope on the temperature. Figure 1.1 shows the simulated relation between Q-factor and temperature.

1.4.3.3. Effect of Temperature on Sensing Output of a MEMS Gyroscope

According to [27], the amplitude of drive and sense mode is dependent on the resonating frequency of resonators. Thus it can be said that the amplitude of the displacement, which is measure of the output of a gyroscope, is dependent on the temperature of its material. Figure 1.2 shows the dependency of gyroscope output voltage amplitude on the changes in the temperature. The output of a gyroscope is measured using this displacement. The displacement governs the gap between the electrodes which determines the capacitance between them. The capacitance is a

measurable quantity and is mapped to the output voltage as the sensor output. Thus the output changes with change in the temperature.

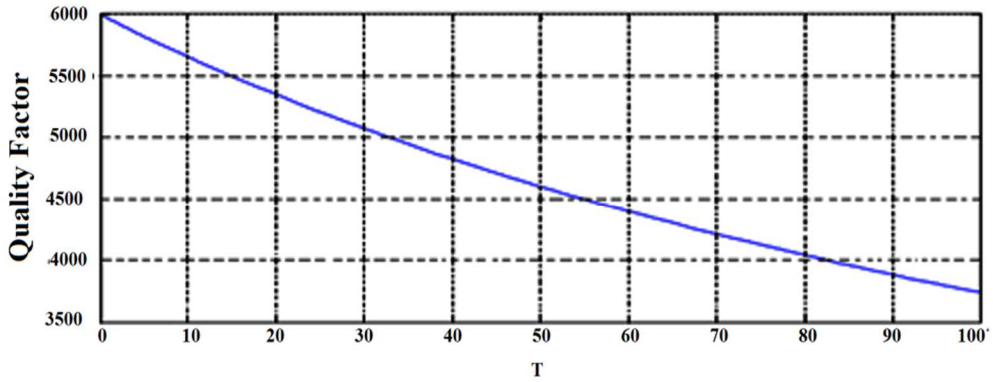

Figure 1.1: The Quality Factor (Q) of MEMS vibratory gyroscope degrades as the temperature change is increasing [27].

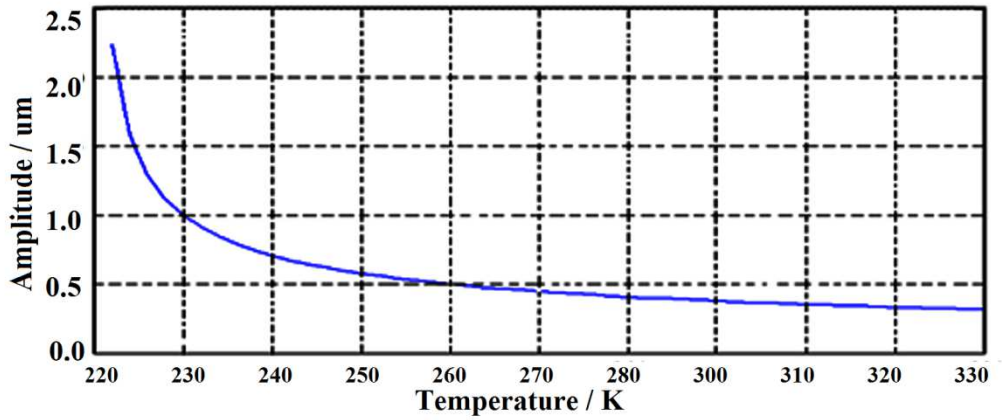

Figure 1.2: The amplitude of the output voltage of a MEMS vibratory gyroscope decreases with increase in the temperature of the sensor [27].

1.4.3.4. Expansion of Materials

When the temperature of the material that makes the structure of a MEMS gyroscope changes, it causes changes in the physical properties of the material as

well which includes dimensions of material. The output voltage (V_o) is a product of input voltage (V_{in}) and some fraction of change in capacitance [19]. Equation 1.7 gives the mathematical form of this relation.

$$V_o = (\Delta C/A) * V_{in} \quad (1.7)$$

A is a scale factor which can be total capacitance or any constant to scale the change, Δ**C** is the change in capacitance due to change in the electrode gap and **V** shows the voltages (subscripts define input and output voltages). The Δ**C** can be achieved either by change in the gap between electrodes or either by change in the overlap surface area. Temperature change causes expansion in the material, that makes a MEMS gyroscope, and that expansion can result in either of the changes that can cause Δ**C**. Thus output of a gyroscope is changed indirectly by expansion of the material.

1.4.3.5. Heating by the sensor packaging

Sensor packages are another factor that determines the temperature of the ambient environment inside a sensor. The amount of heat dissipated by a sensor depends upon the type of package used, and can result in different amount of offsets added to a gyroscope output. The package of a MEMS sensor is designed in such a manner that heat dissipated by the sensor circuitry is transferred outside and the sensor components are not heated. Thus by selecting a suitable package for a sensor, the amount of drift imparted to a gyroscope due to packaging can be controlled.

1.4.4. Effects of Acceleration on MEMS Gyroscope

The effects of acceleration on any MEMS gyroscope output are not much as compared to other factors especially when the value of applied acceleration is less than 5 g [23]. Due to these small effects, the acceleration is not considered as a threat to a MEMS gyroscope output data [22, 23]. However, if there is large amount of acceleration present around gyroscope then it can pose a danger to corrupt the output data. It should be kept in mind that the effects of linear acceleration are different on different designs of gyroscopes, because some designs of MEMS

gyroscopes are based on cancellation of these effects [4]. Equation 1.8 defines the offset voltage $\mathbf{U_y}$ (y-axis direction) in a Double Gimbaled (DG) gyroscope.

$$U_y = K_V * \frac{M_E}{K_y} \tag{1.8}$$

Where $\mathbf{K_v}$ is the scale factor for output voltage, $\mathbf{K_y}$ is the rigidity of y-axis and $\mathbf{M_E}$ is the inertial interferential moment and is defined by following equation.

$$M_E = m(a_x + g_x + \omega_y z_c - \omega_z y_c)z_c - m(a_y + g_y + \omega_x y_c - \omega_y x_c)x_c \tag{1.9}$$

Where **a** is linear acceleration, **g** is gravitational acceleration and **w** is the resonant frequency of the material. The constants $\mathbf{z_c}$ and $\mathbf{x_c}$ represent the expansion in z and y axis respectively. From this equation it is very clear that the output voltage of a MEMS gyroscope is affected by the acceleration experienced by it [28]. Figure 1.3 shows the worst case scenario for effect of linear acceleration. The temperature dependency trend can be inversed by changing the applied acceleration.

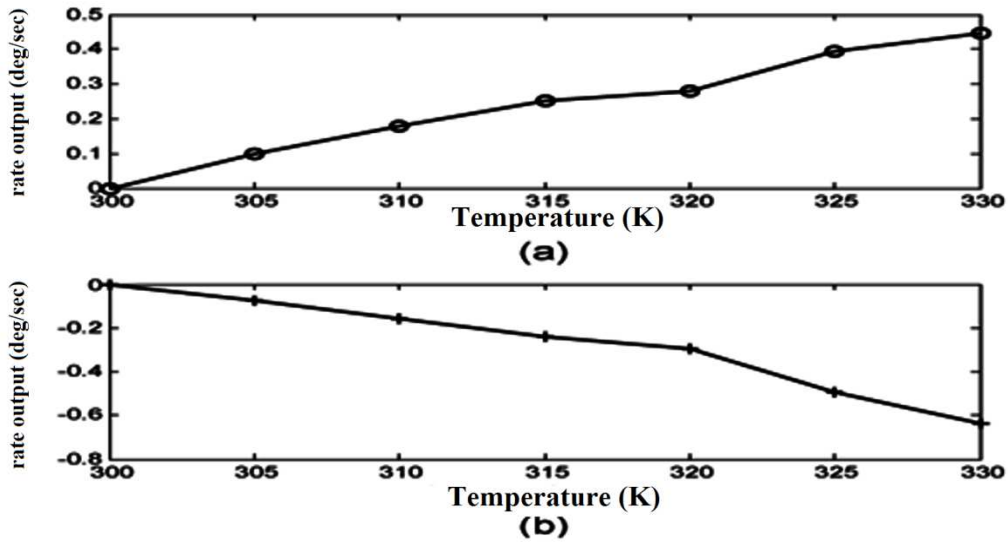

Figure 1.3: The output of the MEMS gyroscope can be seriously affected by the linear acceleration. **(a)** Gyroscope output when z-axis accelerometer (Az) = +1g. **(b)** When Az = -1g, the gyroscope output is inversed also.

The effect of linear acceleration is also shown in the output of a thermal MEMS gyroscope. In a thermal MEMS gyroscope, rotation rate is detected by the flow of temperature to a temperature sensor. The transfer of heat from heater to sensor is done by air present inside the sensor package. The air is not restricted and linear acceleration causes the flow of heat and non-existent rotation is recorded [24].

Consider Equation 1.7 for voltage output of a MEMS gyroscope. The output of the gyroscope is a product of input voltage and the change in capacitance with some scale factor. If there is linear acceleration then the gap between the comb electrodes change, causing change in the capacitance and consequently output voltage of a MEMS gyroscope. The phenomenon is more adverse in single mass MEMS gyroscopes; therefore tuning fork gyroscopes are designed to overcome this error.

Vibration which is also termed as short fluctuating acceleration also affects the gyroscope output rate. The magnitude and frequency of the vibration determine the error it can impart to the output of a MEMS gyroscope. If the frequency of the vibration is of the order of resonant frequency of drive mode, it can cause un-stability in the gyroscope sensor output data [4].

1.5. Literature Review

This literature review mentions all the techniques that are used for compensation of drift data mainly caused by temperature and linear acceleration. This section starts with review of compensation methods for temperature, followed by review of compensation methods for acceleration.

1.5.1. Methods for temperature compensation of a MEMS gyroscope

The thermal compensation can be achieved either by hardware circuit design or by processing the data, after reading from a sensor. Hardware compensation is faster than processing of data, and hence should be the first approach. In certain cases this is not possible and signal processing is the only available option. The designer of a MEMS gyroscope has the option to make amendments in the circuit that caters for drifts imparted to a sensor by temperature effects. This is not the case always,

because many designs require off-the-shelf sensor and their internal characteristics are not known to the user. The temperature compensation in such cases is only possible by processing the data acquired from the sensor. The hardware design to compensate temperature effects are discussed first.

1.5.1.1. Temperature Compensation by Hardware Design

The hardware design can be modified or improved in different ways in order to compensate the drift caused by temperature.

1.5.1.1.1. Using Temperature Control Device

This method is explained by [27] in which the compensation can be achieved by developing a temperature control device. The function of this device is to maintain the temperature of a sensor at an optimum value of temperature. A thermo-electric cooler can be used for cooling or heating a sensor as per requirement. The temperature feedback is used as input to the cooler which then maintains the temperature at a predefined value. This technique gives hardware based design to eradicate the effects of temperature, without changing the actual circuitry of a sensor. The benefit is that the sensor circuit and temperature circuit can be designed separately, thus allowing ease and flexibility in the design. The solution is workable for static conditions and no dynamic conditions of acceleration are discussed.

1.5.1.1.2. Controlling the Oscillators using PTAT

Another method of controlling the effects of temperature is by employing a circuit which has characteristics free of temperature changes. Zhang et. al. [32] used an on-chip circuit that utilizes PTAT (Proportional to Absolute Temperature) current to compensate for the temperature drift. The PTAT current controls oscillators, and lag in the frequency of oscillators due to rise in temperature is compensated by the PTAT current and is valid for a wide range of temperature [32]. The method clearly states that any property of the circuit that is linearly dependent on the temperature can be used as a feedback to the sensor circuit. In this case the current sources are

designed such that they vary the gain with temperature and this variable gain is used as a tool to control the effect of temperature.

1.5.1.1.3. Using Temperature Variable Gain Circuit

Likewise, CTAT (Complementary to Absolute Temperature) current can also be used for compensation of temperature drift in MEMS capacitive Gyroscopes. A linear relation can be found between CTAT current and temperature change in a gyroscope thus paving the way for temperature calibration [34]. Yin et. al. used a capacitive MEMS gyroscope for compensation of temperature drift by making design changes in the readout circuitry using CTAT.

1.5.1.1.4. Design Targeting Temperature Compensation

Other than using the CTAT and PTAT currents, special components can be added to a MEMS gyroscope readout circuit that aim at improving the temperature dependency of a sensor. Such compensation can be achieved by introducing some compensation orientated components at the drive circuit of the sensor [33, 34]. Sun et. al. introduced a Difference Differential Amplifier (DDA) at the inputs of drive mode to compensate the thermal effect on a sensor; a circuit design that achieves low temperature dependency and high gain.

1.5.1.1.5. Using frequency Synthesizer for Core Temperature

The resonant frequency of a drive mode changes with the change in the temperature of a resonator [18, 27]. The difference between the resonant frequencies of two oscillators, that have different oscillation coefficients, can be used to determine the temperature at which they are oscillating [35]. This property is used by Chiu et. al. to read the actual core temperature of a MEMS gyroscope. The temperature compensation is achieved by using an FPGA based frequency synthesizer which provides calibration parameters to adjust the final output of a MEMS gyroscope. The sensor drive mode resonator and an on-chip Si resonator send their signals to a FPGA synthesizer, which calculates the difference in frequencies and then generate a code for calibration parameter. The difference in the frequencies determines the core

temperature of the sensor, and hence is used to compensate the effects of temperature. The calibration parameters then modify the amplitude of the output signal [35].

1.5.1.2. Temperature Compensation by Signal Processing

Compensation by using signal processing is very useful and suitable where hardware changes are not possible. There are different methods which can be used to compensate the changes in a gyroscope output data using signal processing.

1.5.1.2.1. Using Kalman Filter

Many papers have been published where Kalman filter is used for compensation of drift in a gyro data in real time [26, 29, 36]. There are few papers that mention Kalman filter as temperature compensation technique [31, 38]. The paper where the temperature compensation by Kalman filter is mentioned is basically a two step method [31], where first temperature compensation is done by some other technique and then Kalman filter is used for compensation of other drift factors. It can be stated that Kalman filtering cannot be directly used for compensation of temperature based errors. Figure 1.4 shows the basic operation of Kalman filter.

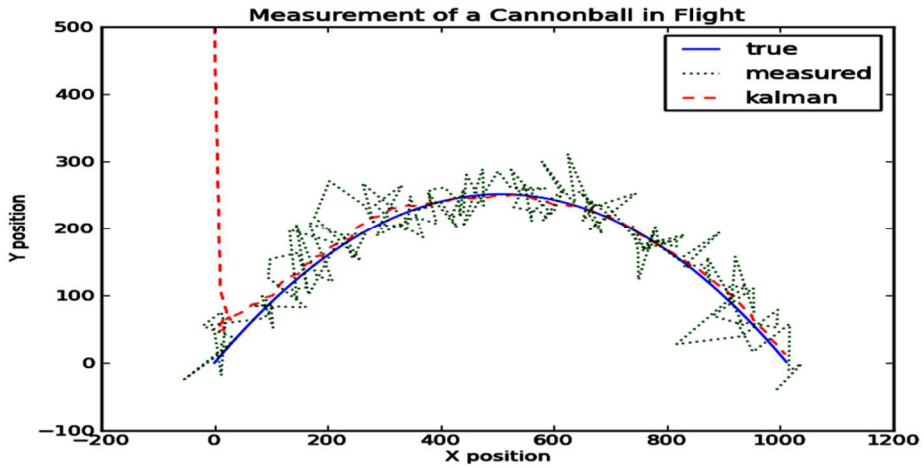

Figure 1.4: The basic operation of Kalman filter shows that the technique is best suited for removing spontaneous random noise.

It can be clearly seen that the predictor is following the data and removing the jumps and noise, and tries to remain on the actual data path. In case of temperature compensation this data path is the error itself and it has to be compensated. Therefore the real time predictor cannot be applied to a temperature compensation problem. The temperature compensation requires knowledge of all the possible outcomes when a certain amount of change in temperature is applied so that it can be compensated later.

1.5.1.2.2. Using Moving Average

Moving average is mostly used for filtering high frequency noise in the data and not for temperature compensation. The moving average cannot be directly used as a compensation method for temperature base effects. Figure 1.5 shows how high frequency noise can be removed from raw data to obtain a visual trend of data. This helps to see dependency of a gyroscope data on temperature or acceleration.

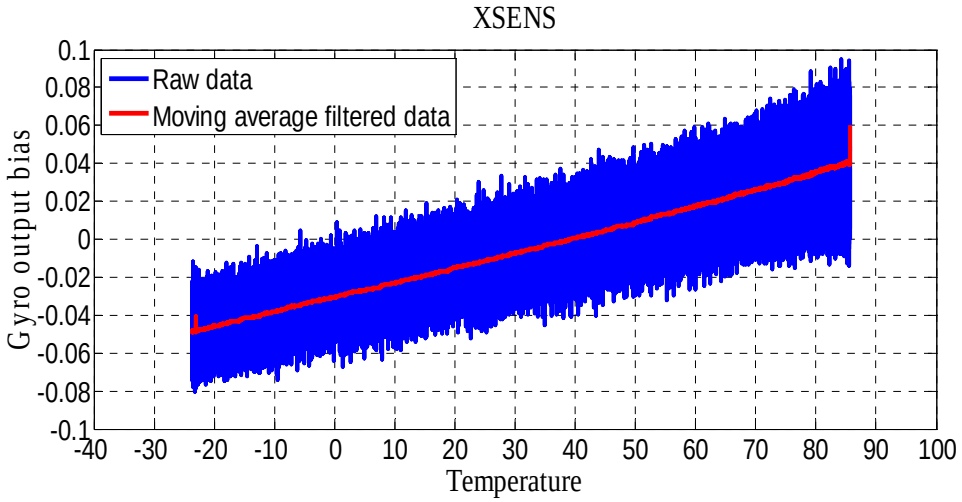

Figure 1.5: The Moving Average Filter is very effective in removing the high frequency noise and the data is filtered.

The moving average (MA) filter is used in this study in every analysis because the high frequency noise makes it difficult to understand the trend of data in raw form. The shown data is taken from XSENS MTi-10 sensor and the relation is quite simple, but some other sensors have too much noise and MA is a must requirement to visualize different trends in data. Also hysteresis analysis requires very fine data plots and it is not possible without the moving average filter.

1.5.1.2.3. Wavelet Decomposition

The wavelet decomposition technique is used for extracting information from a noisy or high frequency data [29]. The trend of drift is overridden by many high frequency noise elements. The wavelet decomposition is a powerful method to acquire information about low frequency pattern of any data. Ji et. al. [29] used the wavelet decomposition to extract the drift trend and used that data to form a drift model. The compensation process is very complex, as it involves four levels of filtering namely median filter, wavelet decomposition, autoregressive modeling and Kalman filtering. Simpler and less complex alternatives are required for use in real time applications which makes this method undesirable.

1.5.1.2.4. Using Polynomial Curve Fitting (CF)

Polynomial Curve Fitting is the most common technique used for temperature compensation [17, 27, 30-31]. Bekkeng et. al. reports 16 times improvement in the bias instability (27°/sec to 1.4°/sec) by using CF for temperature compensation and Kalman filtering for other drift factors [31]. Zhang et. al. provides comparison between CF and other methods and claim that this method is inferior to compensation by neural network [30]. Xia et. al. reports that bias instability can be reduced from 12°/sec to 0.6°/sec by using CF method for temperature compensation. All the research works provide results from a single sensor, and the initial bias instability is not very good and there is margin for correction. Also the effects of temperature are considered and effects of acceleration are completely ignored by the researchers. Hysteresis is an important factor that affects a gyroscope output but it is not discussed or compensated in any of the published literature.

1.5.1.2.5. Using Linear Curves

Linear Curves can be considered as derived form of polynomial curve fitting. The polynomial curves can be of higher order and a non linear system is obtained which is not desired in some cases. The complexity of polynomials can be reduced by dividing the temperature range regions in such a manner that instead of one high order polynomial, first order multiple polynomials are obtained [27]. Thus complexity of the system is reduced significantly and it becomes linear as well. Figure 1.6 explains the phenomenon clearly. The figure clearly shows that the linear curves can be used to divide the main data into smaller parts and each part is modeled more accurately by using lower order equations. Thus more accuracy is achieved and processor resources are also conserved.

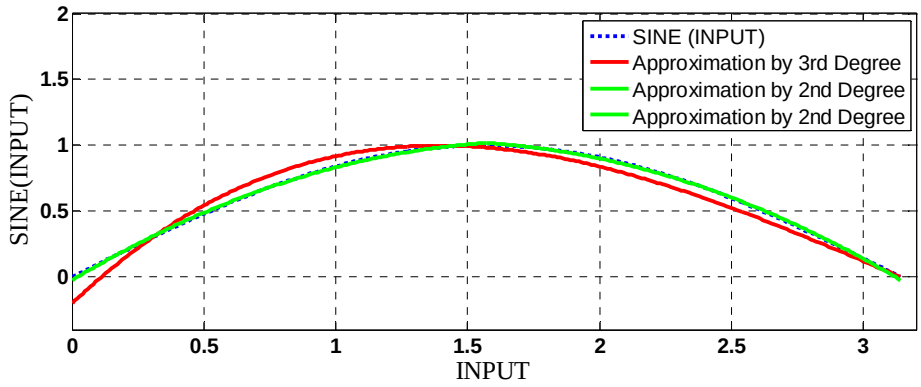

Figure 1.6: The dotted line shows the plot of SINE of some input data and red line shows approximation using a 3rd order equation. The green line shows use of 2nd degree equation more efficiently by dividing into two parts and near to actual data.

1.5.1.2.1. Using Back Propagation (BP) Neural Networks (NN)

BP neural networks algorithm is another commonly used method for temperature compensation [17, 27, 30]. Shiau et. al. reported that neural networks can be used for temperature compensation and the results of compensation are comparable to the results obtained by CF method [17]. Thus NN can be used as an alternative for temperature compensation. Xia et. al. also showed that NN and CF can be used

alternatively and both the techniques help eliminate temperature dependency of a MEMS gyroscope output data [27]. Zhang et. al. showed that temperature compensation by NN can achieve four times better results that temperature compensation by CF method [30]. The sensors used by these three research groups are different and they produced different results when NN compensation is used. Therefore, to better understand the effect of a technique more than one type of sensor should be used for analysis. This method is not very fast as compared to other methods [27] and some tradeoffs have to be done while implementation in real time applications. The most of the work done so for on the BP neural networks is in simulation mode [27, 30], and only one paper reports actual retrieval of constant weights to form compensation equations [17]. Converting the system to set of equations reduces the complexity of this algorithm. Some very basics concepts about neural networks are explained here for understanding point of view. Figure1.7 shows block diagram of neural network.

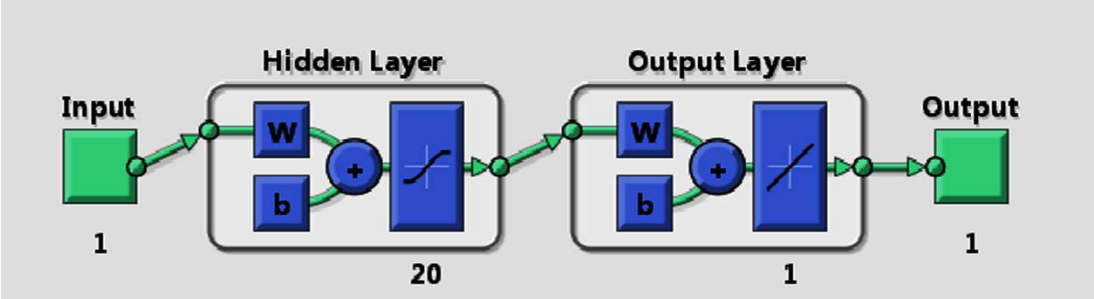

Figure 1.7: The block diagram of neural network which shows different parameters of the method. Output is achieved with calculations based on input and some weights determined from training of a data set.

INPUT is the known data given to the system and OUTPUT is the unknown data which is to be calculated. OUTPUT is known only during the training of the network. TRAINING means finding a relation between INPUT and known OUTPUT data. The layers (HIDDEN & OUTPUT) are set of equations with different weights and bias values. The bias and weights are permutated until a correct relation is established between input and output data.

There are many algorithms that are used to establish relation between input and output data. Once the relation has been established, the weights and bias equations are used to calculate the output based upon the input data. In case of this study inputs are temperature and acceleration values at zero turn rate, and output is the drift at given temperature and acceleration applied to the sensor.

1.5.1.2.2. Using Temperature Coefficient of Resonant Frequency

The resonant frequency of a material that makes the resonator of drive circuit in a MEMS gyroscope is proportional to the temperature value [18, 37]. If the design uses a material for gyroscope whose resonant frequency coefficient for temperature is linear with change in temperature then temperature compensation can be achieved by simply using that coefficient. The resonant frequency is directly proportional to the output voltage of a gyroscope [27], so by knowing that temperature based drifts can be compensated easily in a gyroscope output data [18, 37]. Prikhodko et. al. improved the bias instability from 0.6°/hr to 0.22°/hr, by using resonant frequency coefficient of a vacuum sealed silicon gyroscope [18]. The drawback of this technique is that the material used in the fabrication must have resonant frequency coefficient for temperature which is linear to temperature. This limits the choice of material and also put restrictions on the environment of a sensor.

1.5.2. Compensation of Acceleration Effects on a MEMS Gyroscope

This subject is not found in the literature in abundance as does the compensation for other drift factors [22, 23]. The main reason for this is that the linear acceleration does not affect the output of a gyro as compared to other drift parameters for values less than 5 g [23]. Since most of the applications do not come across higher g value so this is not a much researched area [23]. But for applications where large value of g is expected, the compensation for linear acceleration has to be done for accurate reading. From the very few papers that are available, following methods are selected that can be used to compensate the drift caused by linear acceleration.

1.5.2.1. Using Inferential Momentum Calculations

This method requires detail knowledge about the structure and physical properties of a MEMS gyroscope. The compensation is based upon formulation of static and dynamic thermal error equations using the inferential momentum calculations [22]. The thermo-elastic properties of a sensor material are also required to formulate accurate equations for compensation. The dynamic thermal error due to linear acceleration can be compensated as compared to static thermal error which requires the stationary position of sensor. Temperature and acceleration are input to this method of error calculation [22], and based on these inputs a thermal error is predicted. The method does not require empirical data for formulating the equations for compensation. Jiancheng et. al. reported that both temperature and acceleration effect the output of a MEMS gyroscope, and used this model of inferential equations for its compensation[22].

1.5.2.2. Using modified Kalman Filter

Modified form of Kalman filter can also be used as a method to compensate the effect of linear acceleration on a MEMS gyro output [23]. The Kalman filter is used to predict the position and velocity of object under given conditions. The sensitivity matrix can be added to a regular Kalman filter to gauge the effect of linear acceleration on a gyroscope [23]. Kalman filter is optimal filter for linear systems [26, 29] and if system is modeled using linear equations for acceleration change, then optimal predicted values of a gyroscope output can be obtained. This cannot work as an independent filter for compensation of linear acceleration.

1.5.2.3. Changing Frequency of Operation in Thermal Gyroscopes

This methodology is applicable to MEMS thermal gyroscopes whose output is corrupted by linear acceleration. Feng et. al. reported that the linear acceleration dependency is decreased after the frequency of operation (switching of heaters) is reduced to a lower value. Also the design of the sensor can be adjusted to reduce the effects of linear acceleration. The phenomenon is very similar to the case of tuning fork gyroscopes which are specially designed to counter effects of linear

acceleration. Likewise, in thermal gyroscopes the position of heaters and sensors is placed perpendicular and opposite to each other, to cancel out the false rotation effect caused by the linear acceleration [24].

1.6. Motivation of this Thesis

The drift in the output of a MEMS gyroscope limits its use in inertial applications and all the other benefits are overturned by this error. The structural errors are technology dependent, and not much can be done about them. However, the errors that are caused by the environment and other parameters can be compensated by some methodology, to make a MEMS gyroscope accurate enough to be used for navigational applications.

One such factor that causes the output of a MEMS gyroscope to drift with time is the change in temperature of a sensor [13-21]. MEMS devices, including gyroscopes, require some mechanical movement for operation and the material is heated causing changes in the output of sensors. This is most important parameter that causes degradation in a MEMS gyroscope output [17] and the error accumulates over time because temperature changes. A lot of literature is available that explain the effects of temperature on a MEMS gyroscope output [13-21]. The fact is that the dependency on temperature cannot be removed completely by any technological techniques so far, therefore some form of compensation is required. It can also be said that every MEMS sensor acts as a virtual temperature sensor, because the drift in the output of a MEMS gyroscope has a relationship with temperature.

Another factor that affects the output of a MEMS gyroscope is linear acceleration [22-24]. The effects of linear acceleration on output of a MEMS gyroscope are normally neglected because this error does not add much to drift as compared to other parameters [23]. The effects of linear acceleration become more evident when linear acceleration increases above certain threshold value [23]. Normally MEMS devices do not face acceleration greater than 5g, and hence they are not compensated for linear acceleration errors. But for acceleration values greater than 5g error in a MEMS gyroscope output has to be compensated [23].

There has been a lot of work done on compensation of temperature effects of a MEMS gyroscope, and some work has been done on compensation of linear acceleration effects on a MEMS gyroscope output. The main motivation of this thesis is to work on the compensation of both of these errors simultaneously using the existing compensation techniques. The study results into formulation of a procedure and methodology to improve the output of a MEMS gyroscope to an extent that cannot be achieved otherwise with existing methodology.

The literature shows that the performance of existing methods is verified using only one type of sensor. This is the reason that the improvement efficiency is different in different publications using similar techniques. Therefore different types of sensors are used in this study to generalize the efficiency of the methods. Literature shows that temperature cycles can result in hysteresis in a gyroscope data but no solution is provided. This phenomenon is also analyzed and a workable solution is presented.

1.7. Research Objectives and Thesis Organization

This thesis is focused on the compensation of errors and drifts caused by temperature and acceleration in the output of a MEMS gyroscope data. Section 1.7.1 summarizes the research objectives of this thesis.

1.7.1. Research Objectives

- The first objective of this research is to study different temperature and acceleration compensation techniques and provide a comparison based upon efficiency and complexity of the method.

- Compensation of both the temperature and acceleration effects should be done simultaneously in order to obtain drift free data from a MEMS gyroscope.

- The compensation techniques are implemented on different types of sensors and efficiency of the techniques is analyzed for different sensors.

- Neural network compensation is also used for compensation of acceleration and the results are compared with conventional method.

- Hysteresis should also be studied as drift factor and its compensation is carried out in this study.

1.7.2. Thesis Organization

Chapter 1 summarizes some background knowledge about MEMS sensors and their importance in the modern electronic consumer market. The work done by other researches is also summarized in the literature review. This chapter also explains the limitations imposed on a MEMS gyroscope and its drawbacks.

Chapter 2 gives the details about the methodology that is implemented in this study. The sensors available to this study are discussed in detail, and the equipment used in the study is also presented. The chapter also mentions different testing conditions and methodologies used in this study.

Chapter 3 provides the data and results that are obtained after implementation of the compensation methods. Compensation of temperature, hysteresis and acceleration is discussed for every sensor and comparative figures are presented to understand the improvement achieved after compensation of these factors. Also results for integrated compensation of all the drift factors present in single data set are shown. Allan Variance plots are presented with most of the data to gauge the efficiency of the compensation.

Chapter 4 summarizes the results and provides conclusion to this study. Different numerical parameters are presented in tabular forms to compare the efficiency of different techniques applied to different sensors.

CHAPTER 2

METHODOLOGY OF THIS STUDY

This chapter explains the methodology adopted in this study. The types of sensors used in the study are discussed and their properties are explained. The chapter also explains the setup that is used to collect data, along with limitations provided by the hardware available to this study. The conditions of data collection and samples are discussed to understand the generality of the testing. After explaining all these features, the chapter presents the techniques and algorithms that are adopted in this study for compensation of drift caused by temperature and acceleration.

2.1. Sensors used in the study

There are different sensors used in this study, and it is important to briefly define their characteristics that concern the topic to this thesis. Initial tests are performed on an accelerometer that is fabricated in METU-MEMS Research Centre, and it is named ACC1 for convenience in this study. Later different commercial sensors are purchased to effectively check the compensation algorithms. This section provides a brief introduction of the sensors, and there critical properties like range of rate, bias instability and operating range.

2.1.1. Accelerometer (ACC1)

This sensor is fabricated at METU-MEMS Research Centre, and is used initially in this study. The sensor acted very well for initial study, and working algorithms for temperature compensation are obtained. It is an accelerometer so it is difficult trying to analyze it for acceleration effects, therefore only temperature compensation is implemented on this sensor. Table 2.1 gives main features of this sensor.

Table 2.1: Specifications of ACC1 accelerometer

Range	± 20 g
Bias Instability	7 ug
Operating Range	-40 to +85 ° C
Interface	Analog
Power Supply	3.3 V
Sampling Rate Acc.	250 Hz
Sampling Rate Temp.	50 Hz
On-chip Temperature Sensor	Separate arrangement

2.1.2. ADIS16136

This is a single axis precision gyroscope manufactured by Analog Devices. This is a digital gyroscope with two outputs only, namely gyroscope output rate and temperature. Table 2.2 gives main features of this sensor.

Table 2.2: Specifications of ADIS16136 gyroscope

Dynamic Rate Range	± 450 ° / sec
Bias Instability	4 ° / hour
Operating Range	-40 to +85 ° C
Interface	Serial Peripheral Interface (SPI)
Power Supply	5 V
Sampling Rate	Variable and software controlled
On-chip Temperature sensor	YES

There is a limitation on the operation of this sensor. The sensor has a protective casing made of metal to make it more rugged, but it also limits the range of

operation. The sensor cannot be heated above 50°C, and all the analyses are performed below this temperature. Heating the sensor above this value turns the sensor off, because the metallic casing gets too hot. Also the sensor is very sensitive to vibrations in the temperature chamber, and data collection is not possible when it is experiencing external vibrations.

2.1.3. ADIS16488

This is an IMU manufactured by Analog Devices, and it is a very precise sensor with 3 axes of gyroscope, 3 axes of accelerometer and 3 axes of magnetometer. This sensor is ideal for studying acceleration effects, as there are three accelerometers present on the system, and at any point acceleration value in any direction can be obtained from this sensor. Table 2.3 gives the main features of this sensor.

Table 2.3: Specifications of ADIS16488 IMU

No. of accelerometers	3
No. of gyroscopes	3
Dynamic range (gyroscope)	± 450 ° / sec
Dynamic range (Acc.)	± 18 g
Bias Instability (gyroscope)	5.1 ° / hour
Operating Range	-40 to +85 ° C
Interface	Serial Peripheral Interface (SPI)
Power Supply	5 V
Sampling Rate	Variable and Software controlled
On-chip Temperature sensor	YES

There is also limitation on the operation of this sensor very similar to ADIS16136, as explained in Section 2.1.2. This limits its operation to below 50°C and vibration free data collection is required for analysis.

2.1.4. ADXRS450

ADXRS450 is an analog MEMS gyroscope manufactured by Analog Devices. This sensor is very ideal for this study because the manufacturer has performed no temperature compensation, and dependency on temperature can be seen easily in the data plots. Table 2.4 gives the main features of this sensor.

Table 2.4: Specifications of ADXRS450 gyroscope

Dynamic Rate Range	± 300 ° / sec
Bias Instability	4 ° / hour
Operating Range	-40 to +125 ° C
Interface	Analog
Power Supply	5 V
Gyro Sampling Rate	2 Hz or 500 Hz
Temp. Sampling Rate	2 Hz
On-chip Temperature Sensor	YES

Since this is a single axis gyroscope and no on-chip accelerometers are present, therefore it is not a valid choice for use in the analysis of acceleration effects. However the dependency on acceleration can be studied using alternative methods to obtain acceleration values, which are discussed in relevant sections.

2.1.5. XSENS MTi-10 (XSENS)

This IMU is manufactured by XSENS and is purchased for this study. This sensor is ideal for this study because it provides raw data from the sensor on which no calibration is performed internally by the sensor. Thus the compensation techniques can produce significant improvement in the gyroscope data. The sensor also provides calibrated data, which is used as a reference for compensation techniques used by this study. Table 2.5 gives the main features of this sensor.

Table 2.5: Specifications of XSENS MTi-10 IMU

No. of Accelerometers	3
No. of Gyroscopes	3
Dynamic Range (gyroscope)	± 450 º / sec
Acceleration range	± 10 g
Bias Instability (gyroscope)	18 º / hour
Operating range	-40 to +85 º C
Interface	USB / RS232
Power Supply	5 V / 3.3 V
Sampling Rate	Variable and Software controlled
On-chip Temperature Sensor	Yes / Separate for all sensors

2.2. Setup Used for Data Collection

The data collection for this study is done under different conditions and with different requirements. There are two factors whose effects are to be studied, and they are temperature and acceleration. These conditions are created in a lab to observe their effects on the output of a gyroscope data. The setups required to meet the different criterion can be divided into three main categories; Temperature test, acceleration test and combined (temperature and acceleration) test.

2.2.1. Temperature Test Setup

The first condition that needs to be tested is the effect of temperature. For that purpose, a temperature chamber is used to change the temperature around a sensor in a wide range, so that its effect can be studied on that sensor. The chamber is present in EE Department of METU campus. Figure 2.1 shows the temperature chamber that is used for temperature testing.

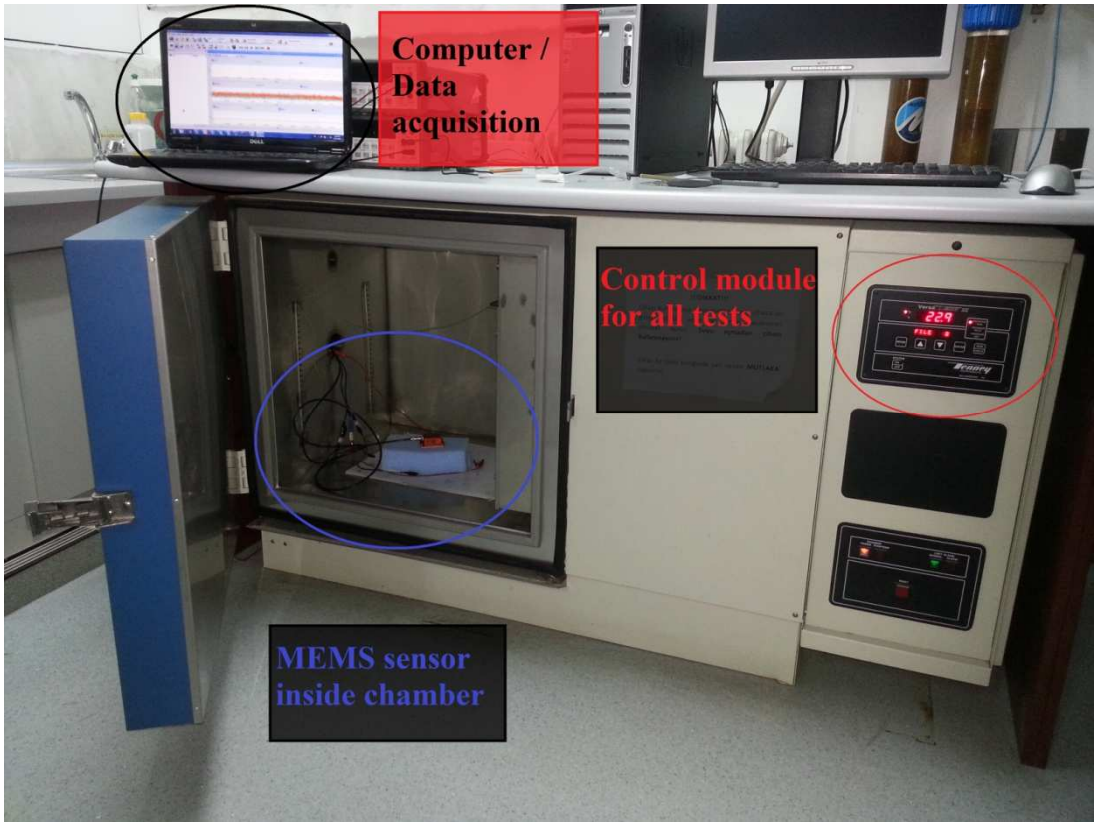

Figure 2.1: Temperature chamber with data acquisition interface, placement of a MEMS sensor in the chamber and control module to control the test conditions.

The data is recorded by placing a sensor setup inside this chamber, and the wires containing data come out of a specified place and are connected to a computer. The chamber is capable of producing temperature range from -80 ºC to 100 ºC. The only problem with this chamber is the vibrations that it produces while the chamber is turned on, and this adds a lot of noise to collected data. This problem limits the use of chamber to collect data from certain sensors. ADIS16136 and ADIS16488 are very sensitive to these vibrations, and data from these sensors cannot be collected while the chamber is on.

Hysteresis is also studied using this setup, because only temperature is changing while testing the effects of hysteresis. No separate setup is required, just the cycles of temperature change using same setup.

2.2.2. Acceleration Test Setup

The second effect that is being analyzed in this study is the effect of linear acceleration on the output of a MEMS gyroscope. The requirement for such a test is that only acceleration is changing, and temperature is not changing. This is very important because the relation between offset and acceleration is valid only when sole source of offset is due to changes in acceleration values. This test does not require any special equipment and can be performed in a lab, where flat surface is available. The data from any sensor is collected while the temperature is also monitored during the test. Figure 2.2 shows the setup required to obtain data for this test. ADIS16488 is connected with the laptop and placed on a flat surface. Using the interface software, the position of this sensor is set to obtain any specific position.

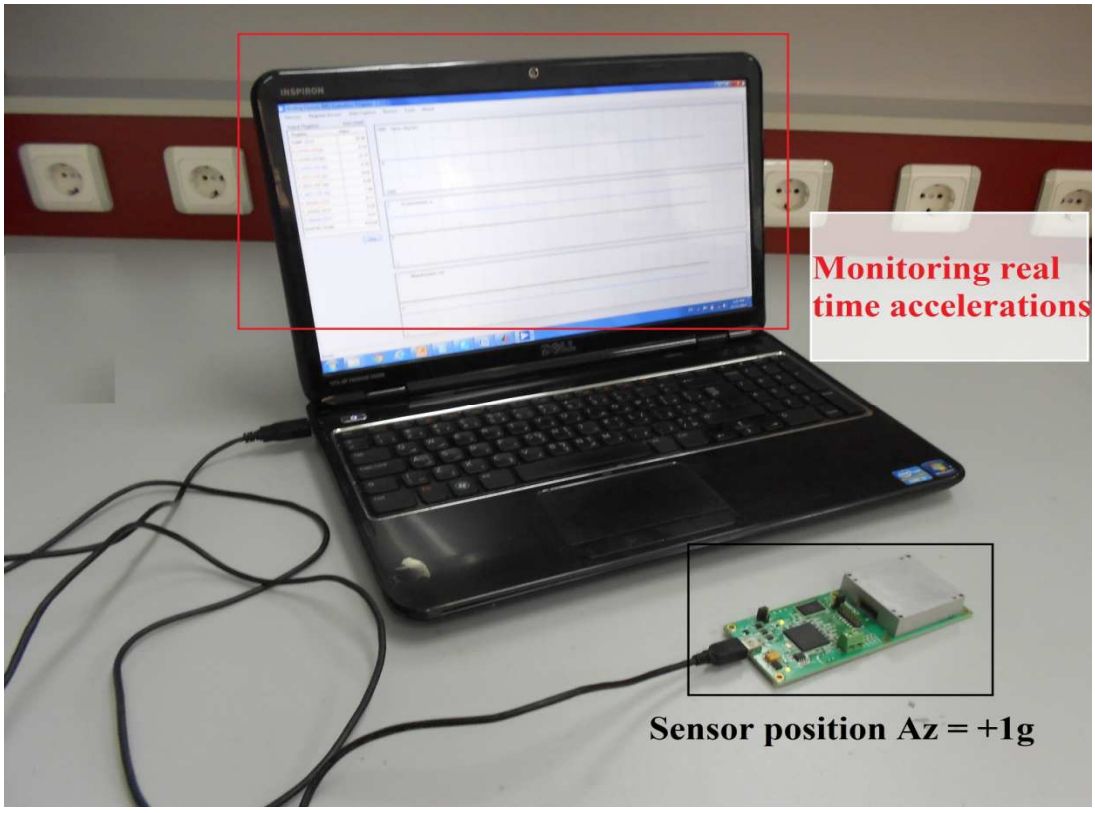

Figure 2.2: The ADIS16488 sensor is placed on a flat surface and real time interface is used to set the position such that the sensor experiences desired acceleration e.g. z-axis accelerometer value Az = +1g.

Figure 2.3 shows how ADIS16488 can be rotated to obtain different positions of accelerations with the help of interface software. The sensor is rotated inversely to obtain +1g and -1g values for y-axis accelerometer using interface software.

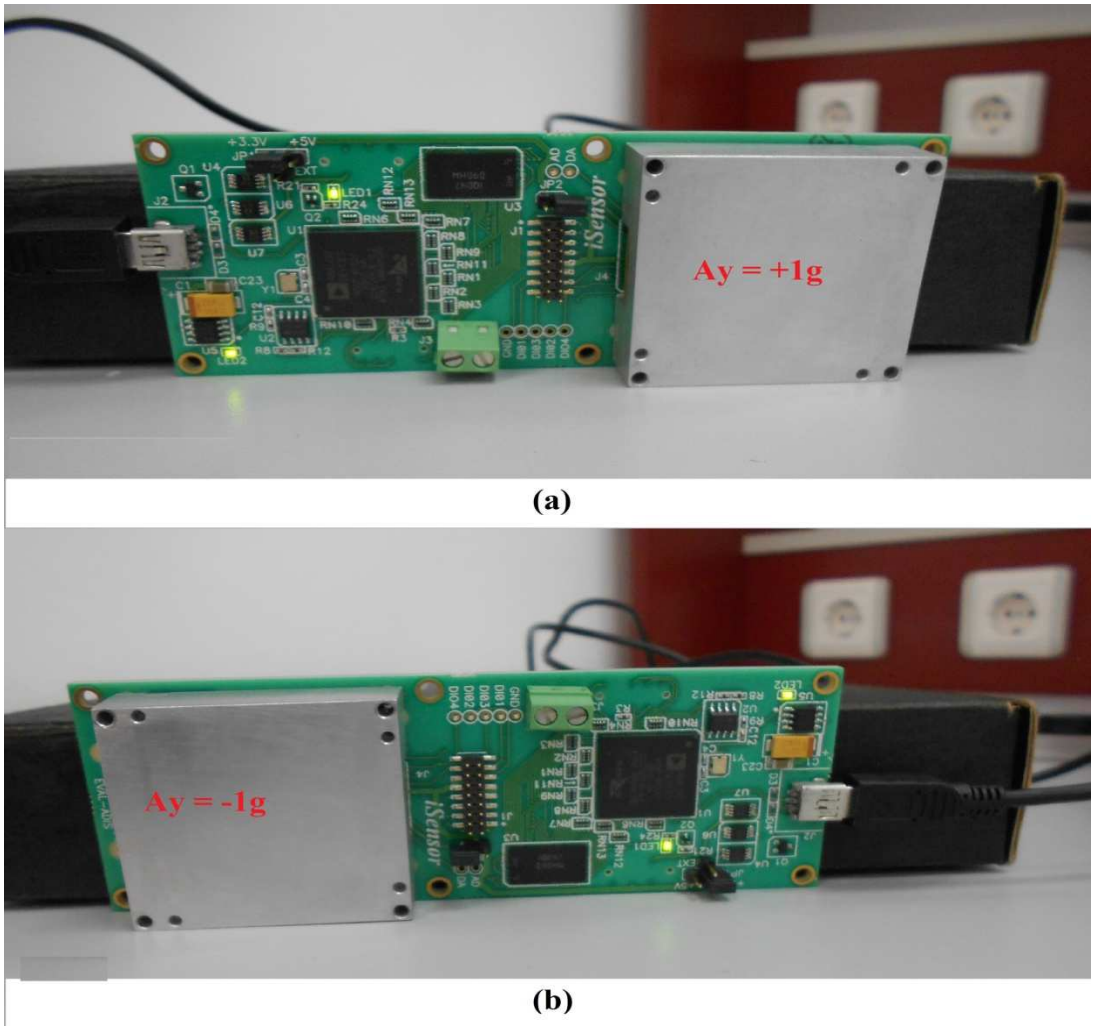

Figure 2.3: The acceleration applied to the ADIS16488 can be changed by positioning the sensor. (a) The sensor is giving +1g acceleration to y-axis accelerometer. (b) -1g is given to y-axis accelerometer

Figure 2.4 shows position of XSENS being changed to obtain +1g acceleration values in all the three axes one by one. These figures give just the basic working principle of how the acceleration values are obtained using the interface software, which gives real time values for acceleration and gyroscope. There are many other positions that can be given to the sensor. The monitoring of temperature is very important while collecting data for acceleration because some sensors are very prone to temperature changes.

2.2.3. Combine Temperature/Acceleration Test Setup

The third setup is requirement for integrated compensation where both temperature and acceleration effects are compensated in a data. For this purpose the temperature and acceleration of a sensor must change simultaneously. The first two setups are combined in this step to attain integrated effect. The acceleration tests, as described in Section 2.2.2, are performed inside a temperature chamber, and temperature is also changing during these tests. Thus the acceleration changes are happening inside a temperature chamber, whose temperature cycle is turned on; thus giving temperature and acceleration based drifts to a gyroscope data.

2.3. Data Collection Procedures

In order to study the effects of temperature and acceleration on a MEMS gyroscope output data, it is very important to follow a set of rules for data collection, and maintain them for all the tests for homogeneous results. All the data collected in this study is according to requirements of this study, limitations imposed by the setups, and specific features of the sensors.

2.3.1. Temperature Range

The ideal range for any temperature test is to change the temperature from -30 °C to +85 °C and then move back to -30 °C (typical temperature range for most of the industrial applications). For ADIS16488 tests are done from -30°C to 40°C because

it can only be operated in this range, but tests that are performed on ADXRS450 and XSENS are done in a much wider range of -30°C to +85°C.

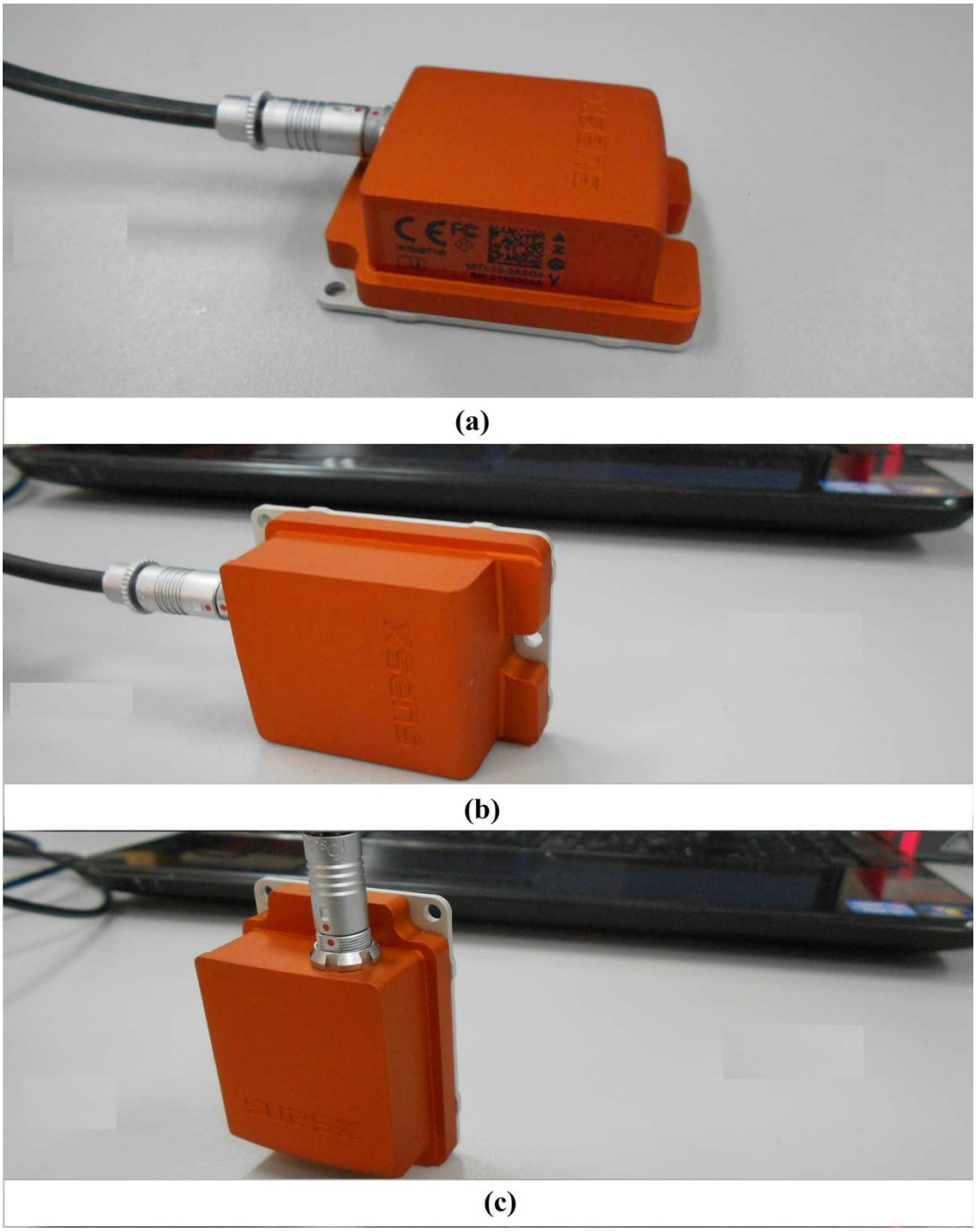

Figure 2.4: The XSENS can be positioned to obtain acceleration value that is required by any test. (a) XSENS is placed to get +1g on z-axis. (b) XSENS is placed to get +1g on y-axis. (c) XSENS is placed to get +1g on x-axis.

2.3.2. Acceleration Range

The acceleration range that can be tested using the available resources is also limited, because there is no specialized equipment that can be used to produce large amounts of acceleration. The study used the natural range of +1 g and -1 g due to the gravitational force of the Earth. The use of interface software makes it easy to read instantaneous value of acceleration of any axis, and thus different values can be used for the analysis purposes.

2.3.3. Duration of Test for Temperature Test

The duration for temperature tests is another parameter that can be discussed here for understanding the duration of any sample. The actual goal of data collection is to collect data over a given range of temperature, and the duration of data collection is not important in this regard. Same range of temperature can be achieved using different amount of time durations under different conditions. Figure 2.5 gives an example of two data sets that are collected in the temperature range of -30°C and +40°C, but the duration of these data collections are 1 and 4 hours. The effect of duration of data collection is also analyzed, and it does not affect any compensation.

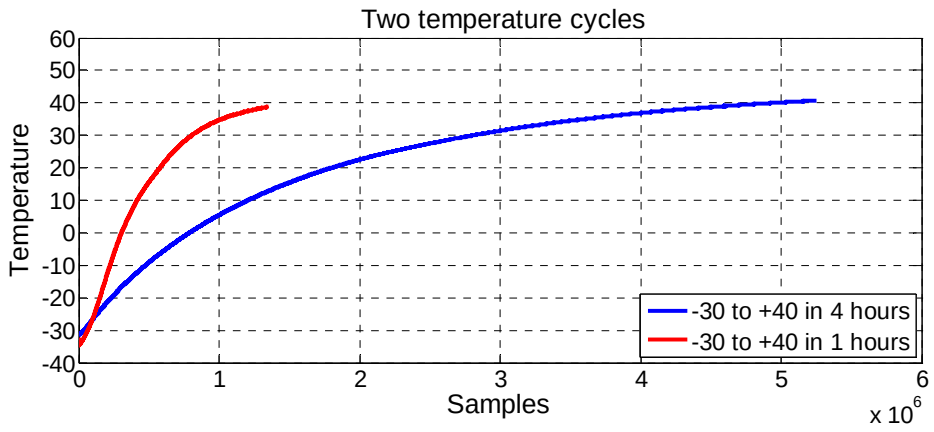

Figure 2.5: The desired temperature range can be achieved in different amount of times depending upon the settings of temperature chamber. Accelerated heating can results in 4 times faster heating of the sensor.

2.3.4. Duration of Test for Acceleration Test

The duration of a test for monitoring acceleration is another important test parameter. The duration of a test is kept small enough to forbid the temperature of a sensor to change to cause any significant error in a data. Also the duration is kept long enough to allow a sensor to attain stable data values. The normal duration of acceleration tests used in this study is around 10 minutes.

2.3.5. Number of Samples

The number of samples (data sets) taken from each sensor is also very important to ascertain the authenticity and generality of these compensation methods. Therefore, more than 10 samples of data are collected from each sensor, in order to verify the consistency of the trend in the collected data.

2.4. Methods of Data Collection

There are different types of sensors used in this study and every one of them requires a separate method to collect data from it. The sensors are selected initially by keeping in mind that readymade data collection is possible. This is decided on the basis of the fact that hardware issues can stall and slow down the process of data acquisition.

2.4.1. Collecting Data from ACC1

This sensor is fabricated at the METU-MEMS Research Centre and has an analog interface. The system used to collect data is Digital Data Acquisition cards installed in a computer. The cards have analog interface, which allows acquiring analog data from any analog sensor. The card has its own interface software that allows acquiring of data from this sensor at any desired rate.

2.4.2. Collecting Data from ADIS16488

The ADIS16488 is an IMU, and a sensor kit is bought along with an acquisition system. The hardware of the acquisition board consists of an evaluation board, on which the ADIS16488 IMU can be mounted easily. The evaluation board has a USB

cable that can be connected to any computer for data acquisition. Figure 2.6 shows the package of ADIS16488 sensor with its metallic casing. Figure 2.7 shows the assembled form of evaluation system, in which ADIS16488 is mounted on the evaluation board, and interface USB cable is also shown.

Figure 2.6: ADIS16488 IMU with metallic casing. This protective casing limits the operation of this sensor by heating up.

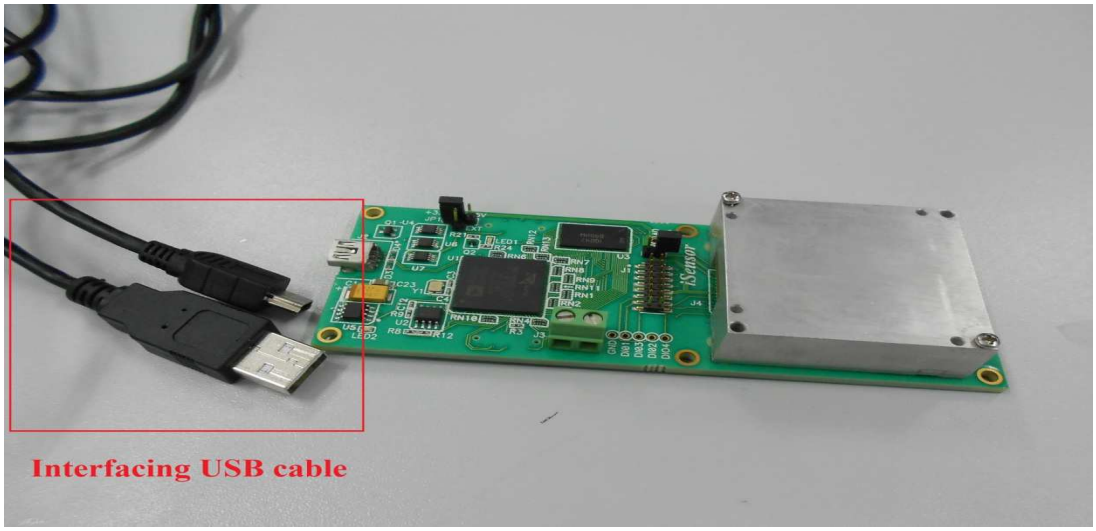

Figure 2.7: Evaluation board with interface USB cable is shown. ADIS16488 is mounted on the evaluation board.

The evaluation system also consists of interface software, which allows communication with the sensor and retrieving data without doing any programming. Appendix B shows different screenshots of this interface software.

2.4.3. Collecting Data from ADIS16136

The data acquisition from ADIS16136 is similar to data acquisition of ADIS16488 sensor because both these sensors are compatible with the same evaluation board, and same interface software is used for data acquisition. Figure 2.8 shows the package of ADIS16136, and it can be seen that it has same connector like ADIS16488. This is mounted on the evaluation board and connected to the computer, from where sensor selection is made from the interface software.

Figure 2.8: The ADIS16136 sensor is shown in the metallic casing. The sensor has same connections as ADIS16488 and hence can be used with same evaluation board.

2.4.4. Collecting Data from ADXRS450

This sensor is also manufactured by Analog Devices, but due to different configuration it is not compatible with the evaluation board discussed in Section 2.4.2. The data acquisition system of ADXSR450 consists of two PCB boards. One board converts the analog voltage into digital value (Satellite Board)

and the second board communicates with a computer using a USB interface (Main Motherboard). Figure 2.9 shows a satellite board with ADXRS450 mounted on it. The sensor is powered up from the power supply provided by the satellite board.

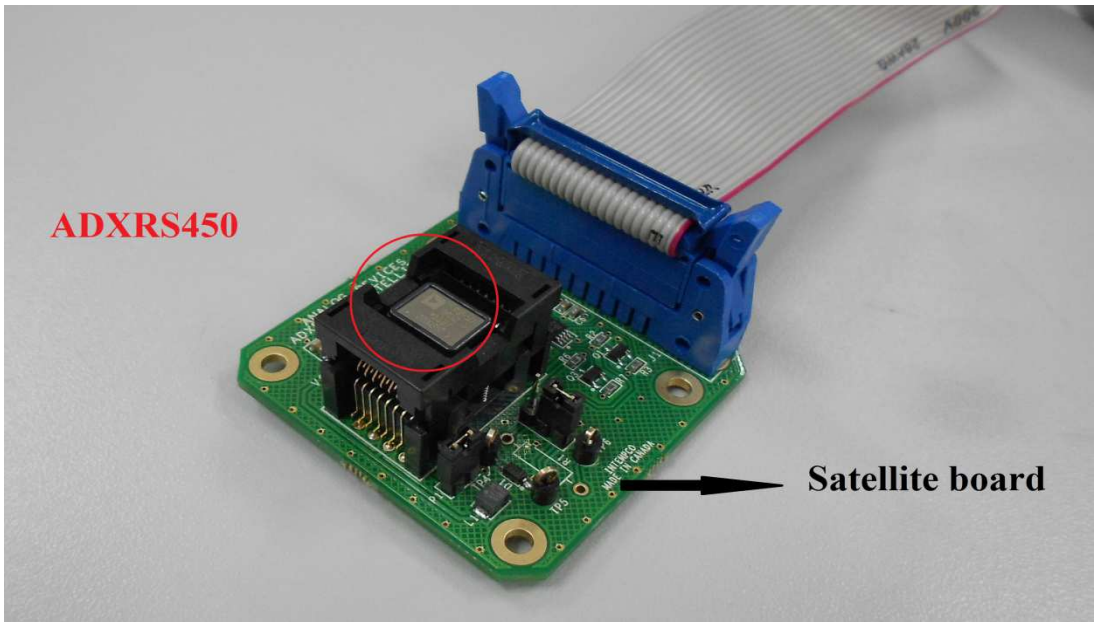

Figure 2.9: The satellite board is shown with ADXRS450 mounted on it. The analog to digital conversion circuitry is also visible in the figure.

Figure 2.10 shows the integrated evaluation system in which both the boards are connected via ribbon and a USB interface is shown for connecting to a computer. The evaluation system takes its power from the USB connector of a computer to which it is connected.

Also this system is equipped with evaluation interface software. The software deals with ADXRS450 only, and it is specialized software for this sensor. Appendix B shows a screen shot of this interface software which gives an idea about the functionality of data recording for this sensor.

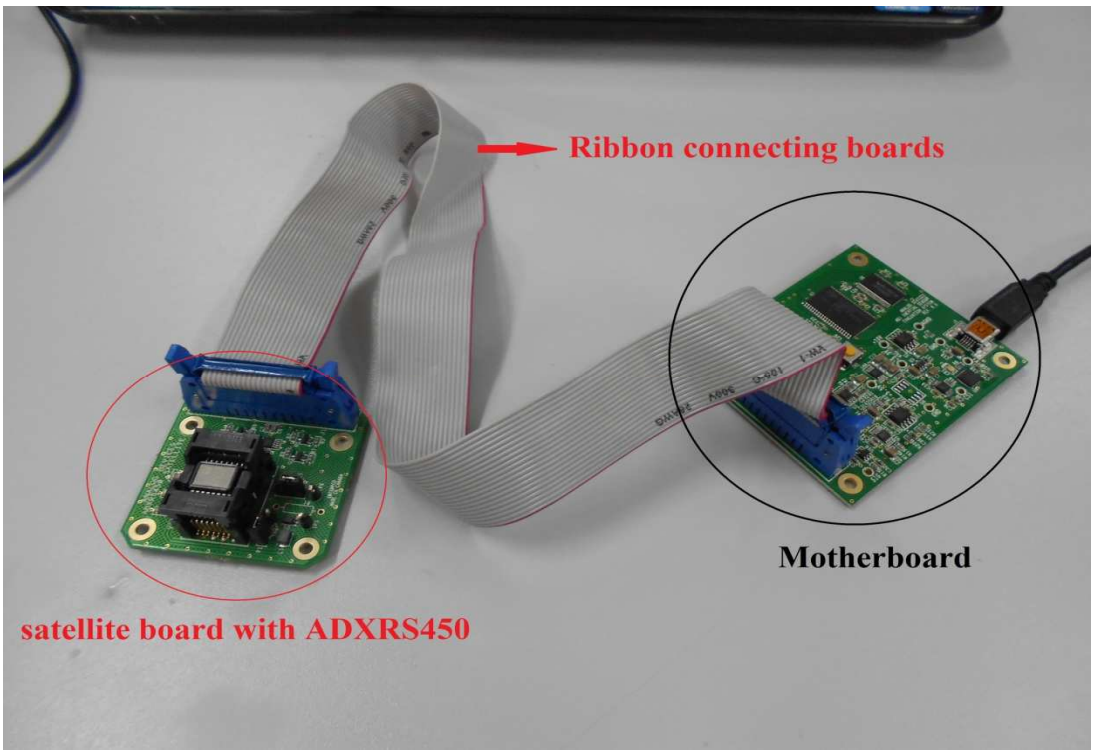

Figure 2.10: Integrated evaluation system with satellite and main motherboard. The boards are connected with a ribbon.

2.4.5. Collecting Data from XSENS MTi-10 (XSENS)

This is a complete IMU package and is manufactured by XSENS. This sensor is the most suitable sensor for this study because it provides raw and calibrated data. The raw data is affected by acceleration and temperature, and their effect can easily be observed. Figure 2.11 shows XSENS and the interface USB cable. The USB interface requires no evaluation board and the sensor is connected directly to a computer. The interface software is also provided with a setup which helps acquire data without any requirement of programming. The use of interface software is very user friendly. Appendix B provides a screen shot of the interface software while it is recording data from the sensor. The real times values of accelerometer and gyroscope can also be monitored during data recording.

Figure 2.11: The figure shows the XSENS sensor and its USB interface. No evaluation board is required for data acquisition from this sensor.

This sensor provides temperature of each gyroscope separately which is not the case in other sensors. The raw data provided by it makes it easy to perform compensation for temperature and acceleration dependent errors.

2.5. Compensation of Temperature

This section discusses the techniques that are used in this study for the compensation of temperature effects.

2.5.1. Moving Average Filter

This is an auxiliary technique, and is used in this study for the purpose of understanding and visualizing a relationship between a gyroscope output data and other parameters (temperature and acceleration). Moving average itself cannot be used for compensation of temperature driven error. It is a type of low pass filter that helps remove high frequency noise, and allows seeing the trends in a data. Figure 2.12 shows raw data collected from ADIS16488. It can be seen that no

relation can be established between ADIS16488 gyroscope data and temperature because of high frequency noise. This forbids seeing any trend in dependence of any gyroscope data on temperature. Figure 2.13 shows the data after moving average filtering is applied. A clear trend in the data can be observed that changes with temperature. Filtering makes it visually easy to see this trend.

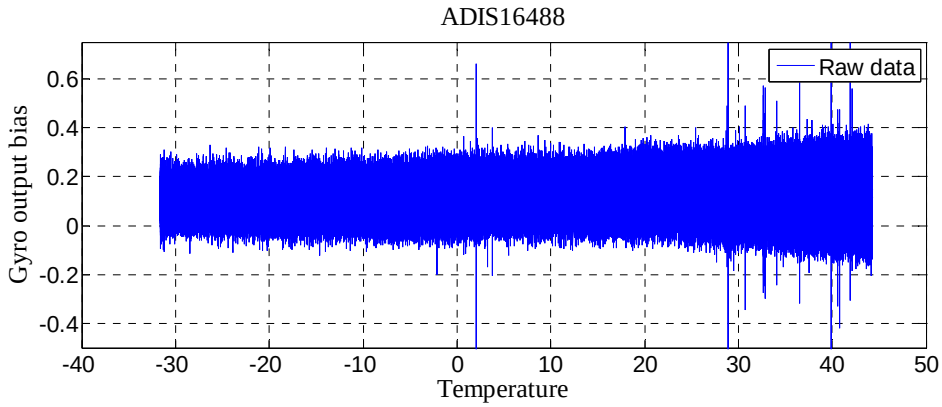

Figure 2.12: Raw data recorded from ADIS16488 IMU without any processing, and plotted against the temperature. No pattern can be seen in the data due to high frequency noise.

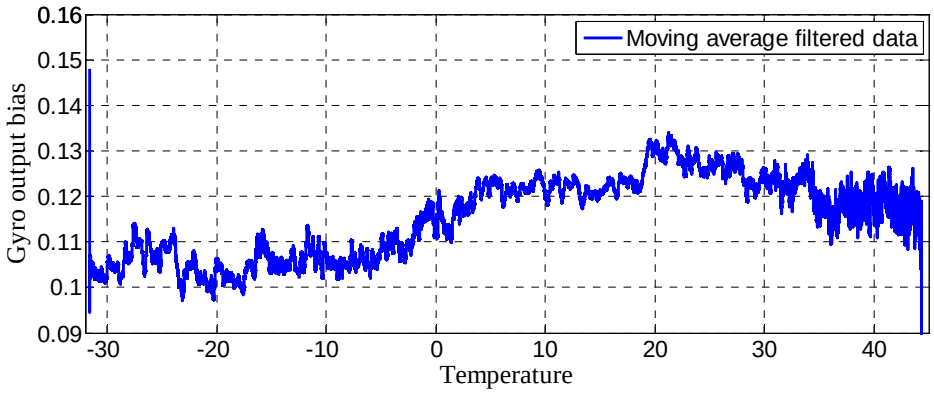

Figure 2.13: Data plot of gyroscope data after passed through a moving average filter. Using moving average filter the trend is visible as high frequency components are removed.

Moreover, data after filtering is different for different values of averaging sample. The moving average filter requires a sampling factor which it uses to average out the data. In this study the optimum sample size is calculated using Allan variance plot of the respective sensors. The minimum bias instability point shows the sample size which will give minimum error for averaging of a data, and is used in this study.

IEEE standard std-592-1997 defines the specification format and test procedures for single axis fiber optic gyroscopes. The standard provides details about theory and applications of Allan variance plots. Allan variance plot is a method of representing random drift noise as a function of averaging time. The plots show amount of noise as the averaging time is increased, and the integration time is determined at the point when the noise is at minimum value. The Allan variance plot gives information about different types of noise factors (quantization noise, flicker noise, rate random walk, correlated noise, sinusoidal noise, angle random noise etc), and bias instability value of a data. Bias instability values shows how stable the system is, and it gives the minimum error value that can be obtained from a data when averaged at that value. Figure 2.14 shows Allan variance plot of ADXRS450 gyroscope data.

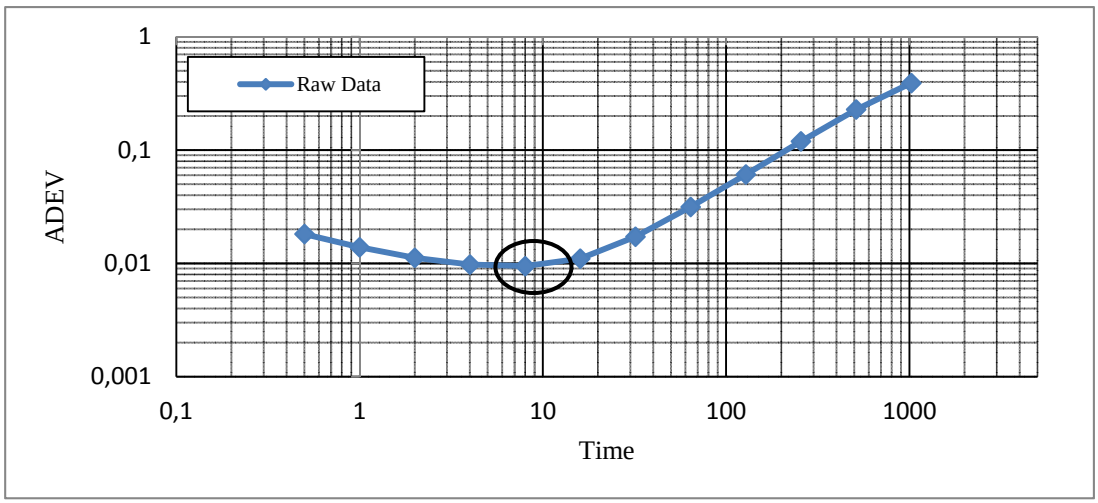

Figure 2.14: Integration time for minimum error is calculated at 8 seconds (encircled) which corresponds to nearly 16 samples. Therefore moving average filter sampling value is 16.

2.5.2. Polynomial Curve Fitting

This is the first compensation technique that is used in this study for compensation of temperature effects. This is the fastest and easiest method because a polynomial has to be used for data compensation, and no complex functions are involved. The technique is applied to zero rate null output data. At no rotation rate, the output rate of a gyroscope should be zero under ideal conditions, but the error sources causes a drift in the null offset. All the environmental parameters are kept constant and temperature is changed, making an assumption that all the non-zero rate output is due to change in temperature. This study also gives importance to the fact that only temperature dependence is modeled, and no other factors are modeled using this technique. This is accomplished by validating the equation on different data sets and getting similar results.

Also same data can be modeled with different degrees of equations. Higher is the degree of polynomial, higher is the accuracy of fitting a data. Figure 2.15 shows how data can be modeled with different order polynomials. 1^{st} order polynomial gives a very vague trend of temperature dependency. 2^{nd} order polynomial gives a better estimate of the data trend, and is more accurate than the first order equation. Increasing the order of polynomial increases the accuracy of the estimation, until 6^{th} order polynomial completely models the data.

Another factor about polynomial curve fitting is the bias offset at the startup. This bias appears as constant in a polynomial equation, and its value is slightly different for every time the sensor is turned on. Figure 2.16 shows two parts of a polynomial. The constant part points towards the initial bias at the startup.

The turn on bias is calculated after the sensor is turned on. The value of averaging time that is used for moving average filter (Section 2.5.1) is used here because it corresponds to minimum drift error, and it also gives sufficient amount of samples to check the trend of data.

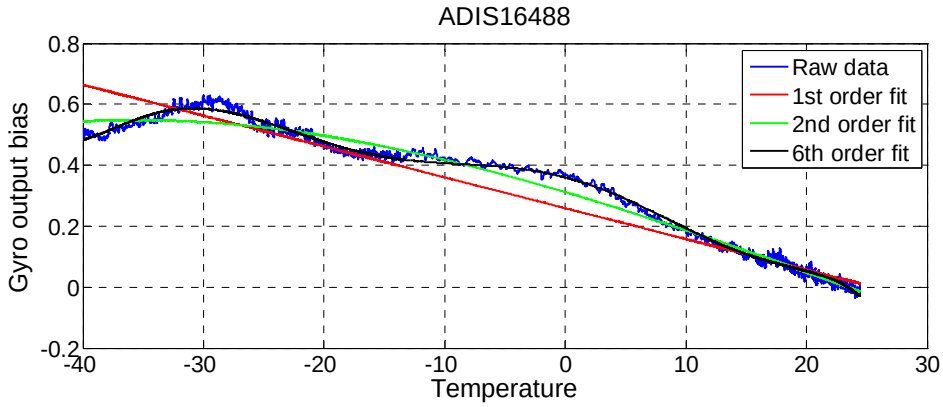

Figure 2.15: Higher the degree of polynomial, higher is the accuracy of the curve fit. The tradeoff between accuracy and speed can be decided by the designer.

$$Offset = -0.000150461 * t^2 - 0.010665 * t + 0.318636$$

Temperature dependent Turn ON bias

Figure 2.16: The turn ON bias is adjusted every time a sensor turns ON, but the relation between the temperature and gyroscope remains constant.

2.5.3. Back Propagation (BP) Neural Network (NN)

The second method that is used for compensation of temperature is Back Propagation Neural Network. This technique also develops a relation between the input (temperature) and output (gyroscope offset due to temperature). This methodology also works on the assumption that the changes in the output of gyroscope, in addition to the initial turn ON bias, are due to temperature change in a sensor. Therefore, the technique is applied on a data that is collected while a MEMS gyroscope is experiencing no rate, and any value other than zero is an error induced

output rate. Since only temperature is changing in these tests, so it is assumed that the drift in the data is due to temperature.

This is also an offline method of calibration. All the compensation is done in the lab environment, and a final updated network is achieved which is used in real time applications later. The complexity of the algorithm can be modified to match the processing capability of a system to implement in real time applications. Back propagation means that the algorithm improves itself based upon the actual output and predicted output from this algorithm. The weights and bias in the networks are updated until minimum possible error values are obtained. There are different algorithms that are used for training the data in back propagation, but the one used in this study is 'trainlm' which is abbreviation for Levenberg-Marquardt. According to Mathworks, 'trainlm' is the fastest algorithm used for back propagation.

In this study the network is created using MATLAB, and an updated network is achieved which can be used in the compensation of any other data set. The Neural Network used in this study has two layers and three neurons (weights assigned to each layer). The function assigned to first layer is Tan-Sigmoid, and the function assigned to the second layer is Pure Linear Function.

The Figure 2.17 shows the shape of a network used in this study. Number of inputs (1), number of outputs (1), number of neurons (3), 1^{st} layer transfer function (tan-sigmoid) and 2^{nd} layer transfer function (pure linear) are shown in the network shape. The number of layers and number of neuron can be adjusted depending upon the level of complexity required.

The NN method is a very specialized method due to levels of weights and bias in the equations, so very precise results are obtained. Errors that result from sources other than temperature are also taken care of, but this is not desired here because they are not repeated errors and not found in all the data sets in the same manner. Therefore before application of a neural network method, special care is taken in this study to get rid of any obvious error data that do not result from temperature change.

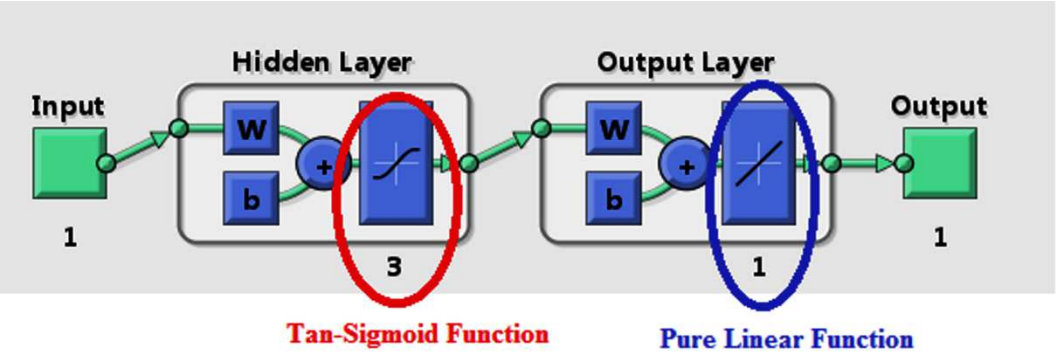

Figure 2.17: Figure shows the shape of a neural network used in this study with 1 Input, 1 hidden layer and 1 Output layer. There are 3 neurons and 1 output in this network.

2.6. Compensation of Hysteresis

This study also discusses the analysis about hysteresis present in a gyroscope output data caused by temperature cycles. Hysteresis is another factor that affects the output of a gyroscope sensor, and for more accuracy hysteresis has to be removed from a gyroscope's data. In this study polynomial curve fitting is used for compensation of hysteresis. Figure 2.18 shows hysteresis present in the data of XSENS sensor, when the temperature is changed between -25ºC and +90ºC degree. The two curves in the figure are first modeled by CF method and two polynomials are obtained. Then the difference between these two polynomials is taken to get a difference polynomial. This polynomial is then modified to make it a function of change in temperature. The hysteresis compensation process is explained by following example. Suppose the temperature is increasing and assumed as the standard response of the sensor. At point 'A' the temperature starts decreasing and there is change from the previous response of the sensor to same temperature values due to hysteresis. The difference in temperature, as the temperature decreases from point 'A', is used as input to the compensation equation. A hysteresis free response of the sensor is calculated using this equation.

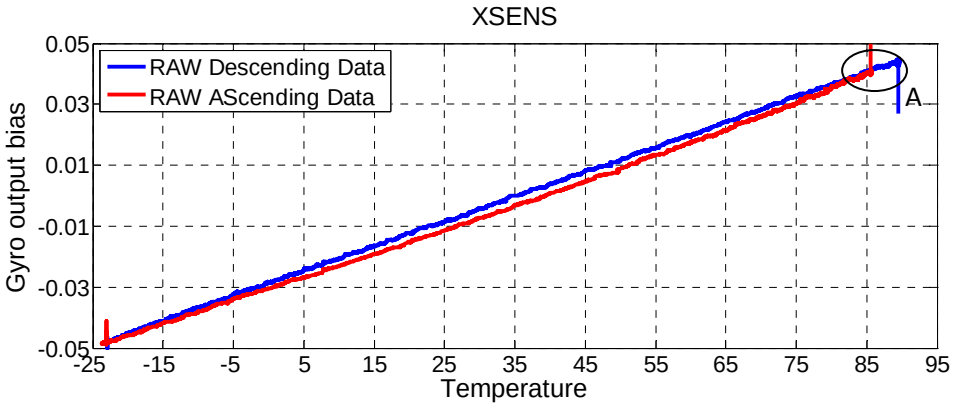

Figure 2.18: Hysteresis in the gyroscope output of XSENS is shown. Temperature cycle is completed between -25°C and +90°.

Figure 2.19 shows the hysteresis compensation equation plotted as function of temperature. It is a quadratic equation that shows that when the temperature starts changing the hysteresis error is at minimum value and it starts increasing with increase in the temperature change. Multiple tests are performed to check the consistency of this trend in different temperature ranges.

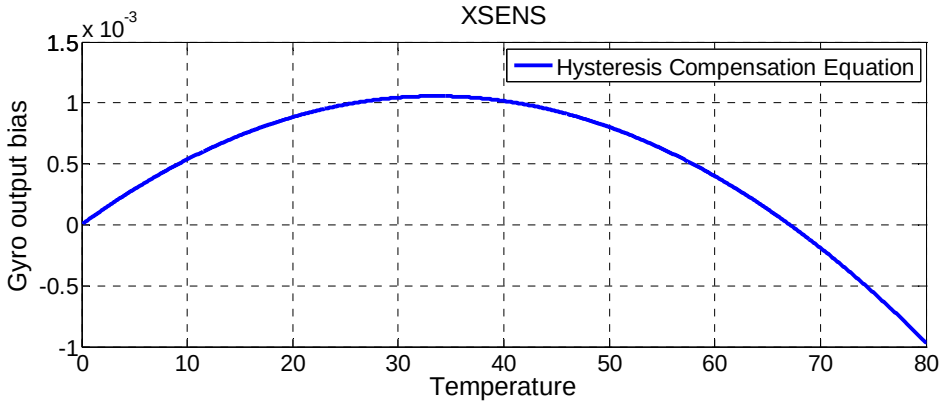

Figure 2.19: The polynomial for hysteresis is obtained which is function of change in the temperature. When the slope of temperature changes this equation is used for compensation of hysteresis.

2.7. Compensation of Acceleration

This section discusses methods for compensation of acceleration. Two methods namely curve fitting and neural networks are explained.

2.7.1. Least Squares Method (Simple Curve Fitting)

This method is very close to polynomial fitting and hence is called curve fitting alternatively in this study. A matrix is formed which includes all the parameters that define dependency of gyroscope on 3 accelerometers, thus a weight matrix is obtained. It is also called G-Sensitivity matrix in literature [23], and it contains all the bias factors associated with three accelerometers. The system that is used in this study for acceleration analysis is an IMU (ADIS16488 & XSENS), so all the values of acceleration are available at all the points.

This analysis is different from the literature [23] because Kalman filter is not used in this study as compared to the work done by [23], where Kalman filter is used for filtering of data and that filter is modified to incorporate the G-Sensitivity matrix. In this study the matrix weights are used to obtain a final offset, and the compensated data is further processed for any other type of errors (e.g. temperature). Equation 2.1 shows the general form of the matrix.

$$\begin{matrix} G_{x-off} \\ G_{y-off} \\ G_{z-off} \end{matrix} = \begin{matrix} G_{11} & G_{12} & G_{13} \\ G_{21} & G_{22} & G_{23} \\ G_{31} & G_{32} & G_{33} \end{matrix} * \begin{matrix} A_x \\ A_y \\ A_z \end{matrix} \tag{2.1}$$

This can be written in reduced form as:

$$G_{offset} = G_{weights} * A \tag{2.2}$$

The $\mathbf{G_{offset}}$ is known matrix because at stationary conditions the output of a gyroscope must point to a zero value, and any non-zero value indicates an offset in that data due to some factor. The **A** matrix is also a known factor because the instantaneous reading of accelerometer can be read from an interface software. The

$\mathbf{G_{weights}}$ is the variable matrix here which can be found out by changing positions of accelerometers, and refined by application of multiple data sets. Here **A** denotes acceleration and **G** denotes gyroscope, and the subscripts show the respective axis.

G_{11} = Weight corresponding effect of A_x on $G_{x\text{-offset}}$
G_{12} = Weight corresponding effect of A_y on $G_{x\text{-offset}}$
G_{13} = Weight corresponding effect of A_z on $G_{x\text{-offset}}$
G_{21} = Weight corresponding effect of A_x on $G_{y\text{-offset}}$
G_{22} = Weight corresponding effect of A_y on $G_{y\text{-offset}}$
G_{23} = Weight corresponding effect of A_z on $G_{y\text{-offset}}$
G_{31} = Weight corresponding effect of A_x on $G_{z\text{-offset}}$
G_{32} = Weight corresponding effect of A_y on $G_{z\text{-offset}}$
G_{33} = Weight corresponding effect of A_z on $G_{z\text{-offset}}$

The study is limited to work in static conditions; therefore the sensitivity matrix verifies all the possible outcomes of acceleration in any axis in stationary positions between +1 g and -1 g. Table 2.6 shows the range between +1g and -1g used for the analysis of acceleration effects on a MEMS gyroscope. These values of acceleration are attained by all the 3 accelerometers of the sensors.

Table 2.6: Acceleration values used in testing for acceleration tests

+1	+3/4	+1/2	+1/4	0	-1/4	-1/2	-3/4	-1

2.7.2. Back Propagation (BP) Neural Network (NN)

The methodology of neural networks has been discussed in Section 2.5.3. The NN is also applied for the compensation of acceleration because NN can take multiple inputs, thus making a very suitable candidate for defining a relation between a gyroscope output and multiple axes accelerations. Figure 2.20 gives the network shape that is used for acceleration compensation. The input in this case is data from two accelerometers (dominant axes used only), and the output is the gyroscope offset corresponding to these acceleration values.

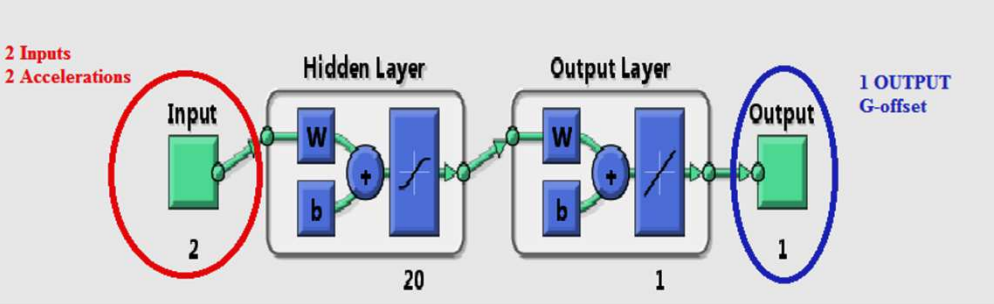

Figure 2.20: The NN has two acceleration inputs that affect the gyro output bias in the third axis gyroscope.

2.8. Integration of Compensation

This section discusses the integration of compensation for both acceleration and temperature effects. There are two different factors affecting a gyroscope output data, and each has its own method of compensation. These techniques can be integrated in different orders to achieve the compensation of both errors at the same time. The compensation of hysteresis in a data is done as a part of temperature compensation, so it is not mentioned separately. In the compensation of temperature by neural network, the hysteresis compensation is also done by curve fitting method.

2.8.1. Polynomial Curve Fitting (acceleration and temperature)

This combination gives the user a set of equations by which the data is filtered twice. The first set of equations remove the offset due to temperature, and the second set of equations remove the offset due to acceleration. Alternatively, the first set of equations remove the offset due to acceleration, and the second set of equations remove the offset due to temperature. The benefit of this method is that the equations are simple and product of different variables. The method is very good for fast processing, and where the computing power is a constraint. Figure 2.21 shows the integrated process in a flowchart.

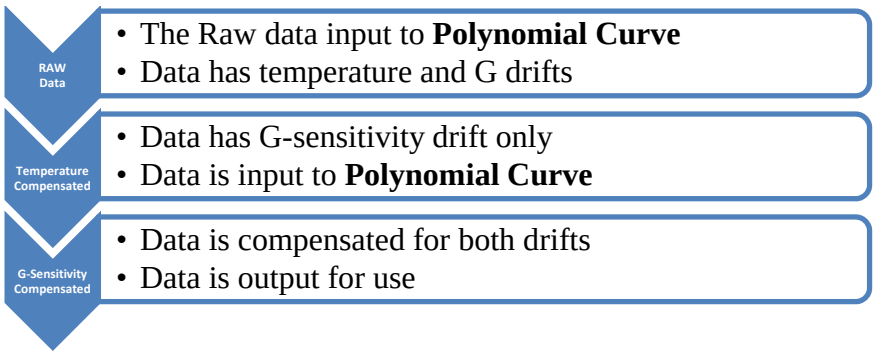

Figure 2.21: The data is first compensated for temperature induced error by CF method, and then compensated for acceleration induced error by CF method.

2.8.2. Neural Network (temperature) and CF (acceleration)

The second method is that the data is first compensated for temperature using the neural network and then curve fitting is used for compensation of the linear acceleration effects on a MEMS gyroscope output. Figure 2.22 shows compensation process in a flowchart form.

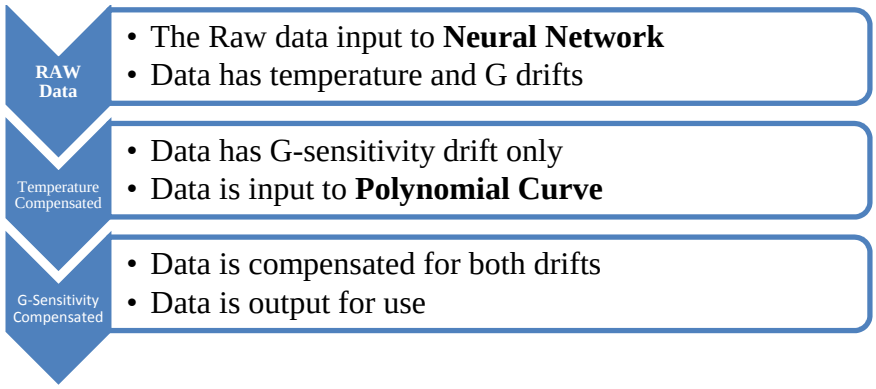

Figure 2.22: First temperature effects are compensated by use of Neural Network, and then curve fitting is used for acceleration induced error compensation

2.8.3. Neural Network (temperature and acceleration)

Third approach is the use of a neural network for both compensation of temperature and linear acceleration effects. The compensation is done separately, and the results are cascaded to obtained integrated compensation. Figure 2.23 shows compensation in the form of a sequential flowchart.

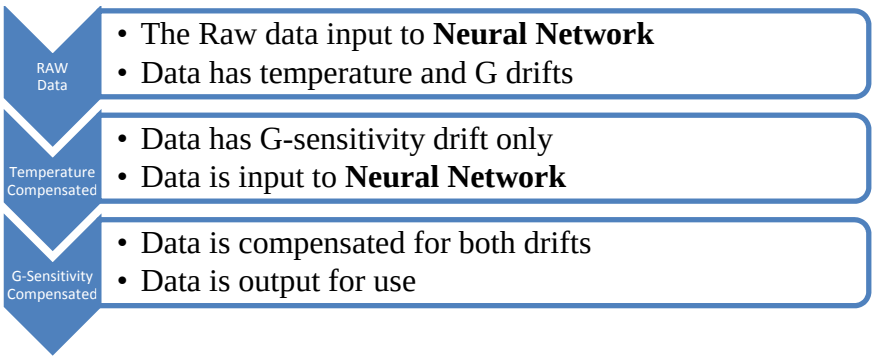

Figure 2.23: Figure shows another integration scheme in which neural networks are used for compensation of drifts caused by temperature and linear acceleration sequentially.

2.8.4. Single Neural Network

Neural networks can have more than one input. This feature is used for the integration of temperature and acceleration effects simultaneously, by treating acceleration and temperature as inputs to a neural network. The gyroscope output bias offset is output to a neural network. Figure 2.24 gives the shape of this network which takes 3 inputs and 1 output. This type of network results in developing a set of equations that have weights and bias, that compensates both the acceleration and temperature driven drifts present in a data. The benefit is that there will be only one network, and only a single technique is used for compensation of both the drifts.

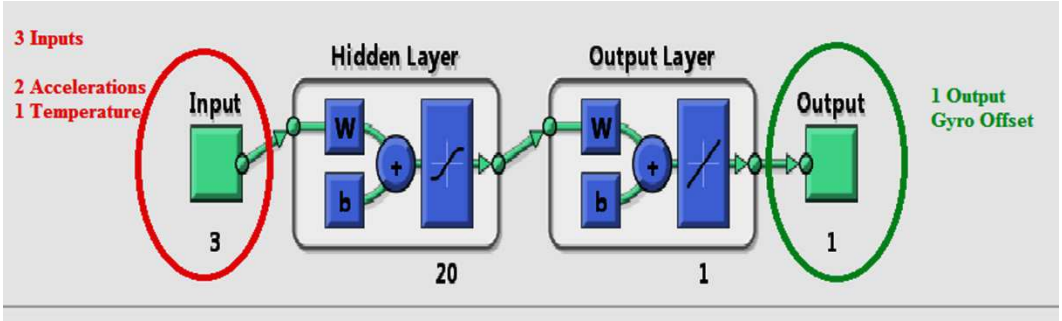

Figure 2.24: Neural Network with temperature and accelerations as inputs, and gyroscope output bias as output of this network. The network can compensate drift caused by both the temperature and acceleration.

2.9. Summary

This chapter presents details about collection of data. The setup used for collection of data for temperature tests and acceleration tests are explained in detail. The conditions under which these tests are conducted are explained. The data collection software and hardware is discussed, and some features and screenshots on the interface software are shown in this chapter. The last sections of this chapter focus on the compensation techniques employed in this study. Polynomial Curve Fitting and Neural Networks are the main techniques for temperature compensation. Their configuration in this study is explained with flowcharts. Sensitivity matrix (curve fitting) and Neural networks are main compensation techniques for acceleration effects, and there configuration is also discussed. The last section is about the integration of these techniques to obtain a final algorithm, which can compensate the effects of acceleration and temperature collectively.

CHAPTER 3

DATA AND RESULTS

This chapter is mainly focused on the results of this study. The methods and techniques have already been discussed in Chapters 1 and 2, and they are applied on the data acquired from various sensors. It is worth mentioning here that all the sensors used in this study are not suitable for all the tests performed in this study. Some features of these sensors prohibit them from testing them under certain conditions, and therefore some of the tests are not performed for every sensor. Example can be of ADXRS450 gyroscope which is an excellent sensor to study the effects of temperature but it has no accelerometers, so it is not suitable to study the effects of acceleration on its output data.

This chapter is divided into five main sections with each section dealing with a certain type of compensation (temperature, temperature with hysteresis, acceleration and hysteresis) and the last section provides a summary. Inside each section, individual sensor data is presented and compensation is performed. The compensation performed by both the techniques is discussed so that a comparative analysis can be achieved.

It is neither feasible nor necessary to present all the results in this thesis. Repetitive measurements are taken from each sensor, but only final results are presented in this report. The aim of repetitive measurements is to increase the consistency of the tests, and eliminate any conflicting results. Also results from two sensors ACC1 and ADIS16136 are not included in this report. ACC1 is an accelerometer, and the results obtained from it are not comparable to other gyroscope sensors used in this study. ADIS13136 has similar features as that of ADIS16488, and the results for temperature compensation are almost repetitive.

3.1. Temperature Compensation

Temperature is the first factor that is compensated in this study. Temperature has different effects on different types of sensors. Since all the sensors used in this study are digital in nature, there is a possibility that temperature compensation has already been performed. ADXRS450 and XSENS are specially selected for this purpose, as they provide gyroscope data without internal temperature compensation performed on them. ADIS16488 IMU is also used for temperature compensation but it is very resilient to temperature changes.

3.1.1. ADIS16488

ADIS16488 is an IMU provided by Analog Devices. The gyroscope data is very resilient to changes in temperature, but the casing of the IMU causes problem for data gathering, and the sensor is also very prone to vibration in its surroundings. The data is collected such that the sensor is cooled down to -30°C and then the temperature chamber is turned OFF. After that data from ADIS16488 is recorded up to 50°C temperature. This data is used for analysis of effects of temperature on ADIS16488 gyroscope output data. Figure 3.1 shows the relationship between temperature change and the gyroscope output of ADIS16488.

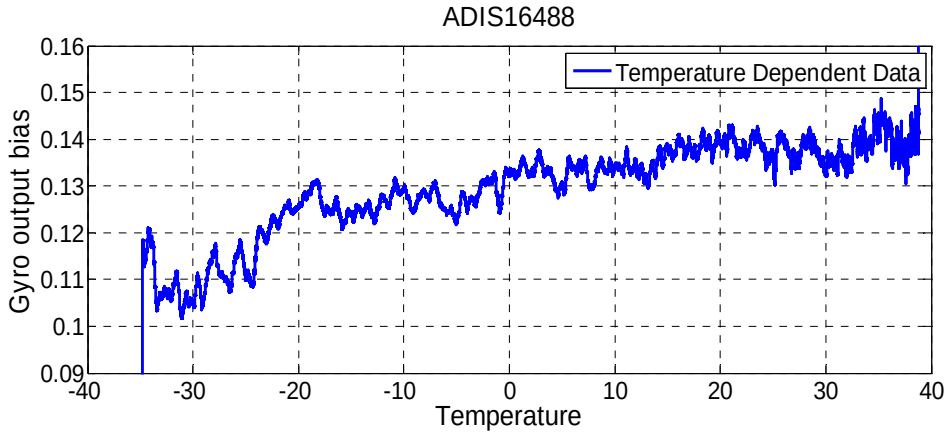

Figure 3.1: Relationship between temperature and gyroscope output bias of ADIS16488. The sensor is very resistant to temperature changes but small temperature dependency can be seen. Bias offset is 0.04°/sec for -30 to +40°C.

The general relation between the gyroscope and temperature shows that the gyroscope data does not change much as the temperature is changing, but still small relation can be found between the gyroscope data and temperature. The offset present in the output bias is approximately 0.04°/sec. The data should be very consistent in order for the techniques to work properly for compensation. Therefore, a number of samples are taken from the sensor and plotted against temperature, to make sure that the gyroscope shows a consistent behavior in this temperature range. Figure 3.2 shows multiples samples taken from ADIS16488 in the same temperature range to see the consistency in the trend of data.

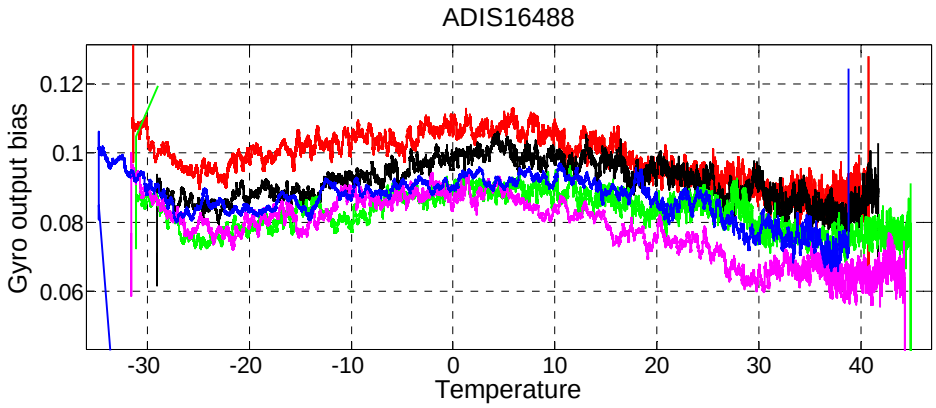

Figure 3.2: Number of data sets show consistency in the trend of data acquired from ADIS16488 in the given temperature range. The relationship between gyroscope output bias and temperature is consistent.

3.1.1.1. Compensation By Curve Fitting

This section shows temperature compensation of ADIS16488 gyroscope output data by using the CF method. Figure 3.3 shows that data can be modeled with different equations, having different degrees. Higher order equations increase the complexity of the processing, therefore lower order polynomial is preferred.

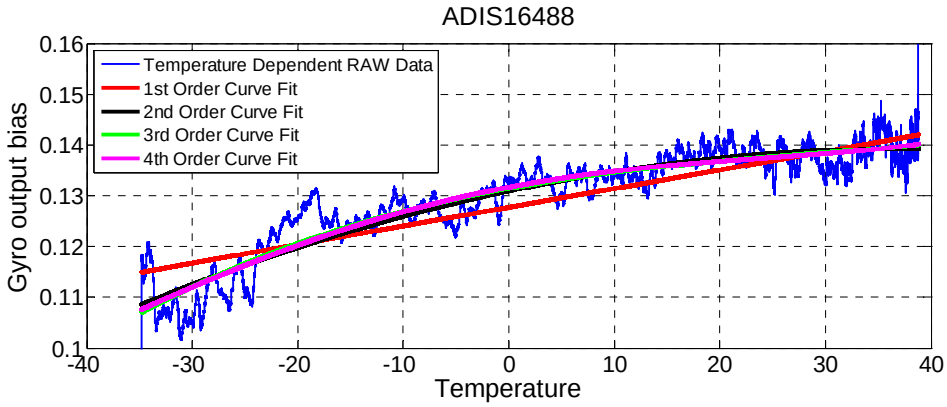

Figure 3.3: The relation between temperature and the gyroscope output bias can be modeled with equations of different degree. 2nd Degree and higher model the data with same accuracy and 1st order does not model very effectively.

The plot shows that using a polynomial of order higher than 2 only increases the complexity and achieve no additional information about the relation between gyroscope output bias and temperature. Hence 2nd order polynomial is selected for compensation of temperature effects.

Out of many acquired data sets, one set is used for compensation of temperature effects by CF method and then by NN method. Figure 3.4 shows raw data and the results of temperature compensation by the CF method. The offset in the output bias reduces from 0.04°/sec to 0.02°/sec which is 2 times improvement. There are still some irregularities in the compensated data, but that do not result from temperature.

The ADIS16488 is very resilient to temperature change and the effect of compensation is not very evident from this figure. To improve the visual effect, the raw and compensated data is modeled using polynomials, and they are displayed with the data. Figure 3.5 shows curve fits of the raw and compensated data.

The temperature dependency reduction in the compensated data is evident from the curve fits, rather than the data itself. The curve fit for the compensated data is very flat as compared to curve fit for the raw data.

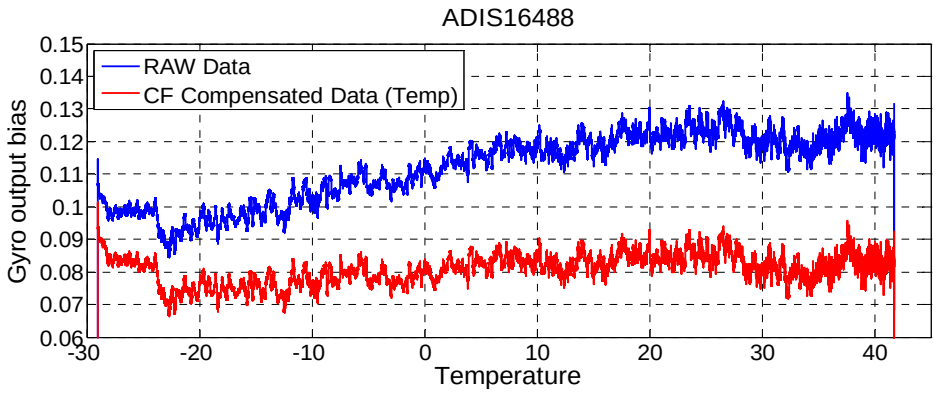

Figure 3.4: Gyroscope bias offset reduces from 0.04°/sec to 0.02°/sec after temperature compensation by CF method, which is 2 times reduction in temperature dependency.

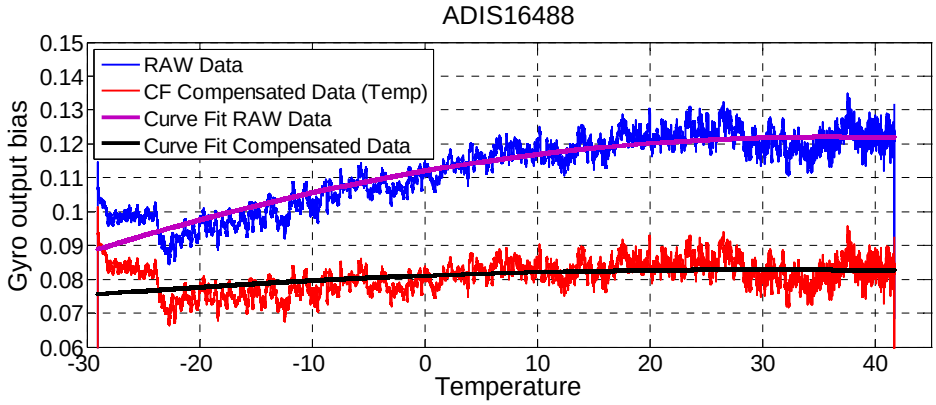

Figure 3.5: Raw and compensated data with curve fits is shown. The curve fits makes it visually understandable that the temperature dependency reduces significantly for ADIS16488, after temperature compensation by CF method

3.1.1.2. Compensation By Neural Networks

The next method is compensation by Neural Networks. The same data set is used for compensation by NN method, which is used in the CF method. The compensation is performed on this data using neural networks. Figure 3.6 shows the raw data and temperature compensated data by NN method.

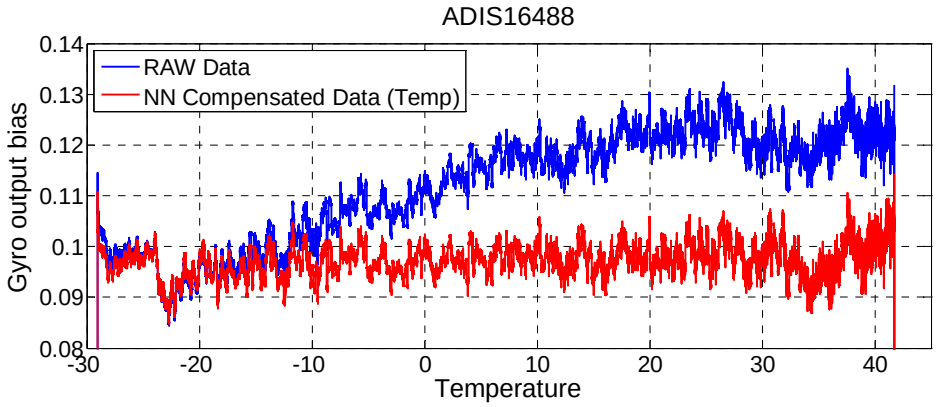

Figure 3.6: Raw and temperature compensated data of ADIS16488 using NN method. Temperature dependency has been reduced significantly. Gyroscope bias offset reduces from 0.04°/sec to 0.02°/sec (2 times improvement).

Figure 3.7 shows curve fits for the raw and compensated data, to visually observe that temperature dependency has been reduced after compensation. The curve fits clearly show reduction in the dependency on the applied temperature after compensation.

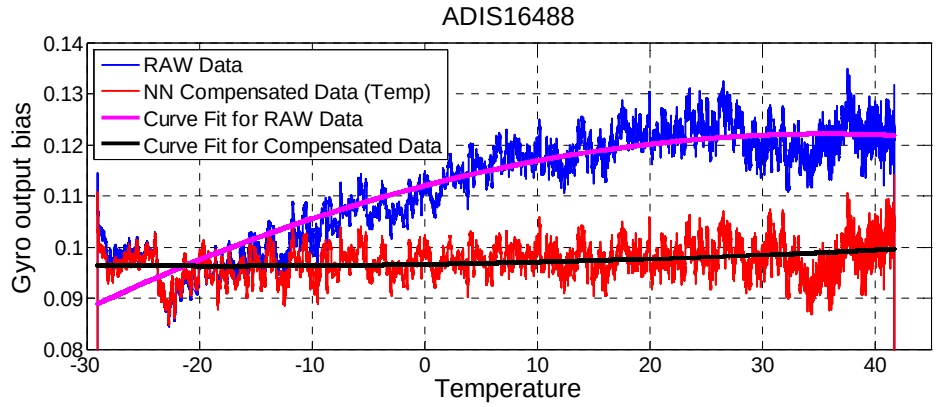

Figure 3.7: The curve fits of raw and temperature compensated data using NN method are shown. The curve fits give a visual understanding how the temperature dependency has been reduced. Gyroscope bias offset reduces from 0.04°/sec to 0.02°/sec (2 times improvement).

The Allan variance plots also provide information about reduction in the dependency of the gyroscope data on temperature. The Allan variance plots of raw and compensated data are presented to see the effectiveness of temperature compensation from another perspective. Figure 3.8 shows the Allan variance plot of raw and temperature compensated data for ADIS16488.

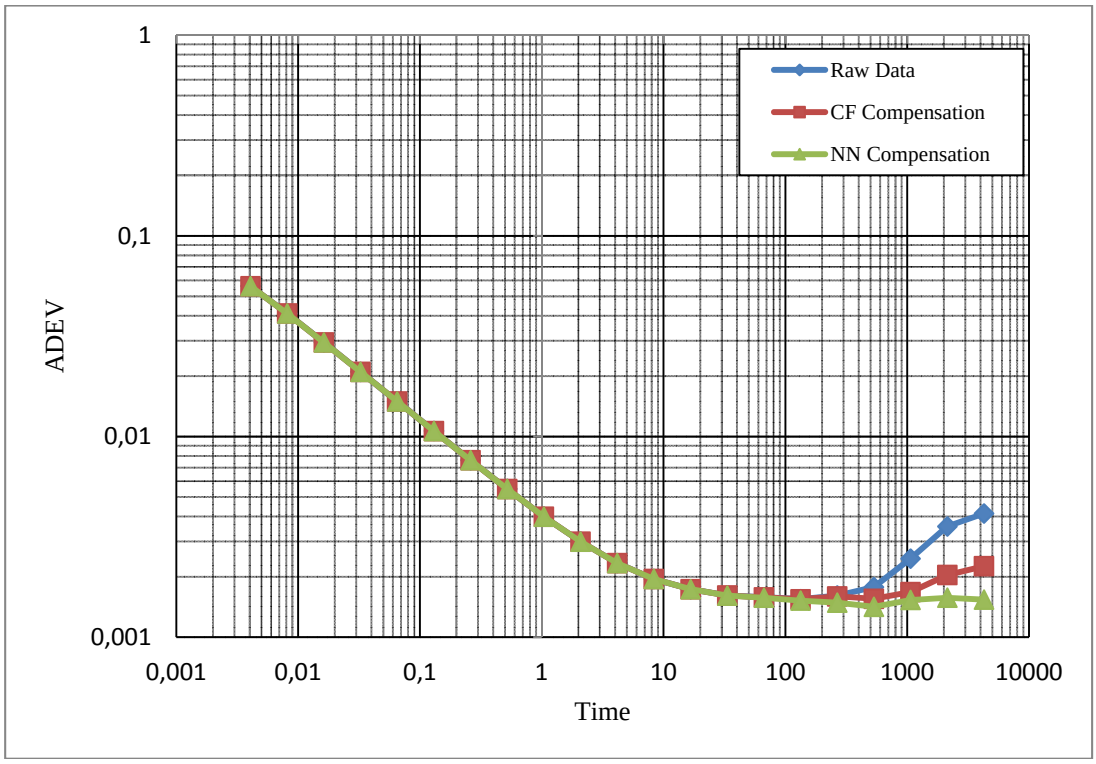

Figure 3.8: Allan variance plot of ADIS16488 shows that after compensation integration time increases 4 times (from 133 to 532 seconds). Bias instability does not change as 1/f noise level is reached.

The Allan variance plot shows that there is no significant improvement in the bias instability after temperature compensation. Both CF and NN produce 4 times improvement in the integration time (from 133 to 532 seconds). The rate random walk is also reduced which is visible from reduction in the slope on right side.

3.1.2. ADXRS450

This is the second sensor that is used for compensation of temperature effects. This sensor is ideal for this study because it operates in the temperature range of -30°C to +85°C, and data can be recorded in ascending or descending trend as per requirement. The sensor shows a very linear relationship with temperature. The sensor is a single axis gyroscope, so only one axis is tested. Figure 3.9 shows the general behavior of this sensor when subjected to temperature change.

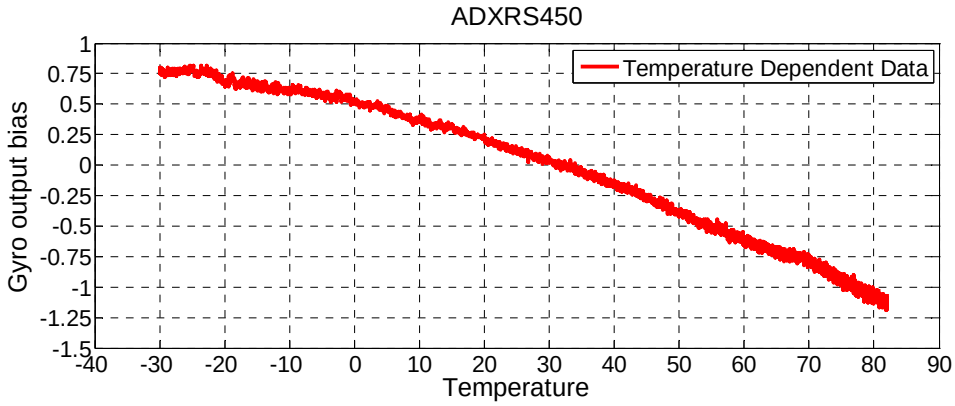

Figure 3.9: The dependency of ADXRS450 gyroscope on temperature can be seen in the temperature range of -30°C to +80°C. The drift in the output bias is around 2°/sec in this temperature range.

This plot shows very clear temperature dependency of ADXRS450 output data. The output rate shows a linear relation with temperature. This data trend must show consistency in order to obtain compensation equations by any of the methods. Data is collected multiple times, and results show consistency in dependency on the temperature. Figure 3.10 shows some of the collected samples of data in one plot to visualize the consistency of data. The data is also collected in different temperature ranges to confirm that they follow the same data pattern. In the plots of Figure 3.10 small hysteresis can be seen, but they are ignored for this analysis. In this section only compensation of temperature is discussed.

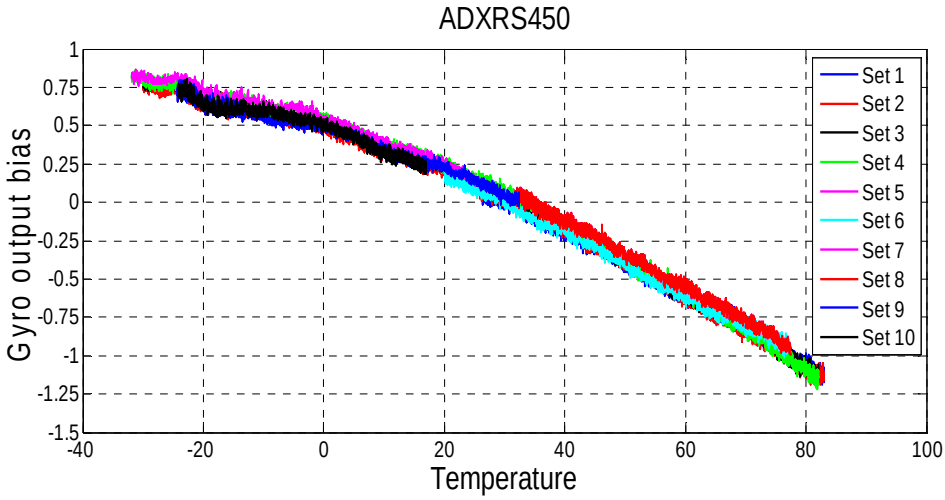

Figure 3.10: Multiple data sets collected from the ADXRS450 sensor are plotted to show the consistency of output rate dependency on temperature. The plot shows that all the samples show similar trend.

3.1.2.1. Compensation By Curve Fitting

Polynomial curve fitting is used first to compensate the drift present in the data, which results from temperature changes. Figure 3.11 shows how the data can be modeled using different order polynomials. It can be seen that 2nd order and 3rd order polynomial fit this data equally good. 2nd order polynomial is the best choice.

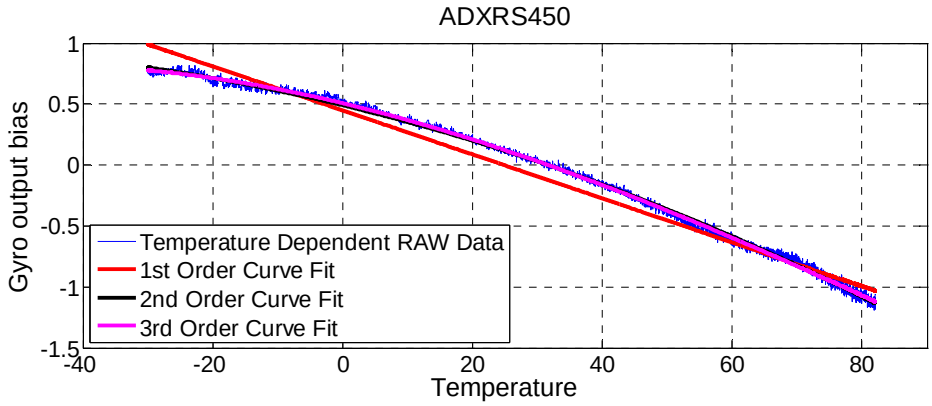

Figure 3.11: The ADXRS450 gyro output bias dependency on temperature can be modeled with equations of different degrees. 2nd and 3rd Degree polynomial fits the data very accurately.

Figure 3.12 shows one of the data sets which is used for compensation. This data set is different from the one that is used to obtain the polynomial for temperature compensation. Figure 3.13 shows the temperature compensated data using CF method. The offset in the output data reduces from 2°/sec to less than 0.1°/sec, which is 20 times reduction in temperature dependency.

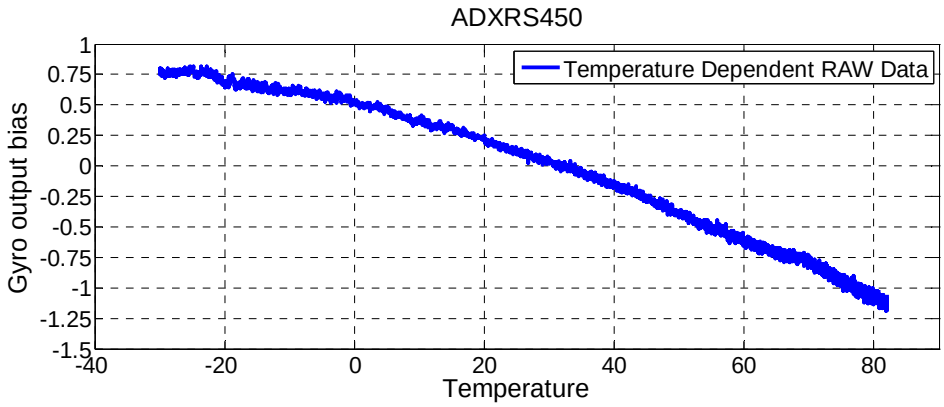

Figure 3.12: Raw data used for compensation of temperature using CF method. The offset in output bias is 2°/sec in the temperature range of -25°C to +85°C.

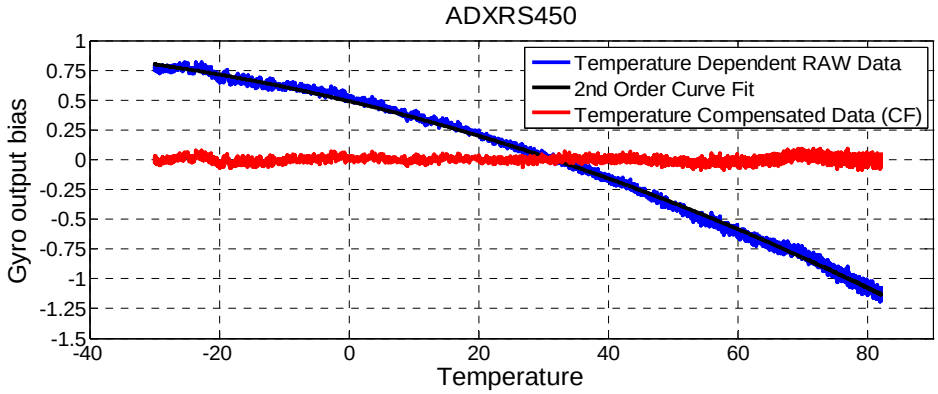

Figure 3.13: Raw and temperature compensated data for ADXRS450 using CF method. The gyroscope bias offset has reduced from 2°/sec to less than 0.1°/sec (20 times improvement).

3.1.2.2. Compensation By Neural Networks

The same data set is used for compensation by NN method. Multiple sets are used to train the network, and obtain a network suitable for compensation of temperature effects in the data. Figure 3.14 shows results after compensation by NN method. The gyroscope bias offset is reduced from 2°/sec to less than 0.1°/sec, after temperature compensation by NN method.

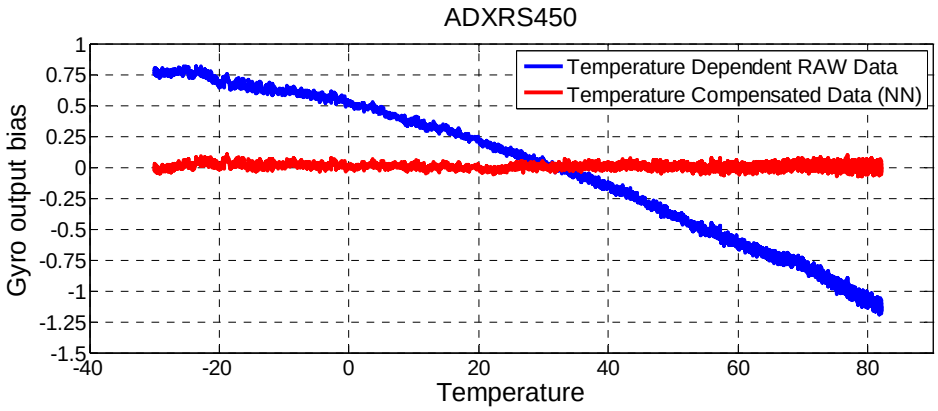

Figure 3.14: Raw and temperature compensated data of ADXRS450 using NN method. The gyroscope bias offset reduces from 2°/sec to less than 0.1°/sec which corresponds to almost 20 times improvement in the data.

Figure 3.15 shows the comparison of both the techniques for compensation of temperature effects. The comparison of the compensation data by both techniques shows that the compensation produces similar results when compensated by either of the methods.

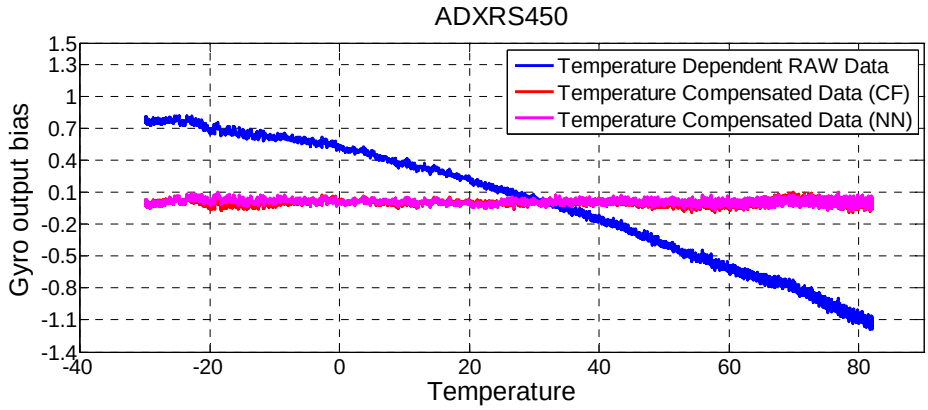

Figure 3.15: Temperature compensation by NN and CF method. Both techniques show 20 times improvement in the bias offset (from 2°/sec to 0.1°/sec) and significant reduction in rate random walk.

The improvement after compensation can be seen using the Allan variance plots of the raw and temperature compensated data. Figure 3.16 gives Allan variance plot of raw and temperature compensated data for ADXRS450.

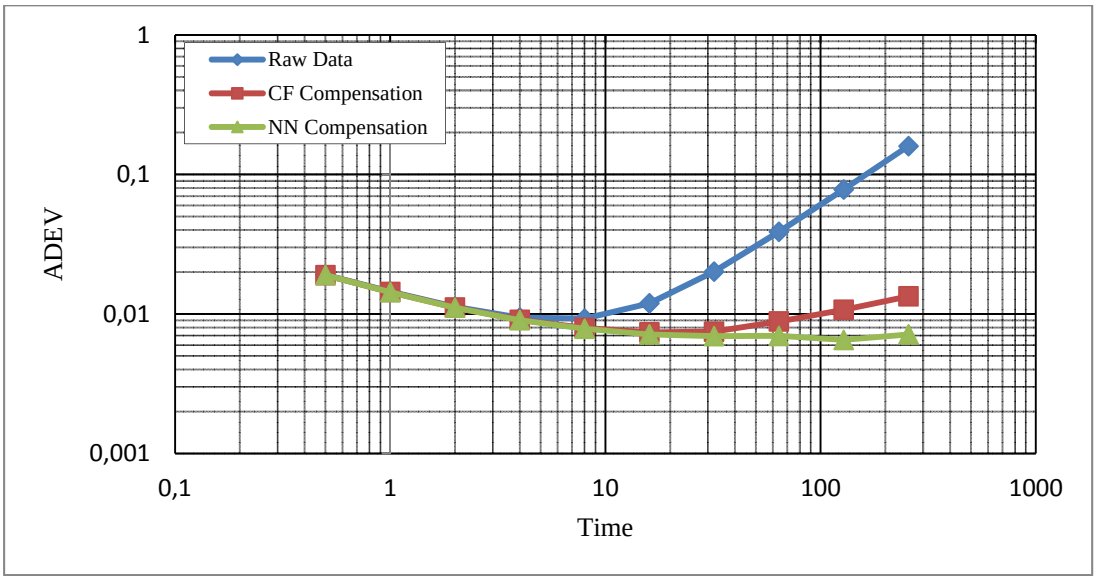

Figure 3.16: The Allan variance plot shows that after temperature compensation, the bias instability reduces from 33.5°/hr to 26.5°/hr (CF) and 24.8°/hr (NN). The integration time improves 2 times by CF (16 sec) and 4 times by NN (32 sec) method.

The Allan variance plot shows that temperature compensation improves the bias instability. Temperature compensation achieves 20% (from 33.5 to 26.5°/hr) improvement by CF method and 25% (from 33.5 to 24.8°/hr) improvement by NN method. The integration time increases 2 times (from 8 to 16 seconds) by CF compensation and 4 times (from 8 to 32 seconds) by NN compensation for temperature. The rate random walk decreases significantly, which is shown by the slope on right side the plot.

3.1.3. XSENS MTi-10

The XSENS MTi-10 (XSENS) is very suitable for this study, because this sensor provides both compensated data as well as raw data. The three gyroscopes in the sensor have similar trends, and therefore results from only z-axis gyroscope are presented in this report. Figure 3.17 gives the general trend of the data from XSENS, when it experiences temperature change. The gyroscope bias offset is about 0.1°/sec in the temperature range from -25°C to +90°C.

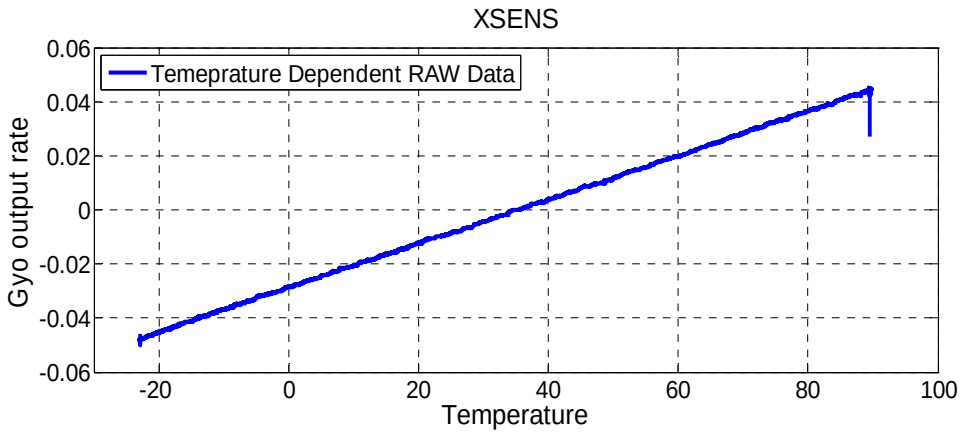

Figure 3.17: The gyroscope output bias is linearly dependent on the temperature. 0.1°/sec offset is present in the data, when temperature changes from -25°C to +90°C.

Consistency in this sensor is also tested using various samples. Figure 3.18 shows four samples of data taken from XSENS, that exhibit similar trend. Only four

samples are shown in the figure because these samples overlay each other and are not visible if more samples are added to the plot.

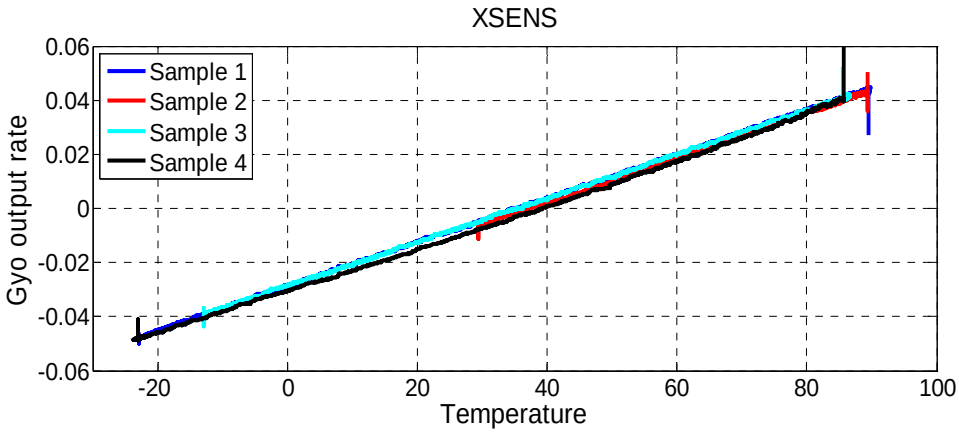

Figure 3.18: Multiple samples taken from XSENS gyroscope are shown in the temperature range of -25°C and +90°C. The consistency of the data can be seen from the fact that all samples overlay each other closely.

3.1.3.1. Compensation By Curve Fitting

The data is first compensated using CF method. The first step is to find a suitable degree of equation for compensation of the data. Figure 3.19 gives different curve fits with varying degree to fit the raw data. All three polynomials of 1st, 2nd and 3rd order overlay each other on the data, and it can be concluded that the 1st order equation is enough to model the trend of data efficiently. The fact that these different polynomials cannot be distinguished from each other; it is enough to understand that using higher order equation just increases complexity and no extra accuracy is achieved.

Figure 3.20 shows the temperature compensated data by using CF method. The temperature dependency has been reduced significantly. The gyroscope bias offset is reduced from 0.08°/sec to 0.0015°/sec which is almost 50 times improvement.

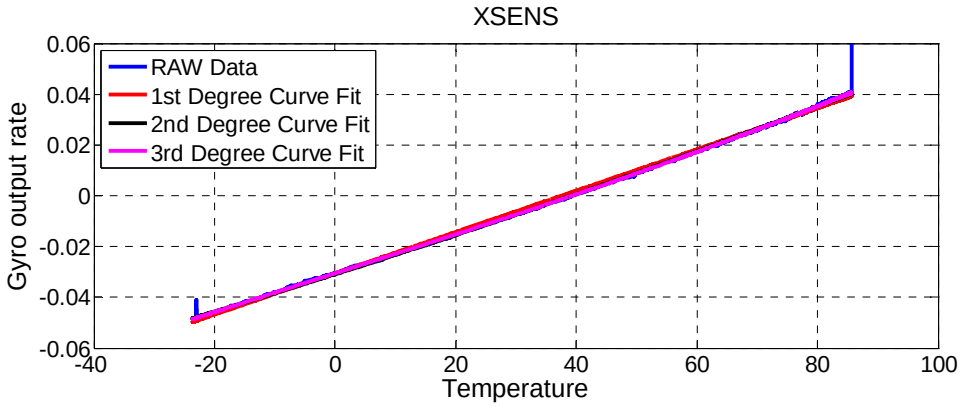

Figure 3.19: The relation between data and temperature can be modeled with polynomials of different degrees. From the plot it is concluded that 1st degree of equation is sufficient for compensation.

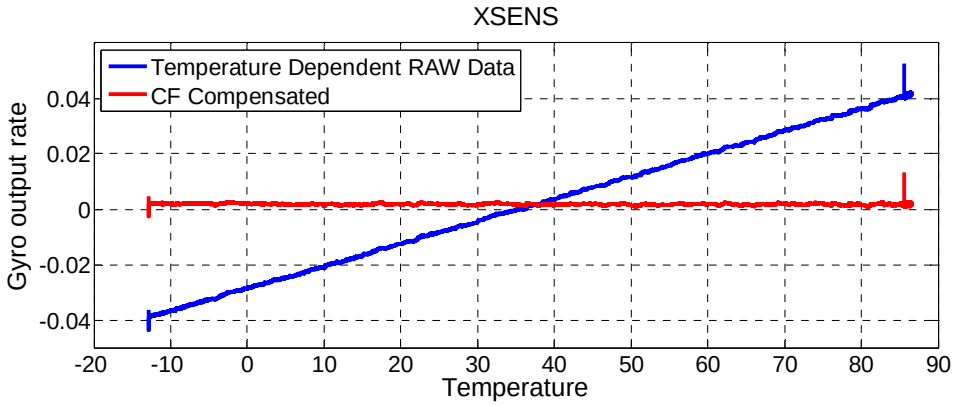

Figure 3.20: Raw and temperature compensated data of XSENS using CF method. Gyroscope bias offset reduces from 0.08°/sec to 0.0015°/sec in the temperature range of -15°C to +90°C, which is 50 times improvement.

3.1.3.2. Compensation By Neural Networks

The next method for compensation of temperature dependent data is NN method. The data set used for compensation by CF method is used here for comparison purpose. Figure 3.21 shows the raw and temperature compensated data using NN method. The gyroscope bias offset is reduced from 0.08°/sec to 0.0015°/sec, which corresponds to 50 times improvement in output offset reduction.

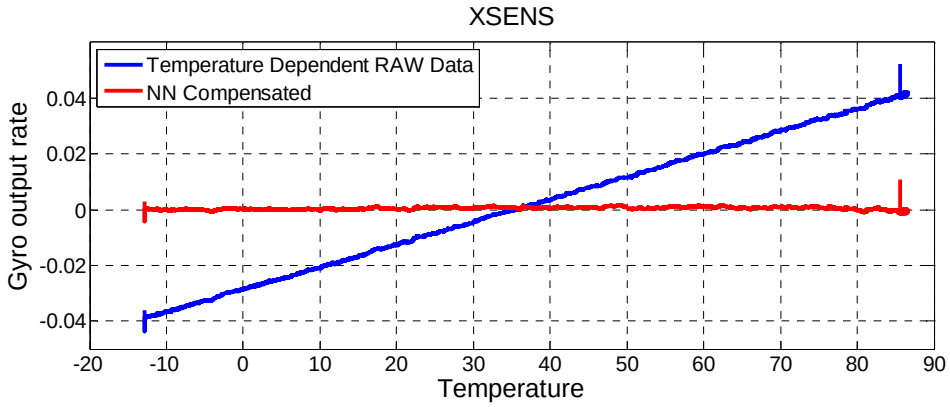

Figure 3.21: Raw and the temperature compensated data of XSENS using NN method. The gyroscope bias offset reduces from .08°/sec to 0.0015°/sec after compensation by NN method, which is 50 times improvement.

Figure 3.22 shows Allan variance plot of raw and temperature compensated data for XSENSE sensor. The bias instability for raw data is 12.24°/hr and the integration time is 5.12 seconds.

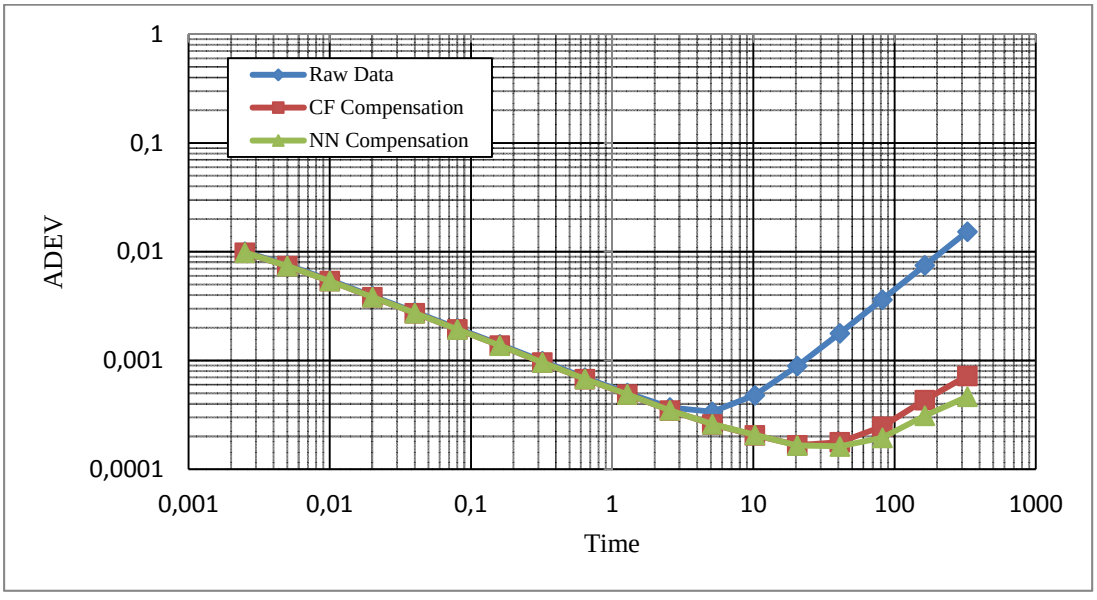

Figure 3.22: The Allan variance plot of XSENS shows that bias instability is reduced from 12.24°/hr to 6.12°/hr (CF) and 5.76°/hr (NN). The integration time is increased from 5.12 seconds to 20.48 (CF) and 40.96 (NN) seconds.

52% (from 12.24°/hr to 5.76°/hr) improvement in the bias instability is seen when compensation is performed by NN method, as compared to CF method which gives 50% (from 12.24°/hr to 6.12°/hr) improvement after compensation. Figure 3.23 gives the comparison of data after compensation by both techniques. Raw data and compensated data are provided by CF and NN methods. Also factory calibrated data is presented for comparison. The improvement in the data is almost 50 times for all methods.

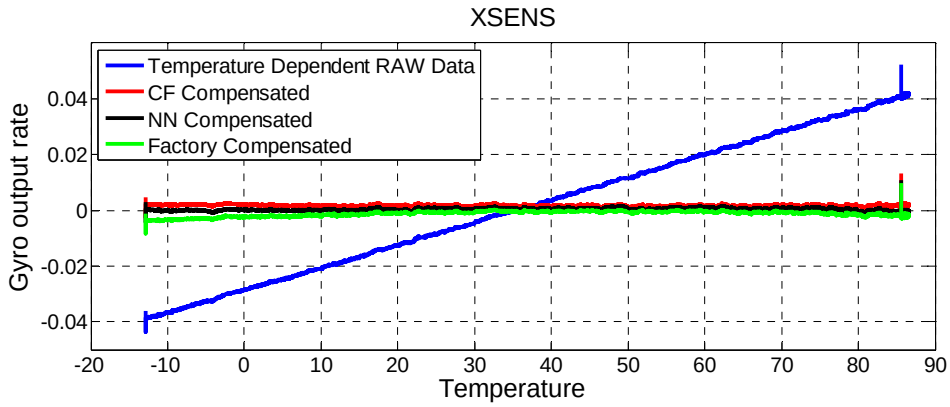

Figure 3.23: Raw data and temperature compensated data by CF, NN and calibration by factory settings. The temperature compensation improves the data by 40-50 times for all the methods.

3.2. Temperature and Hysteresis Compensation

This section explains results for compensation of temperature with hysteresis compensation as well. The sensors used in this analysis are ADXRS450 gyroscope and XSENS IMU. The ADIS16488 is also used but the sensor is very much sensitive to vibrations imparted by temperature chamber, and suitable samples cannot be acquired which is shown in the section of ADIS16488 analysis.

3.2.1. ADXRS450

The first sensor that is used in the analysis of hysteresis is ADXRS450. The sensor has no internal temperature compensation, and thus shows dependency on

temperature. When the temperature is changed between the operating ranges, it is observed that the hysteresis occurs only in a certain range of temperature and only in one direction (descending temperature). Figure 3.24 shows the hysteresis present in the output data of this sensor.

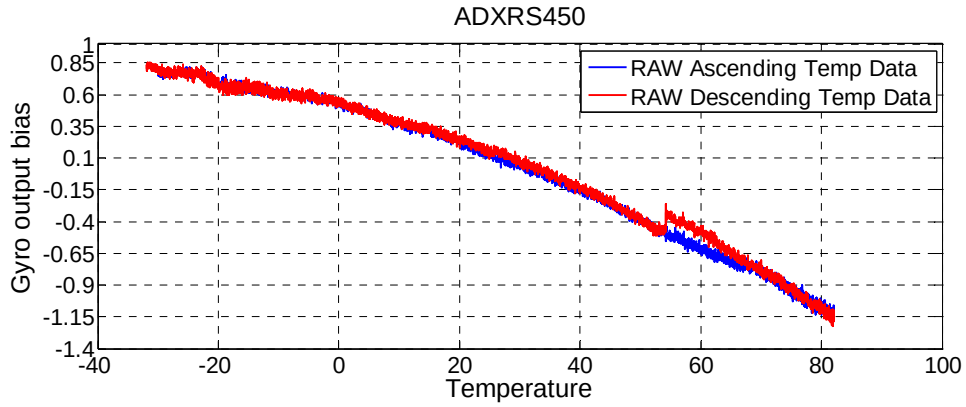

Figure 3.24: Hysteresis is shown in ADXRS450 sensor data. The hysteresis is present in only a certain range of temperature. Hysteresis results in additional 0.2/sec offset in the output bias.

Figure 3.25 gives a closer look of this phenomenon. It can be seen that as the temperature is decreasing from +80°C, the output bias starts drifting until around +55°C temperature and after that it follows the same path as for ascending temperature.

The compensation requires this hysteresis to be consistent in some form. Therefore number of cycles are acquired and plotted to see if it shows a consistent behavior in the given range of temperature. Figure 3.26 shows multiple samples of ADXRS450 cycles, and it can be seen that these samples show consistent behavior and only descending temperature in range between +55°C and +80°C cause drift in the data, that results in hysteresis.

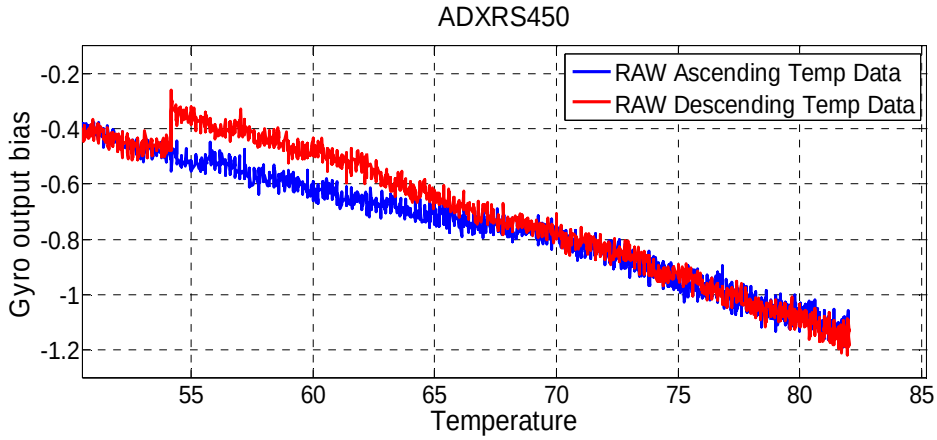

Figure 3.25: Closer look at the hysteresis present in ADXRS450 sensor is shown. The deviant path of relation is present only in a certain temperature range (+55^{0}C and +80^{0}C).

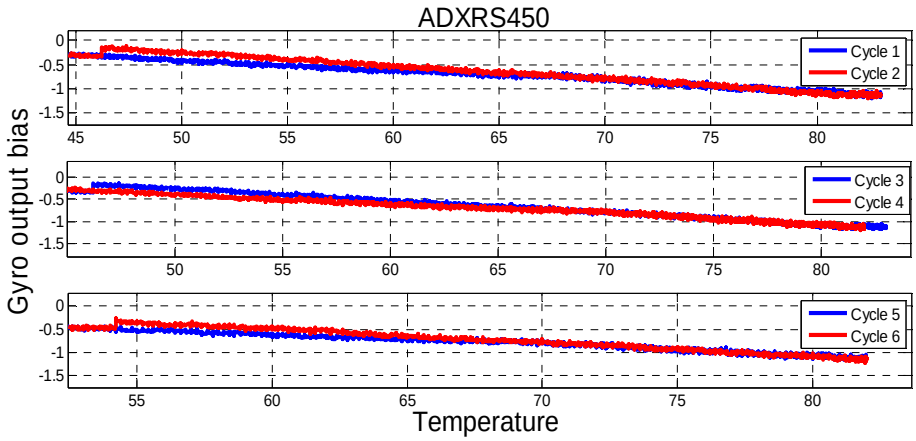

Figure 3.26: Multiple samples of data are taken from ADXRS450 and plotted in this figure. All the samples show hysteresis in the temperature range of +55°C and +80°C and this trend is consistent.

From multiple samples it is established that this phenomenon only exists in 85°C and 54°C temperature range. All the samples taken in any other temperature range do not any form of hysteresis in the data.

Hysteresis compensation is performed on the raw data. Figure 3.27 shows the results after hysteresis compensation. The difference between the standard data path and the

hysteresis based data path is modeled using a first degree equation, and a condition is introduced that limits it to above 55°C temperature.

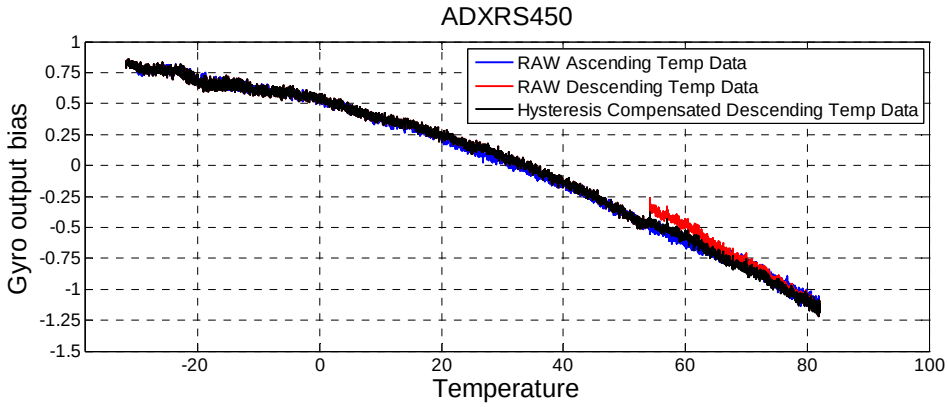

Figure 3.27: After compensation for hysteresis, the descending temperature data follows the ascending temperature data path.

Figure 3.28 shows another view of this compensation as only gyroscope output bias is plotted without temperature. The figure shows how the output bias data changes in time, as there are temperature changes in the environment.

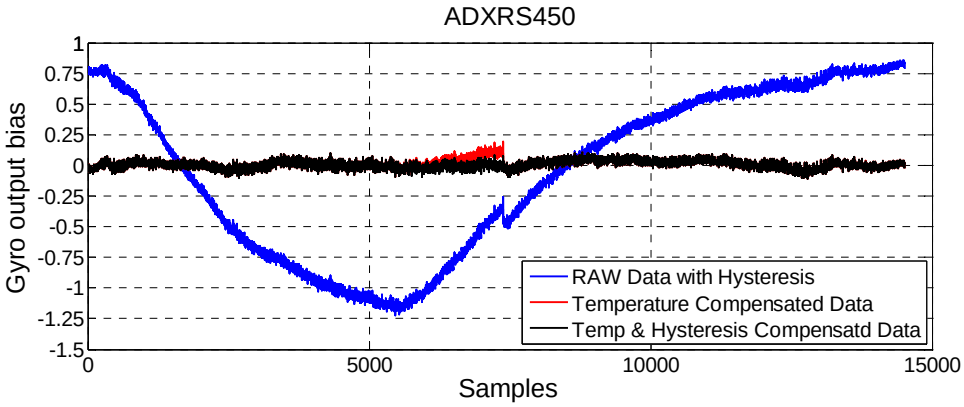

Figure 3.28: Raw data has temperature and hysteresis effects. Compensation of temperature and hysteresis produces reliable output data. Gyroscope output bias offset reduces from 2°/sec to less than 0.1°/sec.

The hysteresis compensation is done only by the CF method, by equating the error between normal and hysteresis affected data. However, the hysteresis compensation can be used in combination with neural networks, such that temperature compensation is done by neural networks and the hysteresis compensation is done by CF method. Figure 3.29 shows plots where NN method is used for temperature compensation and CF method is used for hysteresis compensation.

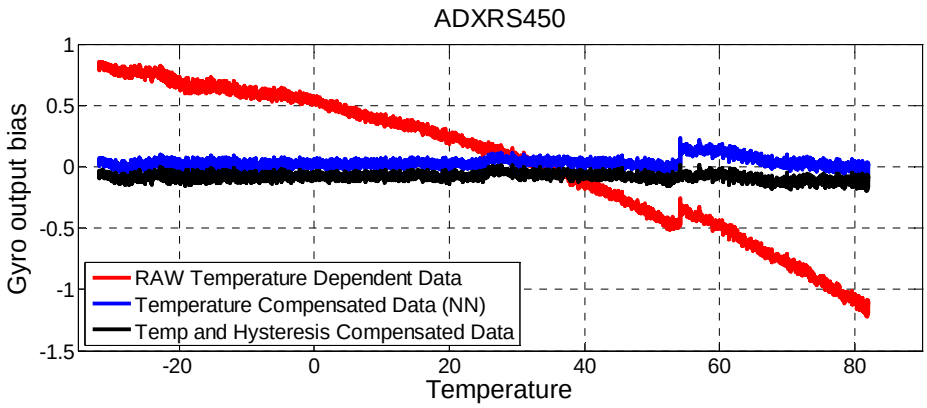

Figure 3.29: Temperature and hysteresis effects are compensated to achieve reliable data. Overall gyroscope bias offset reduces from 2°/sec to less than 0.1°/sec by temperature and hysteresis compensation (20 time improvement).

Figure 3.30 shows the Allan Variance plot of raw and compensated data. The temperature compensated and hysteresis compensated data plots are also shown in the same figure. The bias instability value of raw data is 34.2°/hr, and the integration time is 8 seconds. It can also be seen that the rate random walk is very dominant which shows temperature dependency of data. After temperature compensation by CF, the bias instability reduces to 28.8°/hr (16% improvement) and the integration times doubles to 16 seconds. Rate random walk also reduces significantly, as the slope on the right side of Allan variance plot is more flat. When hysteresis compensation is performed, the bias instability reduces to 25.92°/hr (25% improvement) and the integration time increases to 32 seconds. Rate random walk further reduces significantly as the slope on the right side of Allan plot is more flat.

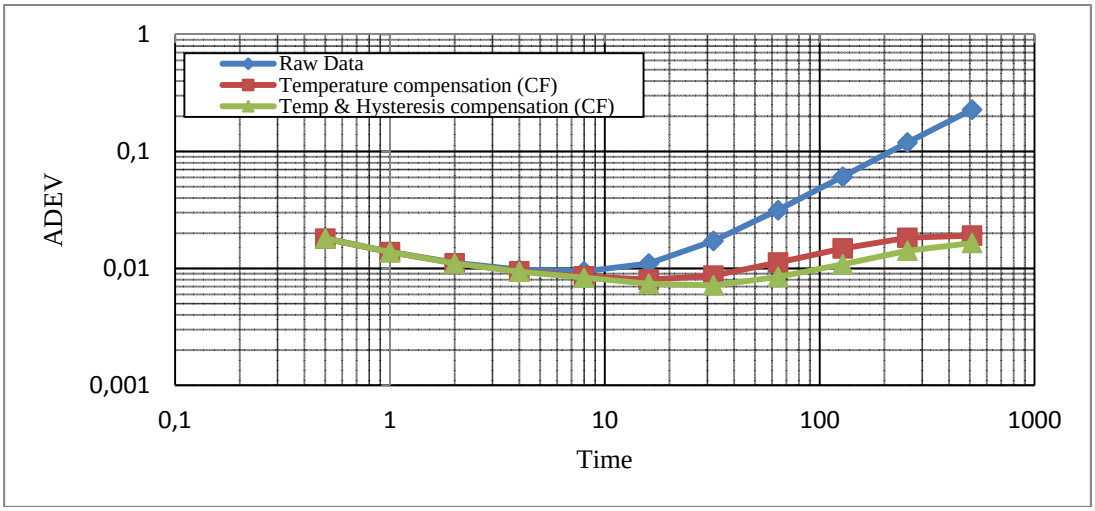

Figure 3.30: After temperature compensation bias instability reduces to 28.8°/hr (16% improvement) and integration time improves 2 times (16 sec). After hysteresis compensation, bias instability reduces to 25.92°/hr (20% improvement) and the integration time increases to 32 seconds.

It can be seen from the plot that hysteresis compensation can further improve the data and reduce temperature dependency. Figure 3.31 shows Allan variance plot of data after compensation by NN method.

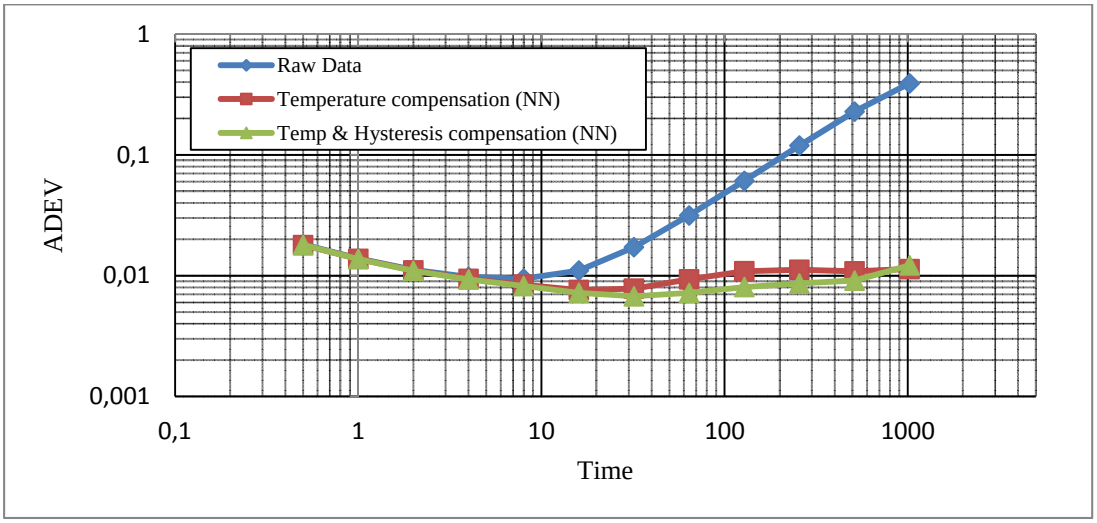

Figure 3.31: Allan variance plot of temperature (NN) and hysteresis (CF) compensated data with bias instability 24.48°/hr (28% improvement) and integration time of 32 seconds which is 4 times better than raw data. The rate random walk also reduces significantly.

The compensation of temperature is done by NN method which results in bias instability of 27.5°/hr which is 20% improvement. Further when data is compensated for hysteresis using CF method, the bias instability is further improved to 28% with value of 24.48°/hr. It can be concluded that for ADXRS450, the hysteresis compensation results in more improved data than simple temperature compensation.

3.2.2. XSENS MTi-10

XSENS is also used for hysteresis analysis because it gives raw data without any compensation for temperature, and hysteresis effect can be seen very clearly in the raw data. Figure 3.32 shows the general trend of hysteresis in XSENS data. The gyroscope bias offset can be up to 0.005°/sec due to hysteresis.

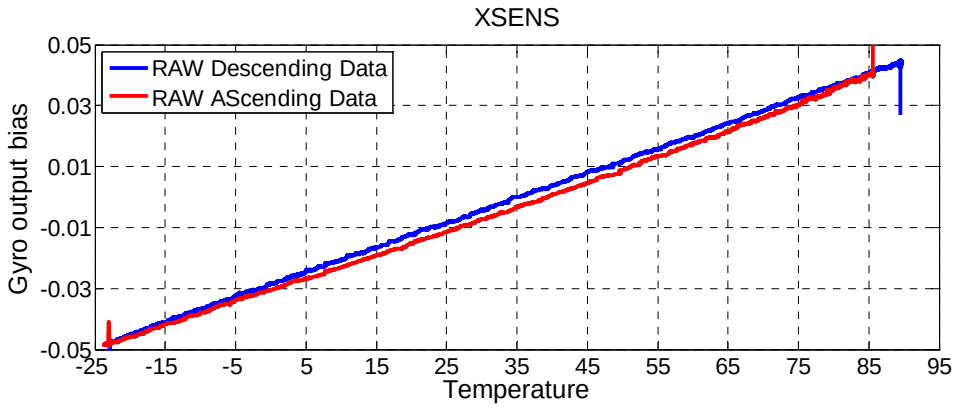

Figure 3.32: Hysteresis in XSENS sensor is shown over a temperature range of -20°C to +90°C. Ascending and descending temperature data are shown in different colors. The bias offset due to hysteresis is up to 0.005°/sec.

The consistency is checked by plotting multiples samples of the data. Figure 3.33 shows multiple samples of XSENS data to show consistency in the trend. The data is also collected at different temperature range, to see the validity in the hysteresis compensation technique.

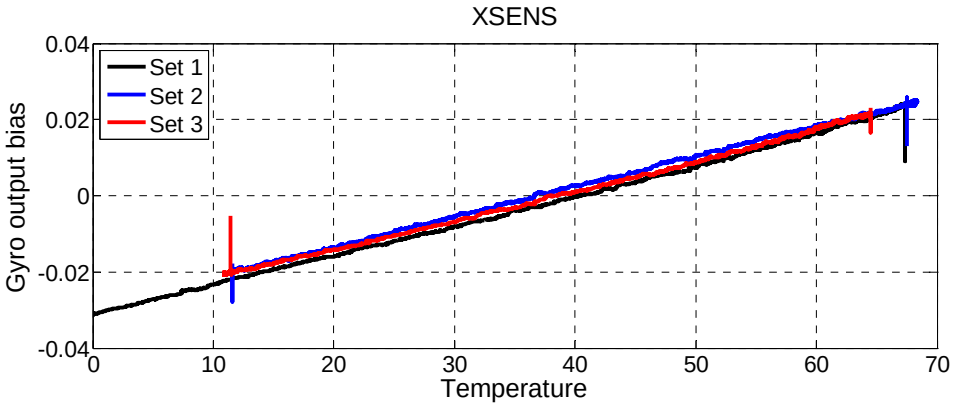

Figure 3.33: Hysteresis trend is shown in smaller range of temperature between -20, +70 and then +10°C. The behavior is consistent with larger range.

Figure 3.34 shows the hysteresis compensation equation plotted as a function of change in temperature. This equation is used to compensate hysteresis effects in XSENSE sensor data.

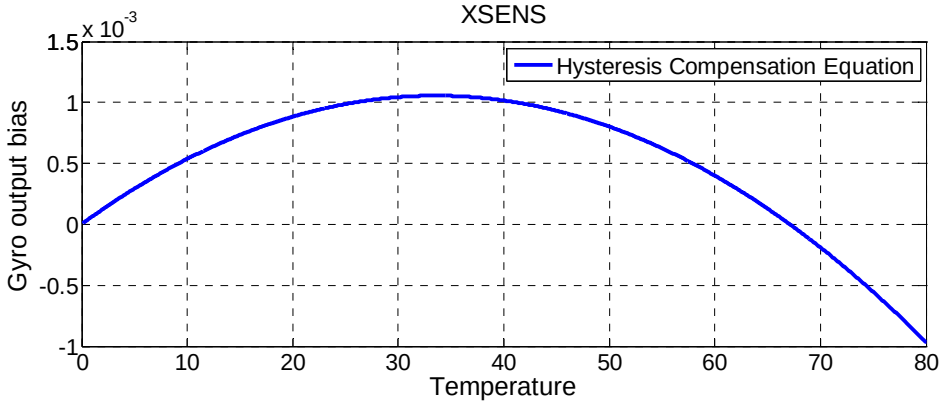

Figure 3.34: Hysteresis is modeled as function of temperature difference from point of change in slope of the temperature curve. The equation tells how hysteresis varies with change in temperature.

Figure 3.35 shows hysteresis affected raw data which is used for hysteresis compensation. The hysteresis compensation is applied on this data using CF method. Figure 3.36 shows a closer view of the results after hysteresis compensation.

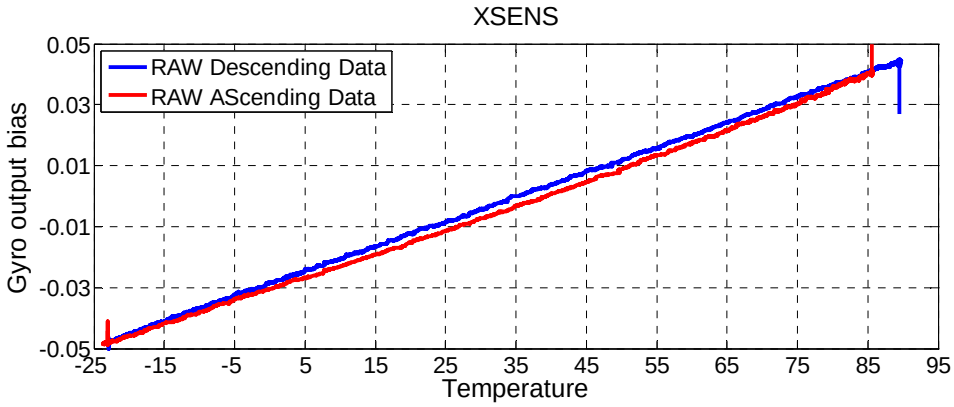

Figure 3.35: Raw data obtained from XSENS which is temperature dependent and has hysteresis in it. The gyroscope bias offset due to hysteresis is 0.005°/sec and the bias drift due to temperature is 0.1°/sec in range -25 to +90°C.

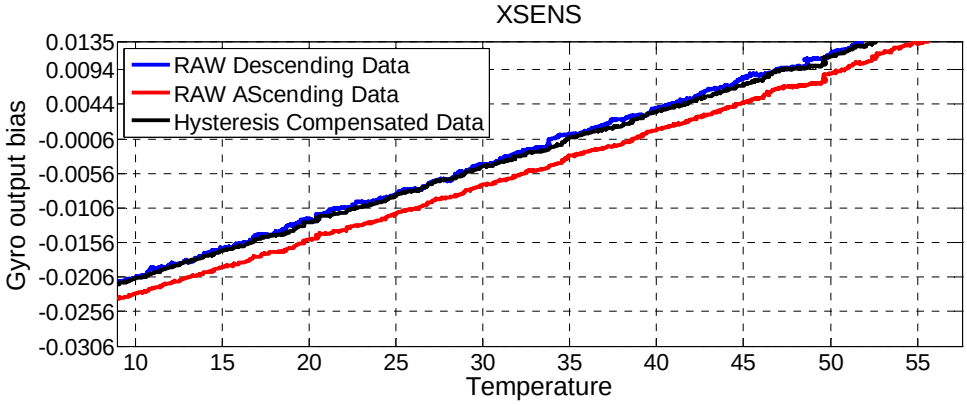

Figure 3.36: Gyroscope bias offset due to hysteresis is 0.005°/sec in raw data which is eliminated after hysteresis. The compensated data has negligible bias offset due to hysteresis.

It can be seen clearly that the bias offset caused by hysteresis has been reduced. Ascending and descending plots aligns accurately to remove any hysteresis error. The amount of error due to hysteresis is 0.005°/sec which is reduced significantly after compensation.

Hysteresis compensated data is the more temperature independent data. The results are even better than the factory based calibration plots (0.005/sec bias offset due to hysteresis is present in the factory calibrated data). Figure 3.37 shows closer view of hysteresis compensation. It can be seen that compensation by this methodology produces better results than factory calibration.

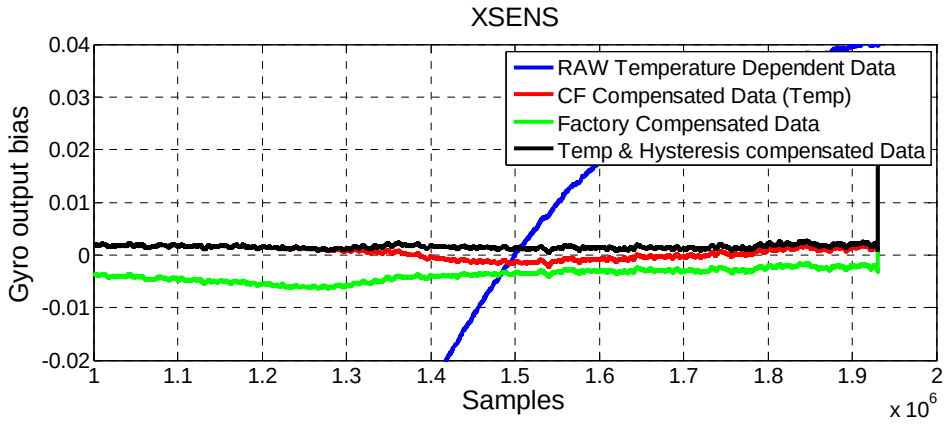

Figure 3.37: The data is shown at different stages of compensation; raw (blue), temperature compensated (red) and hysteresis compensated (black). Green shows the factory based calibration data. The overall compensation eliminates 0.005°/sec bias offset due to hysteresis which is not compensated by factory settings.

Figure 3.38 shows the Allan variance plot of raw and compensated data. It can be seen that the bias instability is reduced from 10.8°/hr to 5.4°/hr (50% improvement) after temperature compensation. Also the integration time has increased 8 times (from 5.12 to 40.96 seconds). After addition of hysteresis compensation, the bias instability is further improved to 4.68°/hr (57% improvement) with integration time of 163 seconds (32 times improvement).

Figure 3.39 shows Allan Variance plot where raw data is compared with compensation method of this study and factory calibration. 46% improvement in bias instability is achieved by factory calibration as compared to 57% improvement by CF method used in this study.

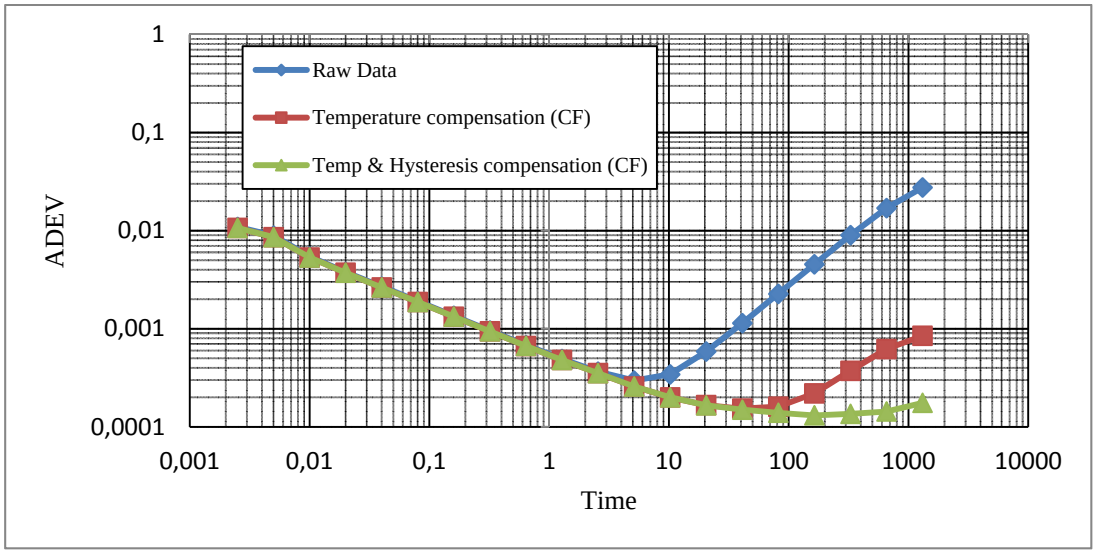

Figure 3.38: Allan variance plot of XSENS raw and compensated data. Bias instability reduces from 10.8°/hr to 5.4°/hr by temperature compensation. It further reduces to 4.68°/hr by hysteresis compensation.

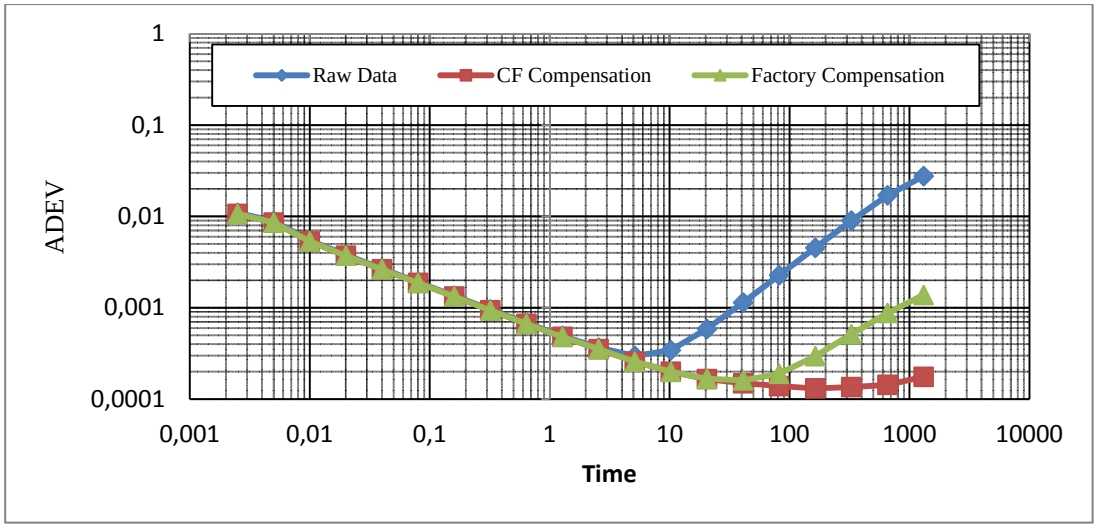

Figure 3.39: Allan variance plot of XSENSE raw and compensated data. The bias instability improves 57% by CF method as compared to 46% by factory calibration.

3.2.3. ADIS16488

ADIS16488 is also used for hysteresis analysis and data is acquired from this sensor. This sensor is very sensitive to vibrations in the environment and the hysteresis

analysis require cycles of temperature, which is attained by turning the temperature chamber ON. Thus data that is collected from this sensor is filled with vibration data from the chamber, which forbids this study to obtain any fruitful results in terms of Allan variance plot. Due to vibrations imparted to sensor by the temperature chamber, Allan variance plots do not show any improvement after temperature and hysteresis compensation. Figure 3.40 shows the effect of vibrations imparted to this sensor. The magnitude of external vibrations shadows the temperature dependent bias offsets. Thus ADIS16488 is not suitable for analysis that requires data to be collected in the chamber while it is ON, because the vibrations degrade the data.

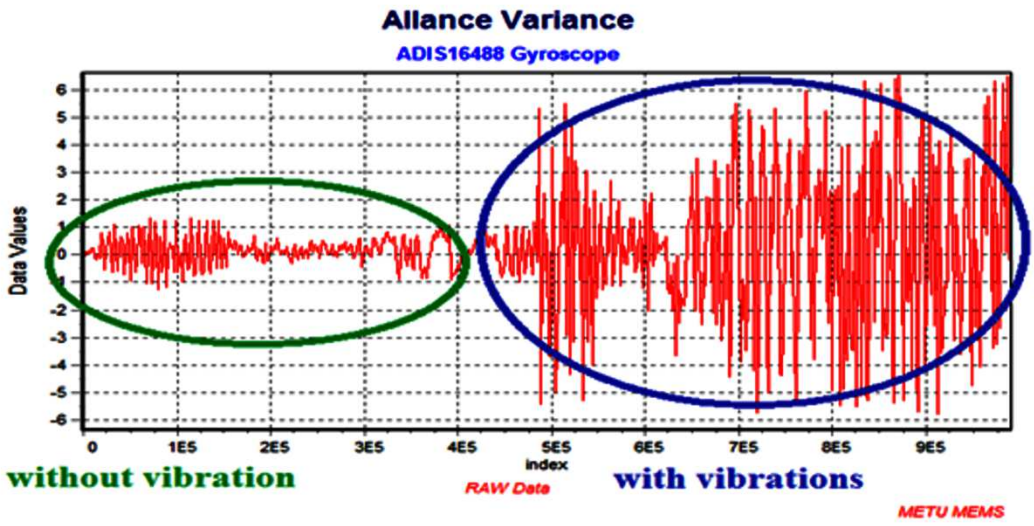

Figure 3.40: The difference between magnitude of gyro bias data with and without vibrations effects for ADIS16488. The magnitude of vibrations (caused by temperature chamber) exceeds the effect of temperature.

.

3.3. Acceleration Compensation

The acceleration compensation is done on the sensors that exhibit dependency on the changes in acceleration applied to that sensor. There is no special equipment available to this study that can produce any desired value of acceleration with accuracy, so the range created by the gravity of Earth is utilized. All the three axes of accelerometer are varied between +1 and -1 g to develop a relationship between

any particular axes of gyroscope and the three axes of accelerometers. The suitable sensors for this study are IMUs as they give the information about acceleration which can be used for its compensation. ADIS16488 and XSENS are used in this study for acceleration analysis. ADXRS450 is also studied but the sensor is not sensitive to small changes in acceleration.

3.3.1. ADIS16488

The first sensor used for this analysis is ADIS16488 IMU. It provides gyroscope data and accelerometer data which are used in this analysis. For this study z-axis gyroscope is selected, and the effect of three accelerometers is taken into account to form compensation equations. Figure 3.41 shows the first set of accelerations applied to the sensor, to see the effect on the gyroscope output.

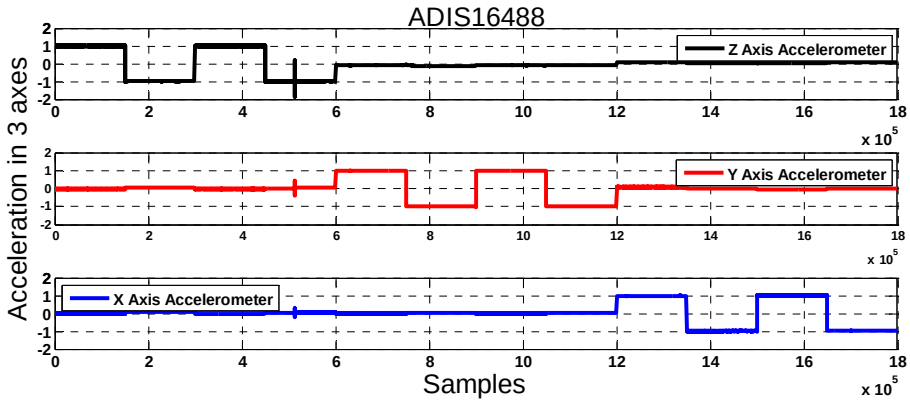

Figure 3.41: The acceleration values of three accelerometers of ADIS1688, applied to see the effects on z-axis gyroscope.

When ADIS16488 is subjected to acceleration values as shown in this figure, the z-axis gyroscope is affected and there is offset in its output bias. Figure 3.42 shows the response of z-axis gyroscope when subjected to acceleration changes. Acceleration can cause bias offsets up to 0.08°/sec.

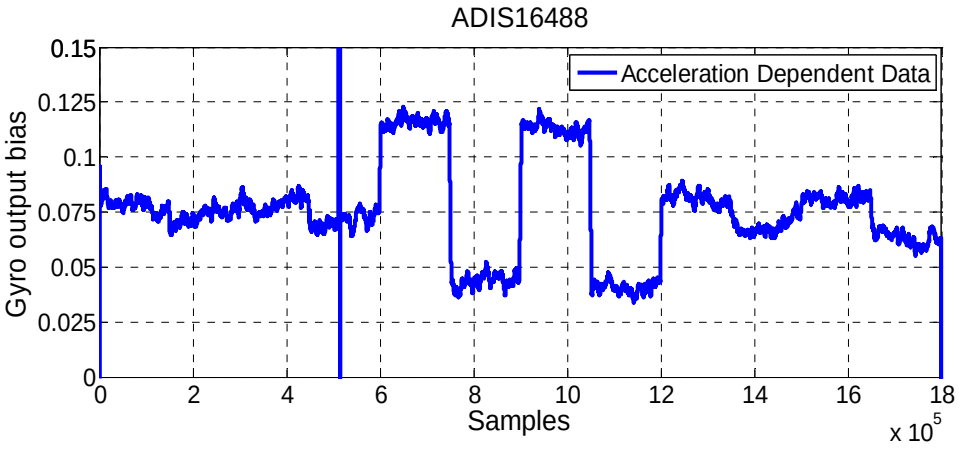

Figure 3.42: Acceleration dependent data of ADIS16488 z-axis gyroscope, when acceleration is changing. Gyroscope bias offsets up to 0.08°/sec results from changes in the acceleration.

Figure 3.43 shows acceleration dependent data along with the acceleration values to see the effects of acceleration. The magnitude of the gyroscope output bias has been scaled up (by factor of 20) to make it comparable to the acceleration values.

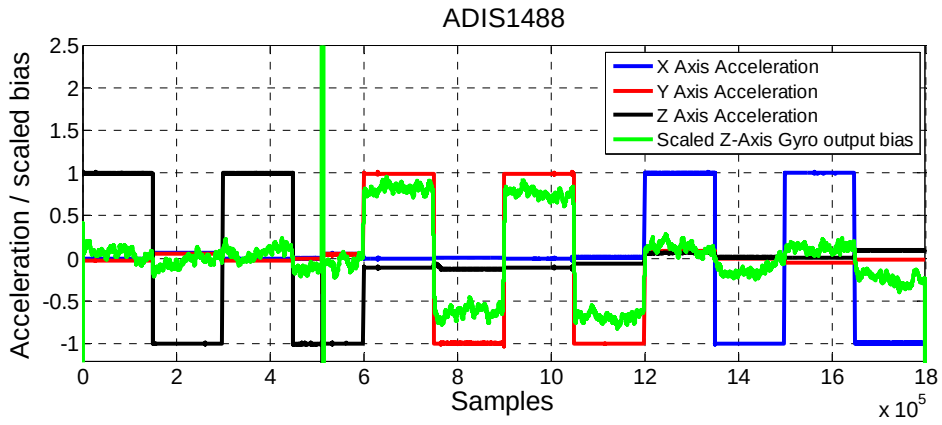

Figure 3.43: The magnitude of the gyro output bias is scaled up 20 times, to make it comparable to acceleration. The magnitude of gyroscope bias changes with changes in acceleration values. Y-axis has more effect on the gyro output bias than x and z-axis.

The sensor is then subjected to more values of accelerations and multiple sets are collected to see the effects of acceleration on gyroscope output bias and the most

reliable solution is obtained. Figure 3.44 and Figure 3.45 show such data sets that are collected for this analysis. These figures show different values of accelerations that are applied to the sensor, and using all these data sets equations are obtained for compensation of acceleration effects.

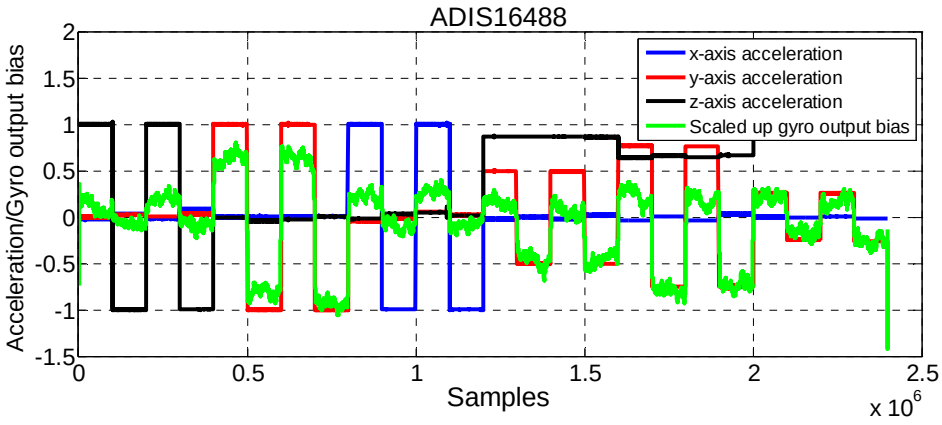

Figure 3.44: The figure shows scaled up (x 20) gyroscope output bias of the z-axis gyroscope, while the acceleration values are changing in all the three axes. The plot shows dependency of the gyro output rate on acceleration.

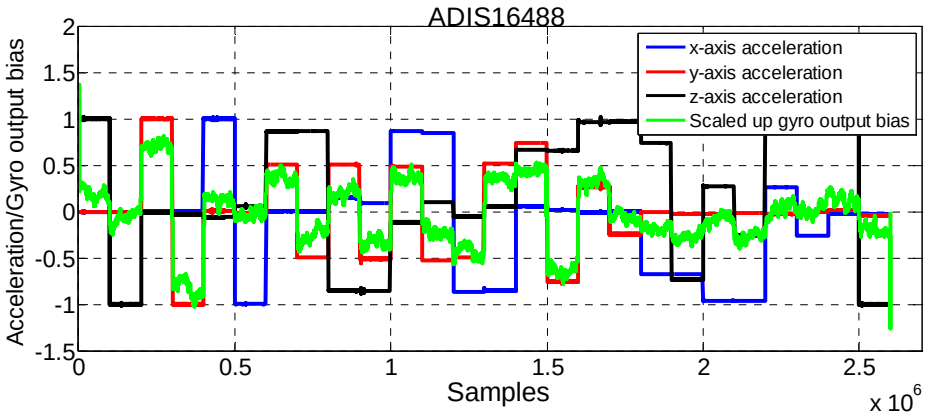

Figure 3.45: The figure shows scaled up (x 20) gyroscope output bias of the z-axis gyroscope, as the acceleration values are changing in all the three axes. The offset caused by accelerations is 0.08°/sec.

3.3.1.1. Compensation by Sensitivity Matrix (Curve Fitting)

The coefficients are obtained for compensation, and they form an equation to compensate the effects of acceleration. The input to this equation is acceleration values from the 3 accelerometers, and it gives the relative drift caused by them.

Figure 3.46 shows the acceleration compensated data using CF method. It can be seen that the acceleration dependency reduces significantly. The offset in the gyroscope bias is 0.08°/sec before compensation, which reduces to 0.02°/sec corresponding to 4 times improvement.

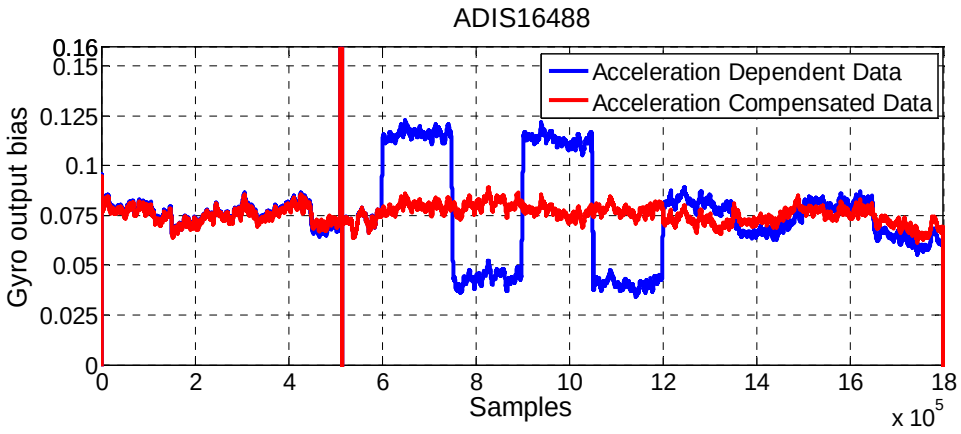

Figure 3.46: The offset in the gyroscope bias after compensation for acceleration effects reduces from 0.08°/sec to 0.02°/sec (4 times improvement).

Figure 3.47 shows another set of data that is compensated for acceleration effects by using CF method. Again it can be seen that the acceleration dependency reduces significantly. The offset in gyroscope bias reduces from 0.08°/sec to 0.02°/sec, which is 4 times improvement.

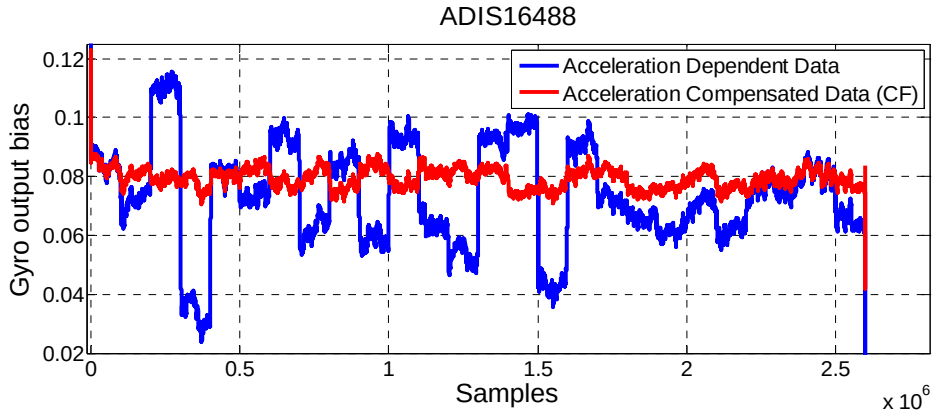

Figure 3.47: This data set also shows 4 times improvement after acceleration compensation by CF method. The offset in the gyroscope bias reduces from 0.08°/sec to 0.02°/sec after compensation.

3.3.1.2. Compensation by NN method

For NN based compensation, multiple data sets are used to train a network, that takes 3 axes accelerometer values as input data and the acceleration dependent error is output of that network. Figures 3.48 and 3.49 show acceleration compensation performed on the same data sets by using NN method. The offset in the gyroscope output bias due to acceleration is 0.08°/sec in both the data sets, and after compensation reduced to 0.02°/sec (4 times improvement).

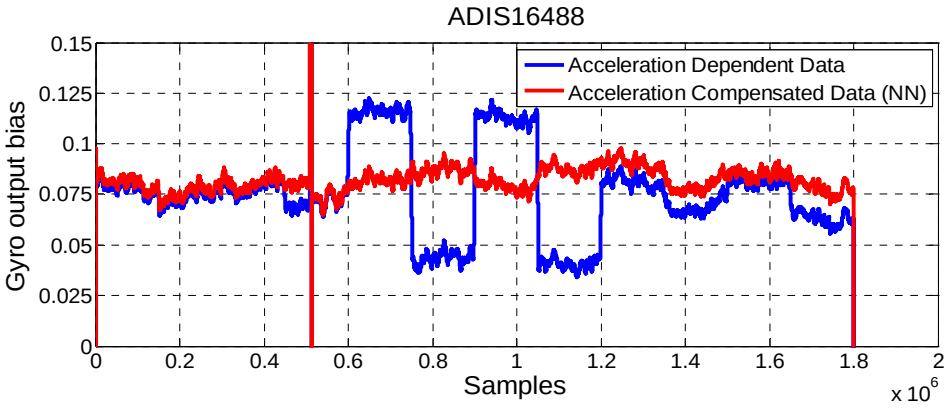

Figure 3.48: The acceleration dependent data is compensated by NN method, and acceleration independent data is achieved. Offset in the gyroscope output bias reduces from 0.08°/sec to 0.02°/sec which is 4 times improvement.

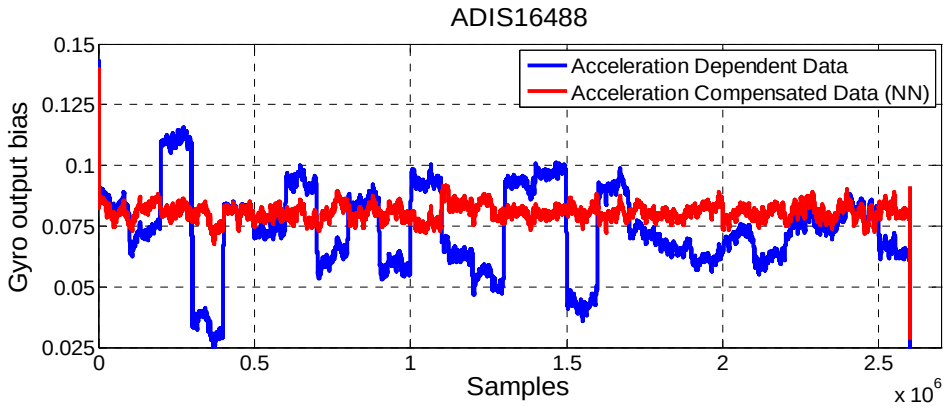

Figure 3.49: The acceleration dependent data is compensated by NN method, and acceleration independent data is achieved. Offset in the gyroscope output bias reduces from 0.08°/sec to 0.02°/sec which is 4 times improvement.

It can be seen from Figures 3.46 to 3.49 that acceleration dependency of the data reduces by using compensation methods. Also both the methods produce almost similar results (4 times improvement). Figure 3.50 gives Allan variance plot of the raw and acceleration compensated data by CF method.

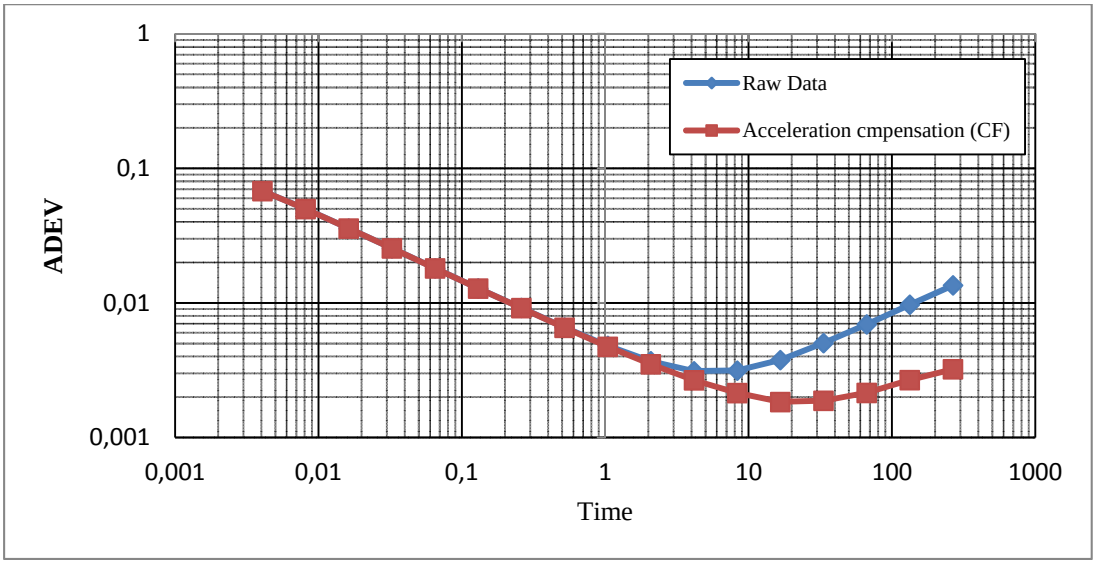

Figure 3.50: Allan variance plot of the raw and acceleration compensated data by CF method. Bias instability reduces to 6.84°/hr and integration time doubles (from 8.32 to 16.64 seconds).

3.3.2. XSENS MTi-10

Z-Axis gyroscope is chosen as the target axis and the effect from all the three accelerometers are studied. Figure 3.51 shows the acceleration values that are applied to this sensor, to see the effect of accelerations on the gyroscope output bias. Multiple samples are taken from this sensor, and different combinations of accelerations are used. Figure 3.52 shows another combination of accelerations applied to this sensor.

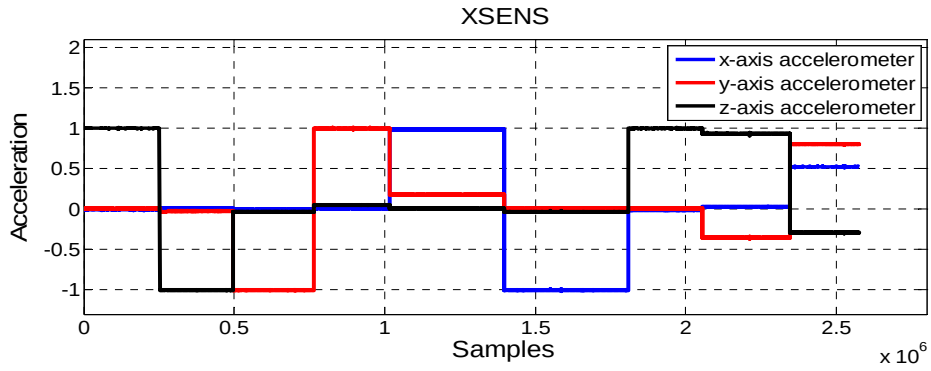

Figure 3.51: The acceleration values applied to XSENS to see effect on the output bias of z-axis gyroscope.

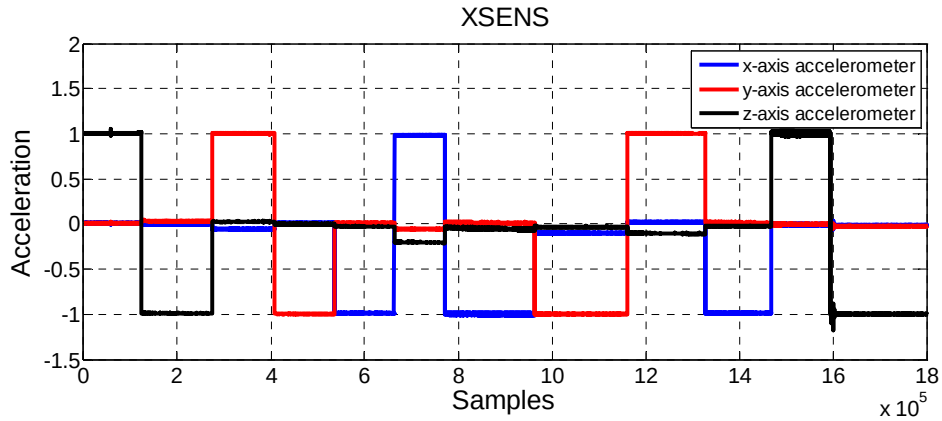

Figure 3.52: Second acceleration combination applied to XSENS sensor to see the consistency of response and formulate a compensation equation.

Figure 3.53 shows response of gyroscope when subjected to acceleration in different axes as shown in Fig. 3.51. Offset in the gyroscope output bias is produced as a result of different accelerations, which go up to .05°/sec.

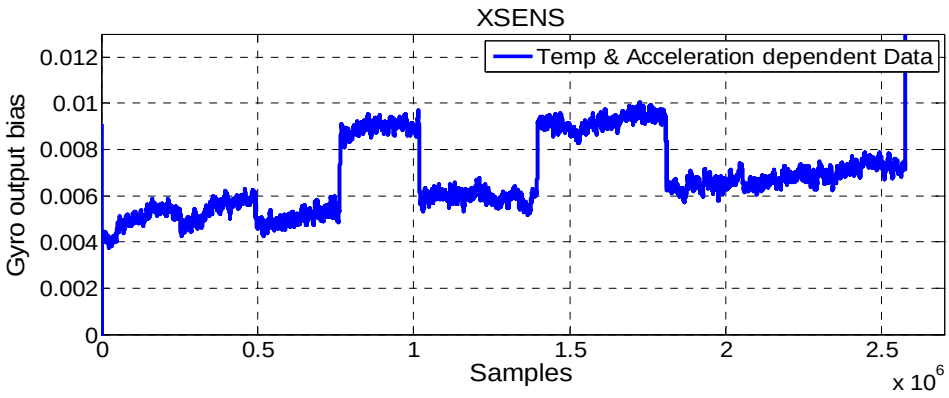

Figure 3.53: Gyroscope output bias of XSENS when subjected to different values of acceleration (Fig. 3.51). Offset of 0.05°/sec is present in the gyroscope output bias.

From this figure it is quite obvious that due to changes in acceleration, the gyroscope output bias also changes accordingly. It is also showing some slope in the data, which is result of change in temperature (1~2°C). To find the correct relation between acceleration and gyroscope output bias, it is very important that all other drifts are compensated first. Therefore, the temperature compensation is performed on the raw data, and it is plotted with acceleration values. The magnitude of gyroscope data is scaled up by multiplying it with 20. Figure 3.54 shows the temperature compensated data plotted with acceleration. The slope in the data due to temperature has been removed, and the data is 100% acceleration dependent.

The acceleration compensation is first done using CF method. As discussed in Section 3.2.1, a compensation equation is obtained using multiple samples that correlate the gyroscope output bias of z-axis with values from all the accelerometers. Figure 3.55 shows the result of acceleration compensation using CF method. The offset in the gyroscope output bias reduces from 0.005°/sec to 0.0015°/sec, which shows 3 times improvement.

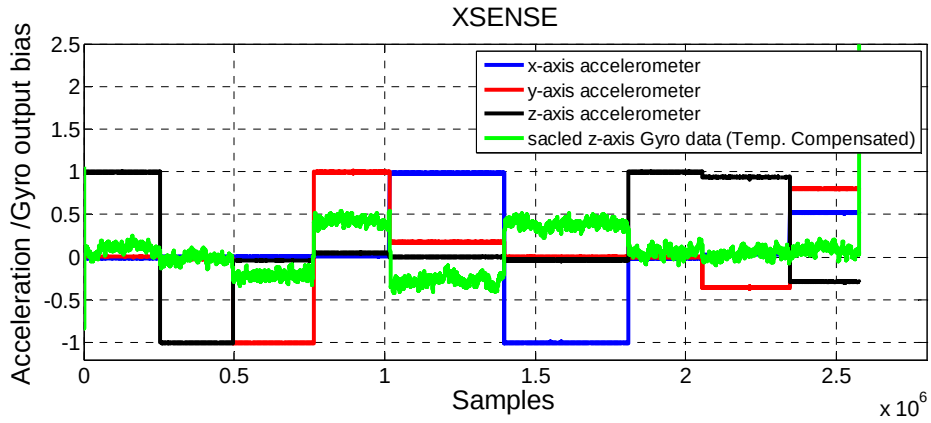

Figure 3.54: The magnitude of the gyro output bias is scaled up 20 times, to make it comparable to acceleration. Strong dependency on acceleration is visible from this plot.

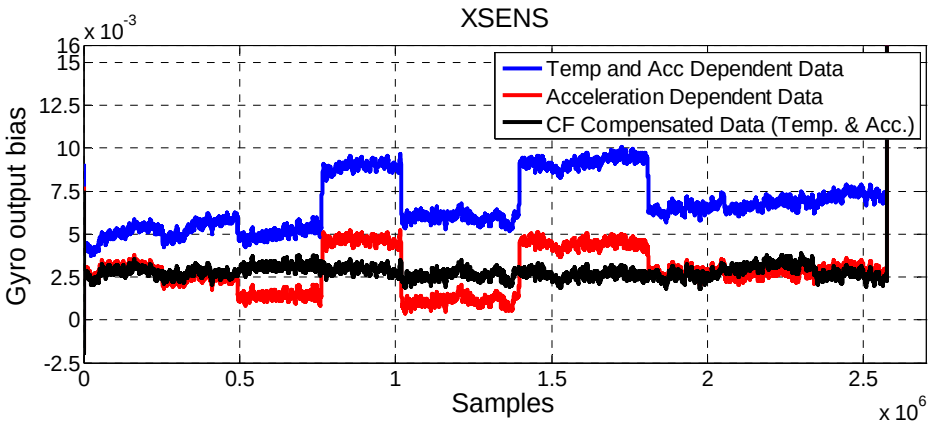

Figure 3.55: The raw data is first compensated for temperature, and then compensated for acceleration. The offsets in gyroscope output bias reduces from 0.005°/sec to 0.0015°/sec (3 times improvement).

Figure 3.56 shows the compensated data with changes in acceleration. This is also scaled up version of the gyroscope output bias. The dependency on acceleration is reduced significantly, and the compensated data is not responding to any changes in the acceleration.

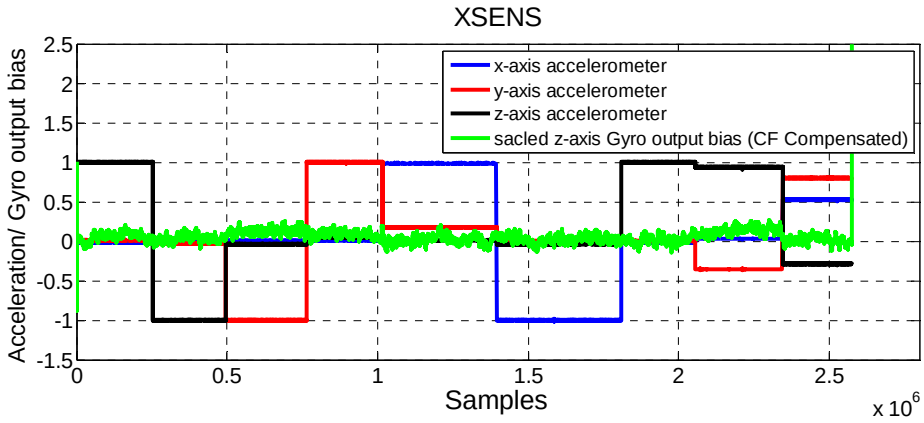

Figure 3.56: The dependency on acceleration reduces significantly after compensation by CF method (from 0.005°/sec to 0.0015°/sec). There is 3 times improvement in the data in terms of offset reduction.

Next, acceleration compensation is performed by using neural networks method. Multiple data samples are used to form a network, which is used to compensate the acceleration effects. Figure 3.57 shows the result of compensation of acceleration dependent data using NN method. The offset in the output bias reduces from 0.005°/sec to 0.0015°/sec after acceleration compensation, which corresponds 3 times improvement in the data.

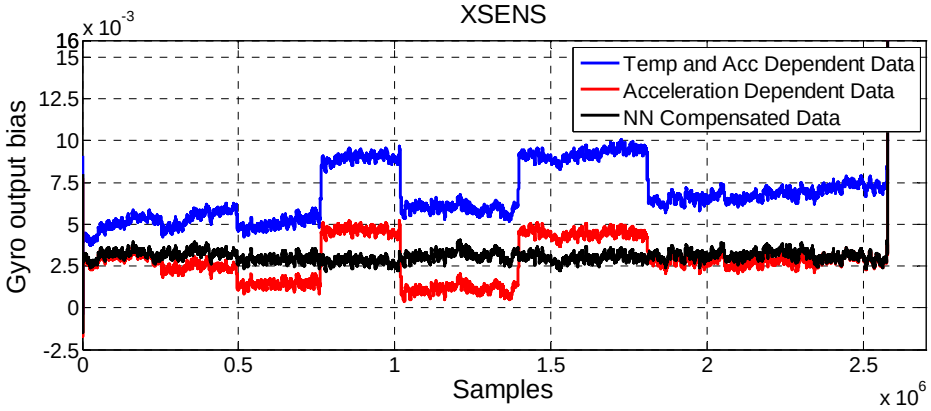

Figure 3.57: The raw data is first compensated for temperature, and then compensated for acceleration by using NN method. The offsets in the gyroscope output bias reduces from 0.005°/sec to 0.0015°/sec (3 times improvement).

Figure 3.58 shows the acceleration compensated data (scaled up 20 times) by NN method, plotted against the acceleration values that are applied to the sensor.

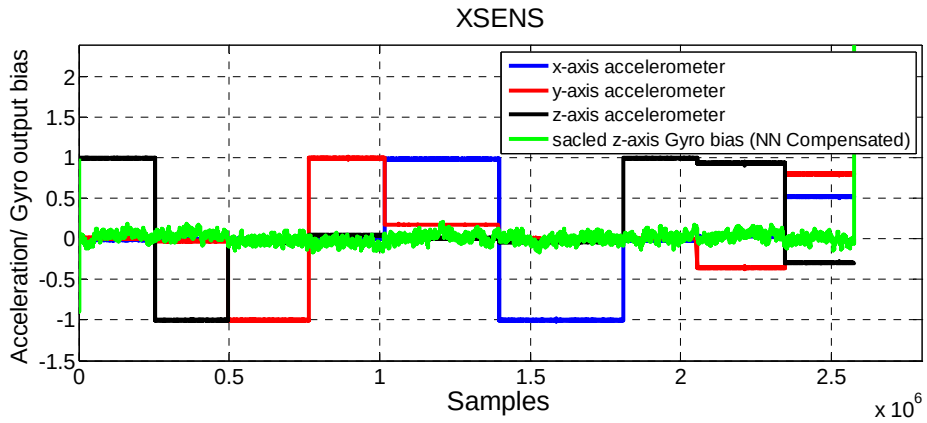

Figure 3.58: The plot shows that after acceleration compensation by NN method the dependency on acceleration reduces significantly (3 times reduction ion bias offset).

Figure 3.59 gives graphical comparison of these two techniques, and shows that both techniques produce identical results for acceleration compensation (3 times reduction in the output bias offsets).

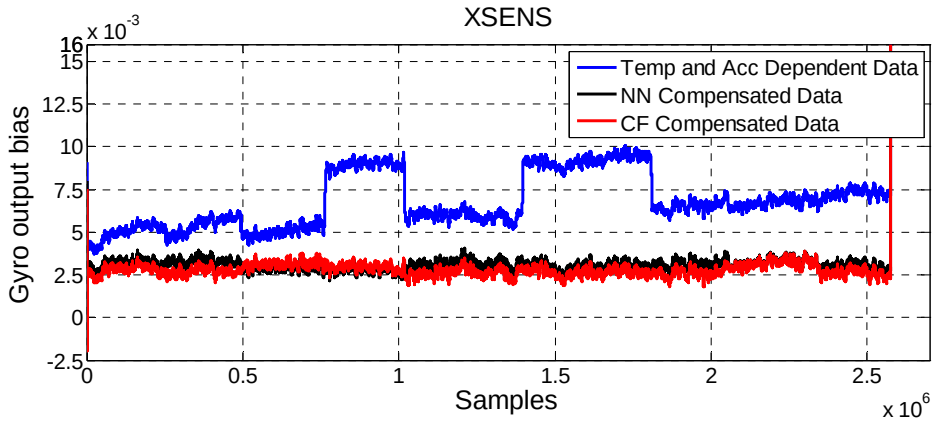

Figure 3.59: Raw and compensated data using CF and NN techniques are shown. Both the techniques show 3 times improvement in the data, where offset in the gyroscope bias reduces from 0.005°/sec to 0.0015°/sec.

3.3.3. ADXRS450

The ADRS450 is a single axis gyroscope, and it gives only information of gyroscope and temperature, which makes it less suitable for acceleration analysis. Still the test is performed to see any dependency on the acceleration values. For this purpose perpendicular positions of the sensor are used to achieve +1g, 0 and -1g in all the directions. Figure 3.60 shows different positions of acceleration and corresponding values of ADXRS450 gyroscope. It can be concluded that this sensor is resilient to changes in acceleration in this range, and the acceleration compensation analysis cannot be performed on this sensor. The sensor shows no dependency on the applied acceleration, and no pattern can be found that relates the gyroscope output bias to the applied accelerations.

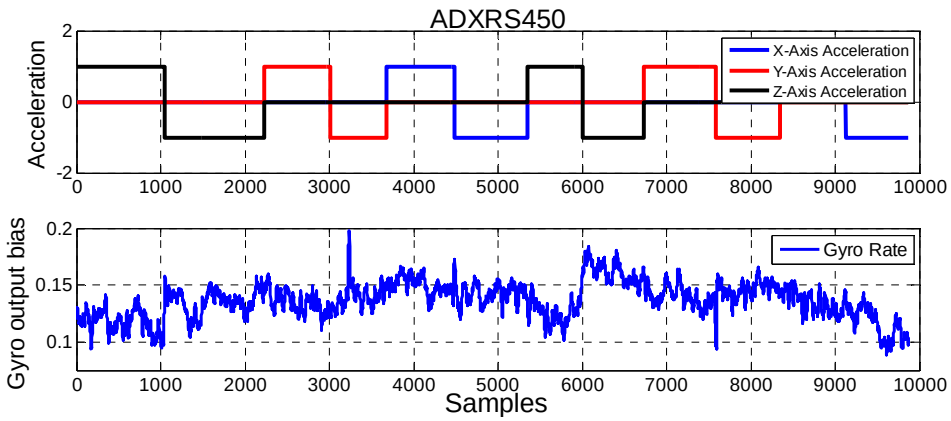

Figure 3.60: Gyroscope output rate of ADXRS450 sensor, when subjected to different positions of accelerations. The sensor shows no dependency on the acceleration values.

3.4. Integrated Compensation

This section deals with the compensation of acceleration and temperature effects collectively. For this analysis, XSENS sensor is used because it provides raw data with no internal compensation. No new equations are formed for this part of analysis, and only the already computed equations and networks are used for compensation of these two errors.

3.4.1. XSENS MTi-10

The compensation of both acceleration and temperature requires a data set that has both temperature dependency and acceleration dependency. For this purpose data is collected in the temperature chamber, and the sensor is moved into different positions. Thus both effects are also included in the collected data sets. Figure 3.61 shows the acceleration changes that are applied to the sensor.

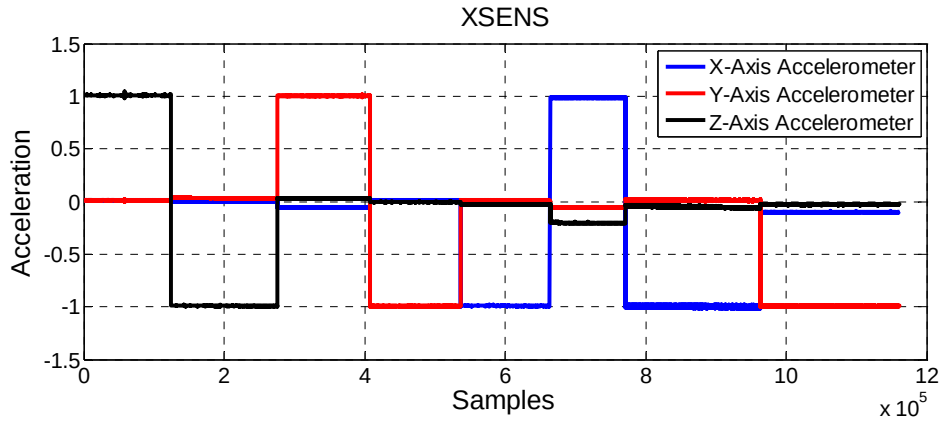

Figure 3.61: Different values of x, y and z axes accelerometers applied to XSENS. The acceleration is applied in parallel with temperature changes, to see the integrated effect of both factors.

It can be seen that the sensor is moved into different positions to get different values of accelerations it experiences. The integrated effect is created by moving the sensor inside the heating chamber, which is first cooled down to -30°C and then data recording is started. The sensor is moved into different position, and data is recorded for about 5-6 minutes at each position. Figure 3.62 gives the temperature range that is experienced by the z-axis gyroscope of XSENS.

The data is subjected to both acceleration changes and temperature changes. Figure 3.63 shows the gyroscope data which results from combined effect of temperature and acceleration.

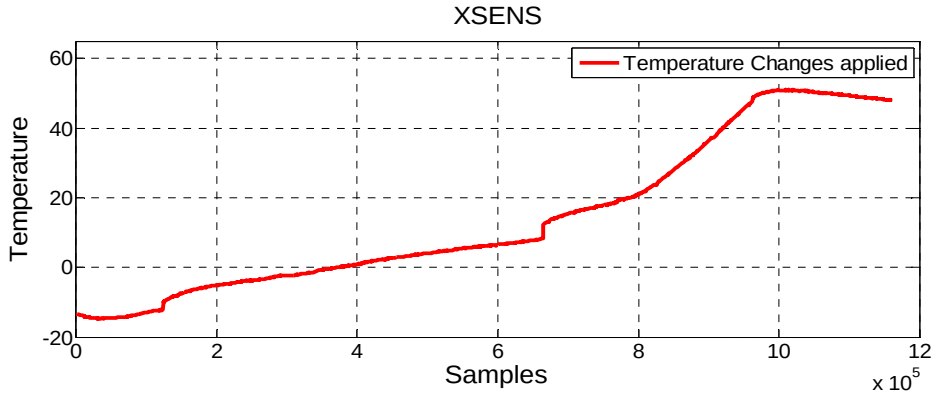

Figure 3.62: The temperature change that is experienced by the z-axis gyroscope of XSENS. The temperature change is in addition to accelerations changes.

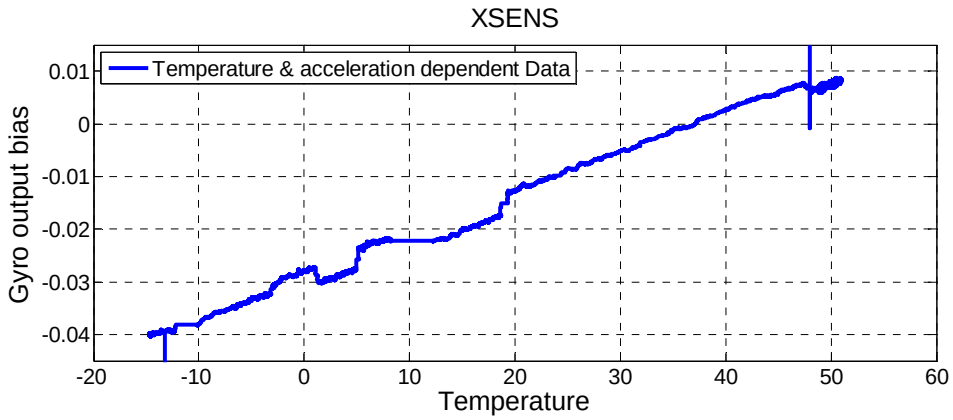

Figure 3.63: The acceleration and temperature dependent raw data of XSENS. Dependency on temperature is shown by the overall slope of data (0.05°/sec offset) and dependency on acceleration is shown by small irregularities in the plot (0.005°/sec offset).

There are two trends in the data which correspond to temperature and acceleration dependency. The overall slope of the data is linearly changing with the change in temperature. The acceleration effects are seen as small patches of irregularities in the data. The compensation of this data is performed by both CF and NN methods. The temperature and acceleration effects are compensated separately in sequential order, and they can be in any combination. First the data is compensated using CF methods for both the temperature and acceleration compensation. The order of compensation is irrelevant because compensation in any order produces similar final results.

Figure 3.64 shows the raw and temperature compensated data using CF method. The offset in the gyroscope bias reduces from 0.05°/sec to 0.005°/sec, which is 10 times improvement. The data is still dependent on acceleration.

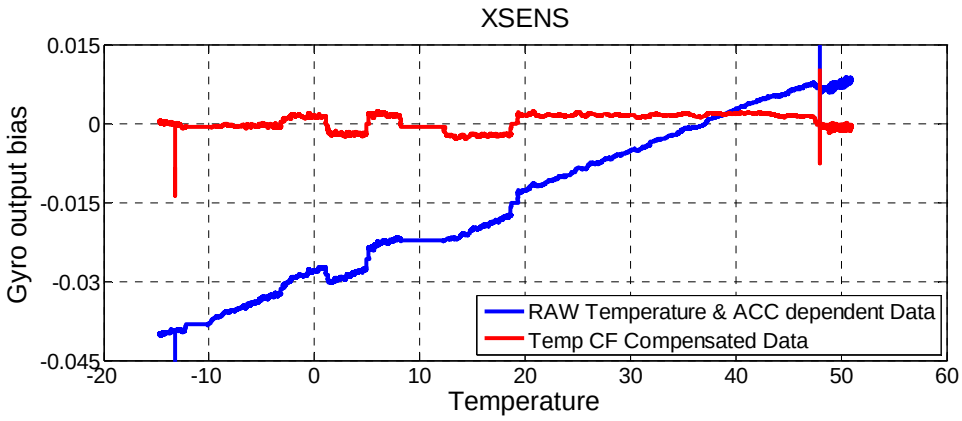

Figure 3.64: Raw data has temperature and acceleration based errors. After temperature compensation by CF method, the offset in the gyroscope output bias reduces from 0.05°/sec to 0.005°/sec.

Figure 3.65 shows the relation between acceleration dependent data (which is compensated for temperature) and acceleration values of different axes. The relation has become clearer after the temperature slope has been eliminated. The data is scaled up 20 times to make it comparable to acceleration values.

Now this data is temperature independent and only acceleration dependency is left in the data. Figure 3.66 shows compensation for acceleration effects by CF method. The offset in the gyroscope output bias is further reduced to 0.001°/sec, which is 5 times further improvement in the output bias data. Overall, the improvement in the bias offsets has become 50 times.

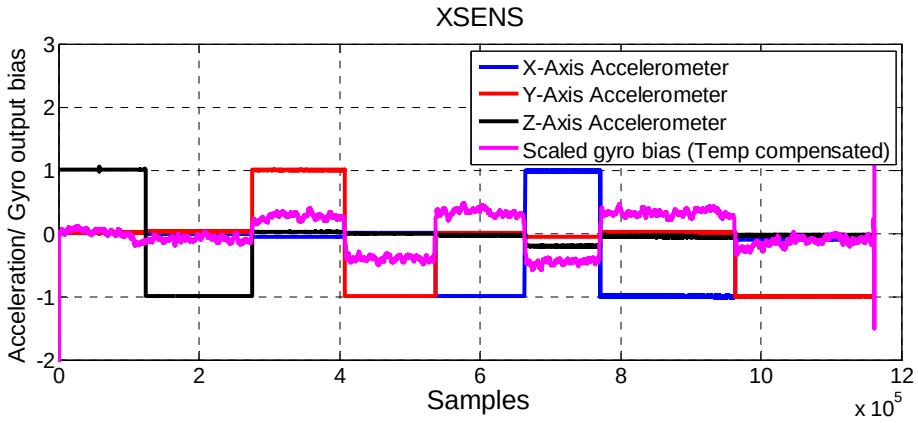

Figure 3.65: The acceleration dependent data is shown with applied acceleration values. The offset due to temperature in the gyroscope output bias reduces, but the offset due to acceleration (0.005°/sec) is still present in the data.

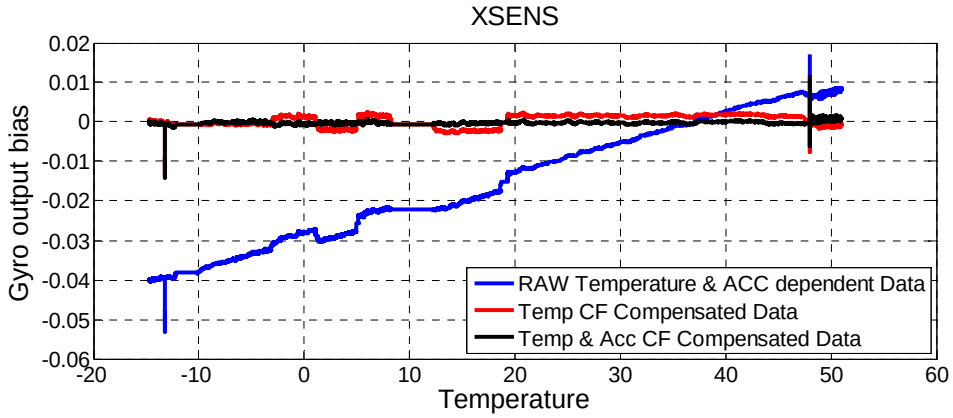

Figure 3.66: The two steps compensation (temperature and acceleration) are shown. Temperature compensation achieves 10 times improvement in the gyroscope bias, and the integrated compensation achieves 50 times improvement in the output bias.

Figure 3.67 gives a closer look at the compensation efficiency. The compensation of acceleration can be seen visually in this figure. Figure 3.68 shows the Allan variance plot of raw and compensated data, which has both temperature and acceleration dependency. The bias instability value is at 11.52°/hr, and integration time is 5.12 seconds. The bias instability value reduces to 5.76°/hr after compensation (50% improvement) and the integration time improves 8 times (40.96 seconds).

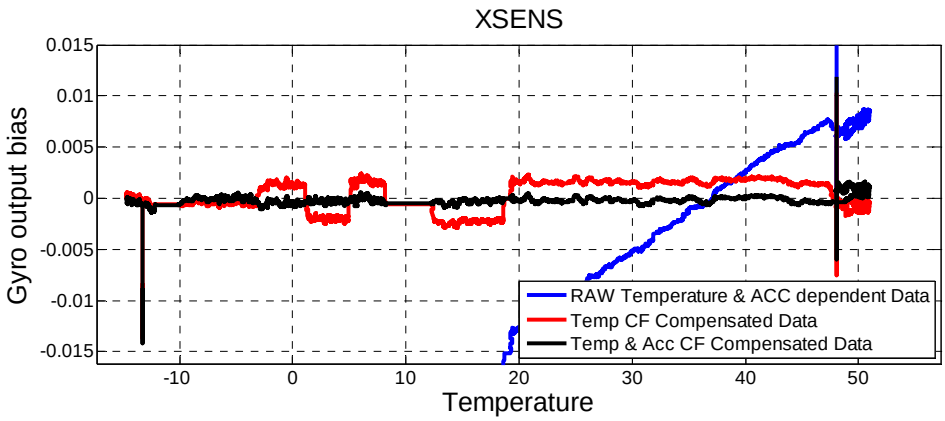

Figure 3.67: The two steps compensation (temperature and acceleration) are shown. Temperature compensation achieves 10 times improvement in the gyroscope bias, and the integrated compensation achieves 50 times improvement in the output bias.

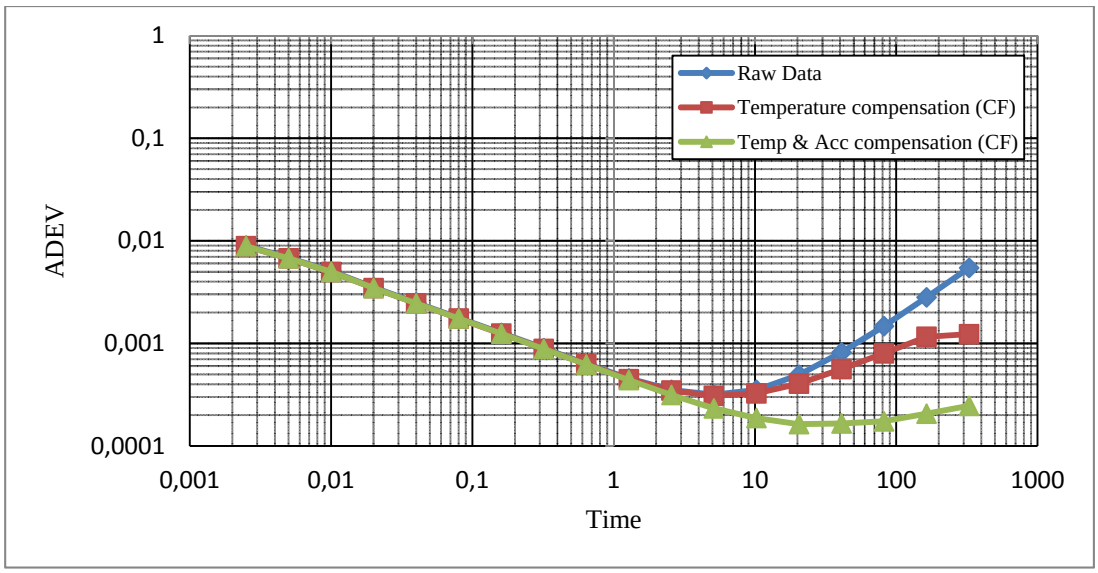

Figure 3.68: The Allan variance plot of XSENS raw and CF compensated data. The bias instability reduces to 5.76°/hr, which is 50% improvement. The integration time increases 8 times (from 5.12 to 40.96 seconds).

The plot shows that by compensating both the factors more reliable and accurate data can be achieved. The data is then compensated by using neural networks method. The order of compensation is reversed (acceleration compensation followed by temperature compensation) just for the sake of making a point that order of

compensation is not important. Figure 3.69 shows the acceleration compensated data by NN method. The offset of 0.005°/sec is removed by acceleration compensation.

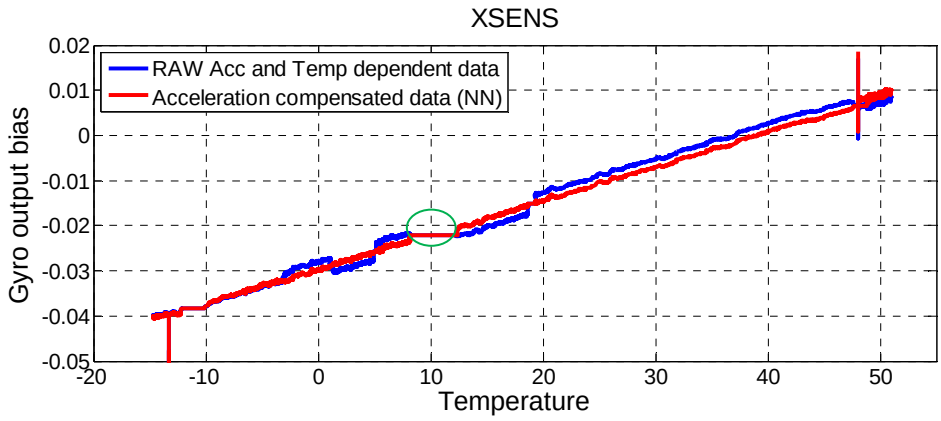

Figure 3.69: The data is compensated for acceleration effects, and the compensated data is linearly dependent on temperature. Offsets in the gyroscope output bias due to acceleration (0.005°/sec) are removed.

The encircled region is showing that there is gap in the temperature range, which actually resulted while data acquisition. The collection of acceleration and temperature dependent data require changing position of sensor into different axis, and data recording is stopped while changing the position of the sensor. The gap in the temperature is due to the time when recording is turned off. Figure 3.70 shows data that is totally temperature dependent. The gap can be extrapolated to form a linear relation between the gyroscope output bias and temperature.

Figure 3.71 shows the data after compensation of temperature (acceleration has already been compensated for this data). The overall offset in the gyroscope output bias reduces from 0.05°/sec to 0.001°/sec (50 times improvement).

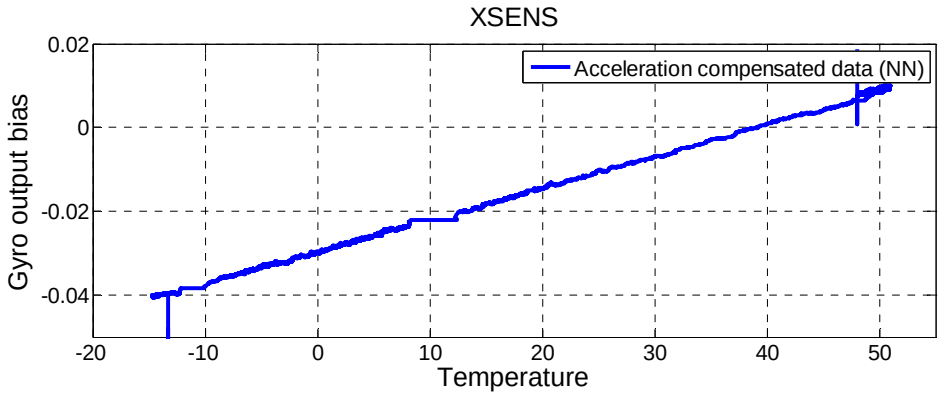

Figure 3.70: After acceleration compensation, the gyroscope data is temperature dependent only. Acceleration dependency is removed.

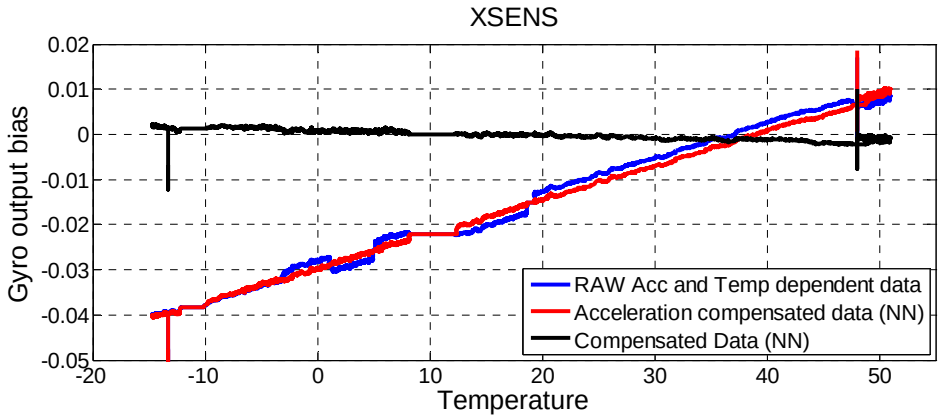

Figure 3.71: The NN compensated data is temperature independent and acceleration independent. The overall offset in gyro output bias reduces from 0.05°/sec to 0.001°/sec (50 times improvement).

Figure 3.72 shows the Allan variance plot of raw and compensated data by both techniques. The performance of both techniques is very similar in terms of bias instability and integration time. Both techniques achieve 50% improvement in bias instability, and 8 times improvement in integration times.

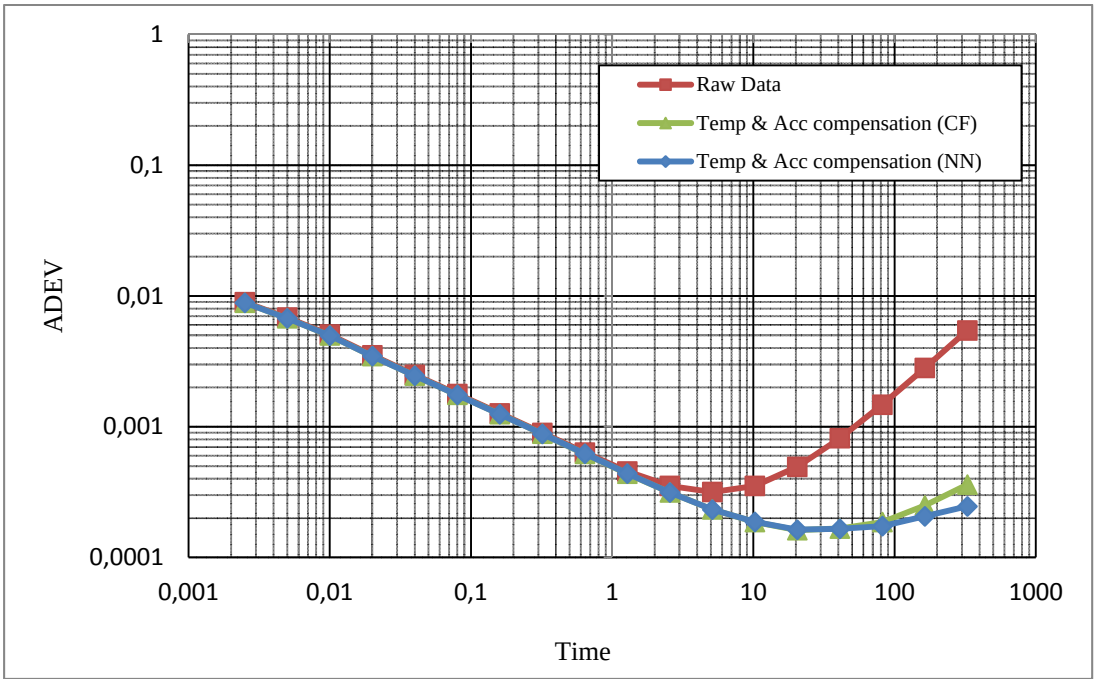

Figure 3.72: Allan variance plot of NN compensated data with bias instability of 5.74^0/hr (50% improvement), and 8 times better integration time. The reduction in temperature dependency can also be seen from reduced rate random walk.

The study also worked on the compensation of hysteresis; therefore another data set is recorded that contain some hysteresis in the samples. For this purpose the recording is done in the same manner but the temperature cycle is elongated, with ascending and descending temperature cycles. Figure 3.73 gives the information about the temperature applied to the sensor. The temperature is first dropped to 10°C and then raised to 70°C.

Acceleration is also applied to the sensor in this duration. Different positions of sensors make different values of accelerations to different axes. Figure 3.74 gives the acceleration values applied to XSENS during the temperature cycle. The first half of accelerations shows a noisy data because the chamber is cooling, and the vibrations are produced by it which is recorded by the accelerometers.

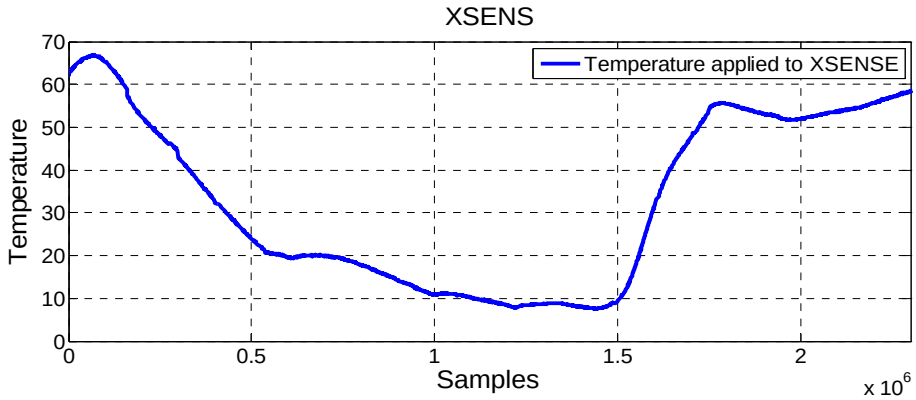

Figure 3.73: Temperature cycle that is applied to XSENS to see the effect of hysteresis, in addition to acceleration and temperature effects.

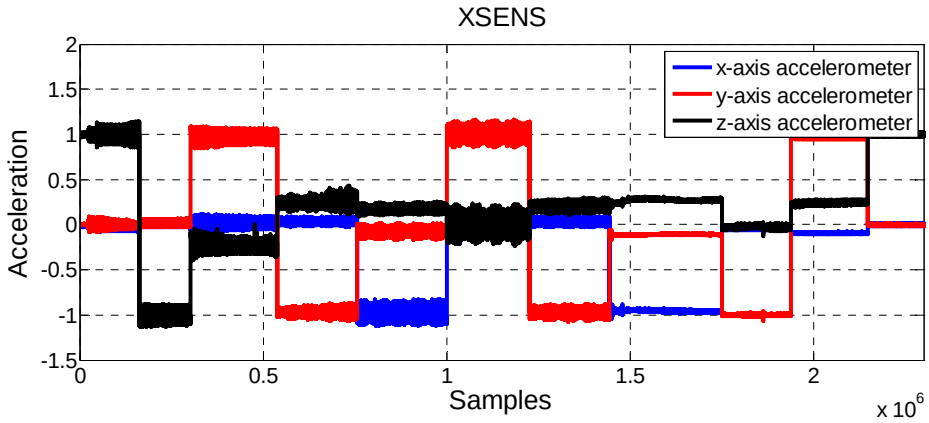

Figure 3.74: Acceleration applied to XSENS sensor while testing its behavior when subjected to temperature and acceleration simultaneously.

Figure 3.75 shows raw data, which results from application of all these factors. The temperature dependency is shown by the overall slope of the data and acceleration dependency is visible by small patches of irregularities in the data. Hysteresis can be seen which makes the ascending data to follow a separate path. The data is first compensated for acceleration effects using CF method. Figure 3.76 shows the data after acceleration compensation using CF method.

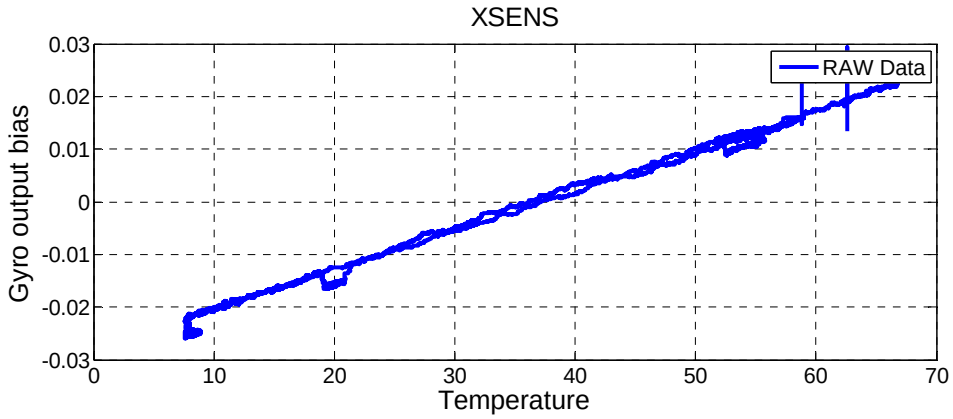

Figure 3.75: Raw data shows temperature dependency, acceleration dependency and hysteresis in the data. Offset is present in the gyroscope bias due to temperature (0.045°/sec), acceleration (0.005°/sec) and hysteresis (0.0015°/sec).

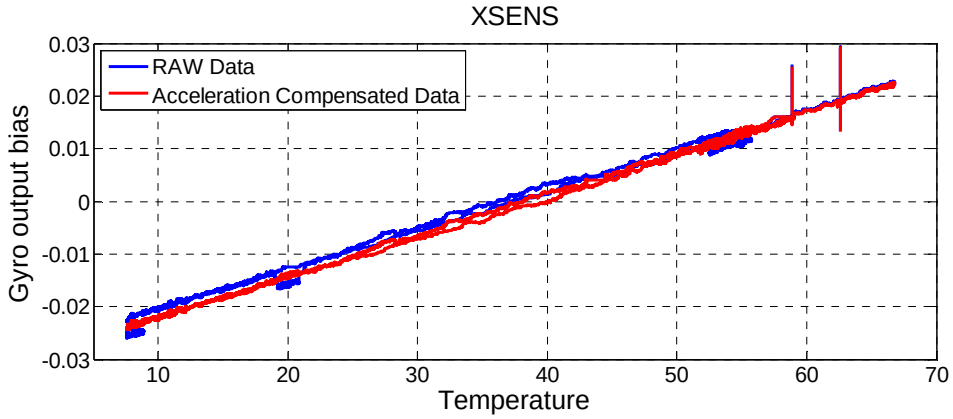

Figure 3.76: The acceleration compensated data shows less dependency on acceleration as the irregular patches in the data reduces, and the offset in the gyroscope output bias due to acceleration (0.005°/sec) is removed.

The next step is removal of hysteresis from the data which is also done using CF method. Figure 3.77 shows a closer view of the data where hysteresis compensation has been performed. The complete plot is not presented because the data paths are very close to each other and compensation cannot be detected easily. The plot shows that after acceleration dependency the hysteresis is removed from the data as well. Now the remaining plot is just data with linear temperature dependency which is compensated next.

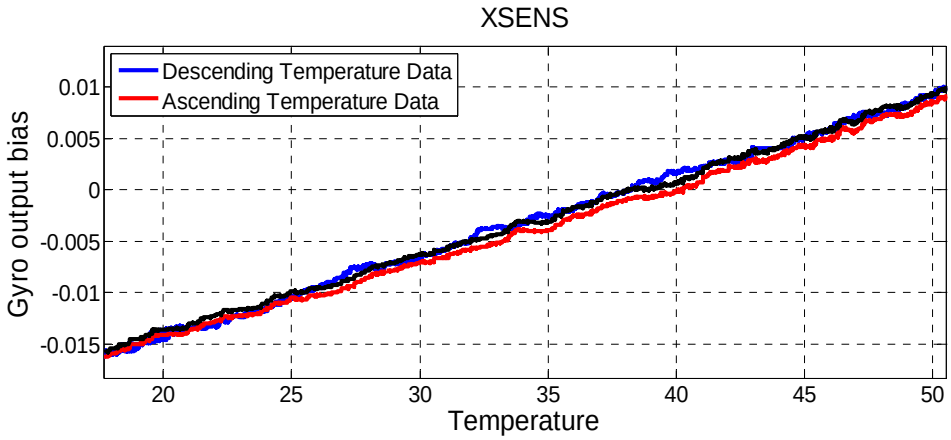

Figure 3.77: Compensation for hysteresis by CF method is shown. The compensated data aligns itself with the other temperature cycle data. Hysteresis reduces significantly (2~3 times improvement).

Figure 3.78 shows the data after compensation of temperature using CF method. This data is now free off all the errors namely temperature, acceleration and hysteresis.

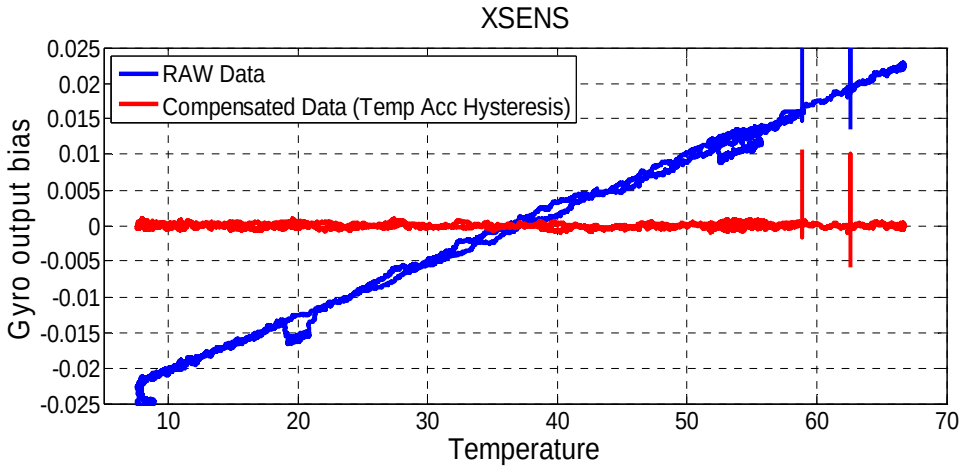

Figure 3.78: Raw data with acceleration, temperature dependency and hysteresis is shown. Compensated data is independent of temperature, acceleration and hysteresis. The offset in gyroscope output bias reduces 45 times after overall compensation.

The compensated data is compared with the results obtained from the factory calibration. Figure 3.79 shows that the overall compensation provided in this study produce better results as compared to factory calibration. The offset in the gyroscope output bias is reduced to 0.001°/sec by CF compensation (45 times improvement) as compared to 0.002°/sec by factory calibration (23 times improvement).

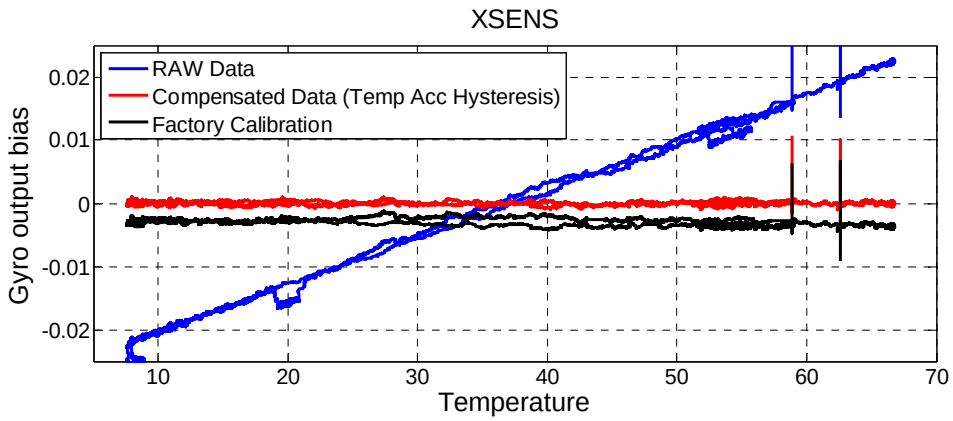

Figure 3.79: CF compensation improves the data 45 times (offset reduces from 0.045°/sec to 0.001°/sec) as compared to factory calibration which improves the data 23 times (from 0.045°/sec to 0.002°/sec).

Figure 3.80 gives Allan variance plot of raw and compensated data by CF method. The bias instability value is at 16.56°/hr for raw data and integration time is 5.12 seconds. After compensation, the bias instability reduces to 5.04°/hr (70% improvement) and integration times is 81.92 seconds (16 times improvement). The right side of plot is more flat which indicates reduction in rate random walk.

Figure 3.81 gives Allan variance plot of raw and compensated data by factory calibration. After compensation the bias instability is reduced to 5.74°/hr and integration times is 81.92 seconds. CF method has better performance than factory calibrated data.

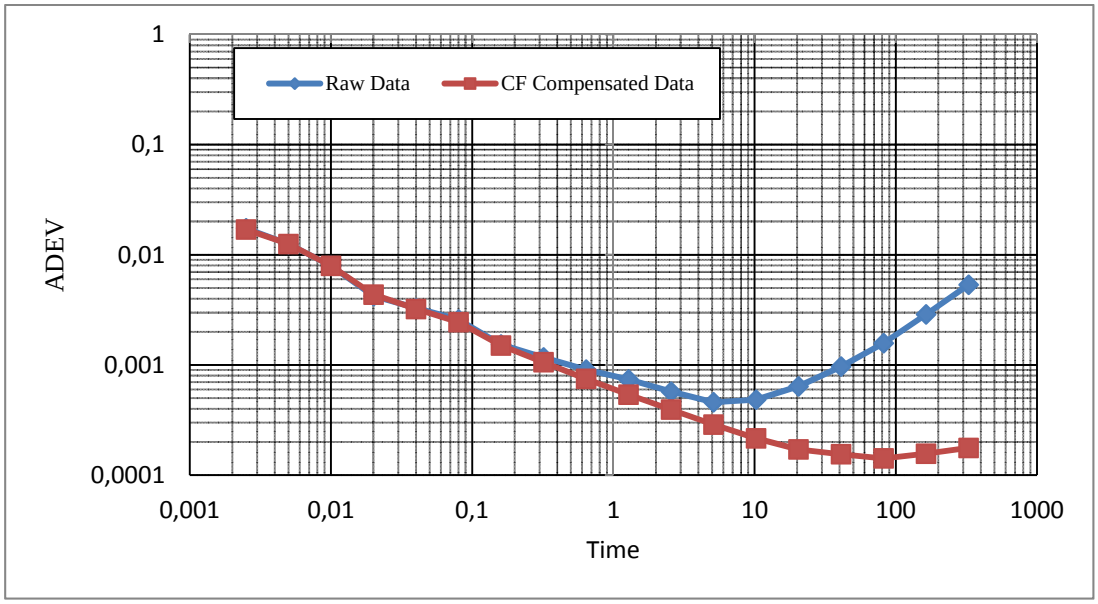

Figure 3.80: The Allan variance of XSENS raw and CF compensated data. The bias instability improves from 16.56°/hr to 5.04°/hr (70% improvement). Integration time improves 16 times (from 5.12 to 81.92 seconds).

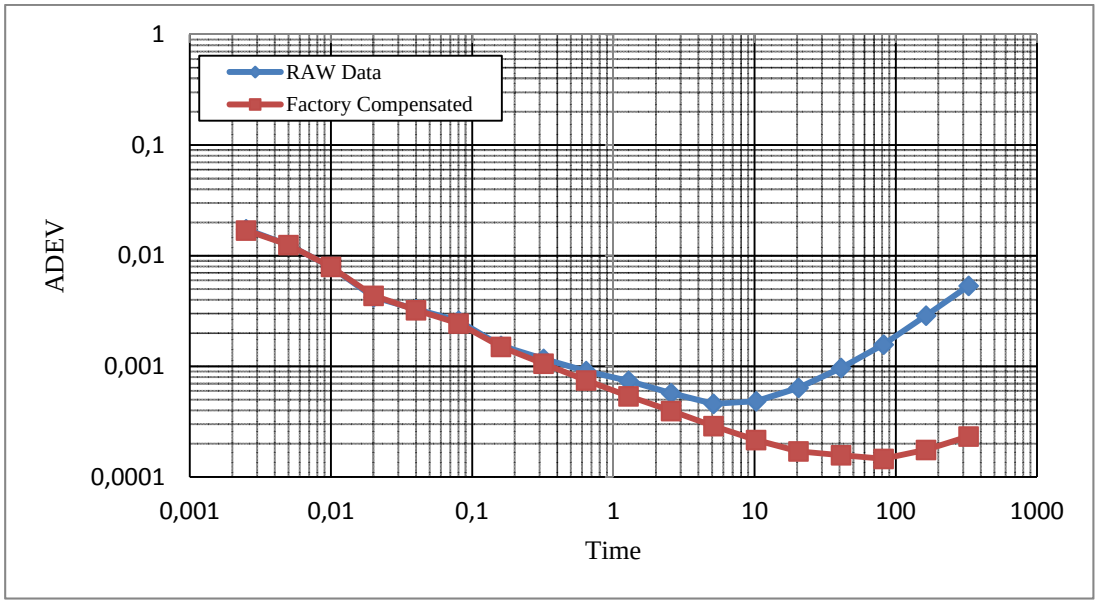

Figure 3.81: The Allan variance of XSENS raw and factory compensated data. The bias instability improves from 16.56°/hr to 5.76°/hr (65% improvement). Integration time improves 16 times (from 5.12 to 81.92 seconds).

From these two Allan variance plots, it can be seen CF compensation resulted in 70% improvement in the data as compared to 65% improvement by factory calibration. The improved margin results from inclusion of hysteresis compensation in the integrated compensation process. It can be concluded that CF based compensation produces better results than existing compensation techniques if hysteresis is included in the compensation process.

3.5. Summary

This chapter discusses compensation of temperature, temperature with hysteresis, acceleration and integrated effects of temperature and acceleration. CF and NN methods are used for compensation of these factors that cause drift in the output of a MEMS gyroscope data. The three sensors (ADIS16488, ADXRS450 and XSENS MTi-10) are used in different tests, based upon their characteristics and suitability to certain type of analysis. The data is successfully compensated, and it is seen that up to 70% improvement can be achieved in the bias instability of the gyroscope output bias after temperature compensation. The rate random walk is significantly reduced and data becomes less temperature dependent after its compensation. The acceleration compensation also results in achieving acceleration independent data by use of both compensation methods. The results from both the compensation methods produces comparative results and can be used interchangeably depending upon the requirement of complexity. The last section shows the integrated compensation of the data which is both temperature and acceleration dependent. The 2nd example also includes hysteresis in the data that results due to change in the slope of temperature. After compensation the data becomes significantly independent of acceleration and temperature effects, and in case of hysteresis it is also removed.

CHAPTER 4

CONCLUSION

This chapter concludes the work done in this study. This study is focused on compensation of temperature and acceleration effects on a MEMS gyroscope output data. Different compensation techniques are implemented on different types of sensors. The study used the existing compensation techniques (polynomial curve fitting and neural networks) and implemented them on available sensors, with slight modifications in the methodology. Following sections summarizes the conclusion on research objectives of this study.

4.1. Performance comparison of different sensors

The first research objective is to use different types of sensors for this study, so that comparison can be made about how each technique improves data when applied to different sensor data. This makes the performance of any technique generalized rather than restricted to a particular sensor. There are different types of sensors used in this study including ADIS16488, ADXRS450 and XSENS MTi-10. Initially an in-house built accelerometer is also used for testing compensation techniques. The study utilized these three main sensors for the analysis of different techniques. These three sensors have different characteristics, and they behave slightly differently from each other when subjected to acceleration and temperature changes.

ADIS16488 is an IMU, and its gyroscope data is very resilient to changes in temperature. The compensation of temperature results in improved bias (from 0.04°/sec to 0.02°/sec), but not much improvement is seen in Allan variance plots. The reason is that the sensor data is internally temperature compensated, and there is no room for further improvement in terms of bias instability. When subjected to acceleration changes, this sensor shows dependency on applied accelerations.

Compensation methods reduce the dependency on linear acceleration very significantly (4 times improvement). Hysteresis is not analyzed using this sensor because it is very prone to vibrations produced by the temperature chamber, which limits the sensor operation while changing slopes of temperature.

ADXRS450 is a single axis gyroscope that gives gyroscope rate and temperature data as output. The sensor is not internally compensated for temperature and the effects of temperature on the gyroscope are almost linear with temperature changes. The compensation performed on this sensor results in improved bias instability values (up to 28% improvement) and improved integration times (up to 4 times). The rate random walk reduces significantly after temperature compensation. This sensor is also very good for analysis of hysteresis, and the compensation of hysteresis is performed with progressive results.

XSENS is an ideal IMU for this study, as it provides raw data that is temperature dependent and acceleration dependent. The raw data of gyroscope shows a linear relationship with the changes in temperature, and compensation produces very significant results. The dependency on the temperature reduces with 50% improvement in the bias instability (by temperature compensation only), and rate random walk reduces significantly. The sensor also shows hysteresis in the data when subjected to change in the slope of temperature. Study shows that the compensation of hysteresis further improves the data, and makes it more temperature independent. The sensor also shows dependency on accelerometers when different acceleration values are applied between -1g and +1g. The effects of acceleration are also significantly compensated using the compensation methods (offset reduces 3 times in the output).

Table 4.1 shows which of the sensors are used for different type of analysis in the study. It should be noted that a sensor is selected based upon its characteristics and operating conditions of the test.

Table 4.1: The sensors used for different analysis according to their characteristics and operating conditions of the tests.

Sensor	Temperature Compensation	Hysteresis Compensation	Acceleration Compensation
ADIS16488	Applied / Improvement (2 times in bias offset) (4 times integration time)	Not Applied	Applied / (4 times improvement in bias offset)
ADXRS450	Applied / Improvement (27% in bias instability) (4 times integration time) (20 times in bias offset)	Applied / (7% improvement in bias instability)	Not Applied
XSENS	Applied / Improvement (70% in bias instability) (8 times integration time) (50 times in bias offset)	Applied / (7% improvement in bias instability)	Applied / (3 times improvement in bias offset)

4.2. Compensation of Temperature and Acceleration Effects

Second research goal is to perform temperature and acceleration compensation simultaneously on raw data from the sensors. There is no published research that deals with both the factors simultaneously. This study presents results that show the compensation of both the factors, and their importance for accurate data. Results from this study show that acceleration range between -1g and +1g has significant effect on the output of a MEMS gyroscope data. The effects of temperature are well known and lot of work has been done on its compensation. The effects of linear acceleration for small values are ignored, as they do not pose any threat to accuracy of the data. This study shows that some sensors are prone to even small values of linear acceleration, and they need to be compensated for error free data.

ADIS16488 and XSENS show dependency on temperature and acceleration, when subjected to these factors. ADXRS450 is not affected by acceleration changes in the

±1g range, and hence is not used in acceleration related analysis. XSENS provides raw data which is neither compensated for temperature nor for acceleration, therefore, it is very ideal for the integrated compensation analysis. Table 4.2 shows summary of integrated compensation performed on XSENS, which shows that acceleration dependency has to be removed for more accurate data.

Table 4.2: Importance of acceleration compensation and its effects.

XSENS	**CF Compensation**		**NN Compensation**	
	Offsets contribution to output bias	**Improvement**	**Offsets contribution to output bias**	**Improvement**
Raw Data	0.05°/sec	-	0.05°/sec	-
Temperature compensated only	0.005°/sec	10 times	0.05°/sec	10 times
Temperature and acceleration compensated	0.001°/sec	50 times	0.001°/sec	50 times

4.3. Compensation of Hysteresis

Third research objective is to study hysteresis present in MEMS gyroscope output data. The compensation of basic level of hysteresis is also performed in this study, which is not present in any of the published research. The study shows that compensation of hysteresis improves the sensor data in terms of reducing the dependency on the temperature. The rate random walk is also reduced significantly by compensation of hysteresis in any gyroscope output data. The hysteresis compensation also improves the bias instability of a MEMS gyroscope data. Table 4.3 summarizes some benefits achieved by hysteresis compensation.

Table 4.3: Improvement in data before and after hysteresis compensation.

	Bias instability without hysteresis compensation	**Bias instability with hysteresis compensation**	**Offset due to hysteresis in output bias**
ADXRS450	16~20% Improvement (34.2°/hr to 28.8°/hr)	25~28% Improvement (34.2°/hr to 25.92°/hr)	0.2°/sec
XSENS	50~65% Improvement (12.24°/hr to 6.12°/hr)	57~70% Improvement (10.8°/hr to 4.68°/hr)	0.005°/sec

The hysteresis compensation improves the bias instability of gyroscope output data by 7-8 % more than when only temperature is compensated. The Allan variance plots also show that rate random walk is reduced after hysteresis compensation. Table 4.4 shows an updated version of Table 4.2 with addition of hysteresis results.

Table 4.4: Effects of hysteresis compensation in integrated compensation of data.

XSENS	**CF Compensation**		**NN Compensation**	
	Offsets contribution to output bias	***Improvement***	***Offsets contribution to output bias***	***Improvement***
Raw Data	0.045°/sec	-	0.045°/sec	-
Temperature compensated only	0.005°/sec	9 times	0.05°/sec	9 times
Temperature and acceleration compensated	0.0015°/sec	30 times	0.0015°/sec	30 times
Temp, acceleration and hysteresis compensated	0.001°/sec	45 times	0.001°/sec	45 times

4.4. Comparison of Different Techniques

There are two techniques used for compensation of acceleration and temperature effects, namely Polynomial Curve Fitting (CF) and Neural Networks (NN). There are different parameters which can be used to compare these techniques. Table 4.5 gives comparison of these techniques based upon bias instability improvement by temperature compensation.

Table 4.5: Comparison of compensation techniques based upon bias instability, integration time and offset reduction improvement by temperature compensation.

	Bias Instability Improvement		**Integration time Improvement**		**Offsets in gyroscope output bias**	
	CF	***NN***	***CF***	***NN***	***CF***	***NN***
ADIS16488	0%	5%	4 times	4 times	2 times	2 times
ADXRS450	20%	25%	2 times	4 times	20 times	20 times
XSENS	50%	52%	4 times	8 times	50 times	50 times

The results in the table show that NN method is slightly superior to the CF method. When complexity of the methods is taken into account, then NN method is much more complex than CF method. The decision to use one of these techniques is based upon the tradeoff between accuracy and complexity of a system. Another factor that determines the efficiency of a compensation method is reduction in the rate random walk due to compensation of temperature. It is observed from the data in this study that both techniques significantly reduce rate random walk after compensation. The second thing that can be used as criterion for performance between these two techniques is compensation efficiency of acceleration effects. Table 4.6 summarizes comparison based upon the improvement in the bias offset reduction by acceleration compensation.

Table 4.6: Comparison of compensation techniques based upon improvement in the bias offset reduction as a result of acceleration compensation.

	Offsets before acceleration compensation		**Offsets after acceleration compensation**		**Improvement**	
	CF	***NN***	***CF***	***NN***	***CF***	***NN***
ADIS16488	0.08°/sec	0.08°/sec	0.02°/sec	0.02°/sec	4 times	4 times
XSENS	0.0045°/sec	0.0045°/sec	0.0015°/sec	0.0015°/sec	3 times	3 times

4.5. Future Aspects of this Study

The work done in this study is based upon compensation of temperature and acceleration effects using processing of data. The results show that the temperature dependency and acceleration effects can be reduced efficiently by using processing methods. This is an alternative to changes in the hardware design of sensors, to make them resilient to the temperature and acceleration changes.

Compensation of acceleration and temperature effects can be compensated by hardware design up to certain limit, and it also makes a design more complex. Adding complexity to a design limits a designer to add extra features to any design, as the resources are used for compensation of these unwanted errors. If the designer does not have to worry about compensation of errors like these, then there is room for improvement in other aspects of a design. For example the size of a MEMS gyroscope can be reduced significantly, if circuitry for temperature compensation can be avoided in the design.

This study proposes a hardware design for a MEMS gyroscope, which is made under the assumption that errors can be compensated efficiently by data processing. Thus

the complexity of a hardware design can be traded off with signal processing for compensation of errors that result from less complex design.

REFERENCES

1. K. Maenaka, "MEMS inertial sensors and their applications," *5th International Conference on Networked Sensing Systems, INSS 2008*, pp. 17-19, June 2008.

2. C. Acar, A.R. Schofield, A.A. Trusov, L.E. Costlow and A.M. Shkel, "Environmentally Robust MEMS Vibratory Gyroscopes for Automotive Applications," *IEEE International Sensors Journal*, vol. 9, no. 12, pp. 1895-1906, December 2009.

3. S. Lee, C. Kim, S. Jung, I. Song and Y. Cho, "MEMS for IT applications," *Proceedings of 2001 International Symposium on Micromechatronics and Human Science*, pp. 17-23, September 2001.

4. S. E. Alper, K. Azgın, and T. Akın, "A High-Performance Silicon-on-Insulator MEMS Gyroscope Operating at Atmospheric Pressure," *Sensors and Actuators A*, Vol. 135/1, pp. 34-42, March 2007.

5. N. F. De Rooij, S. Gautsch, D. Briand, C. Marxer, G. Mileti, W. Noell, H. Shea, U. Staufer and B. Van der Schoot, B., "MEMS for space," *International Solid-State Sensors, Actuators and Microsystems Conference, TRANSDUCERS*, pp. 17-24, June 2009.

6. M. Perlmutter and L. Robin, "High-performance, low cost inertial MEMS: A market in motion," *IEEE Position Location and Navigation Symposium (PLANS)*, pp. 225-229, April 2012.

7. R. Antonello and R. Oboe, "Exploring the Potential of MEMS Gyroscopes: Successfully Using Sensors in Typical Industrial Motion Control Applications," *IEEE Industrial Electronics Magazine*, vol. 6, no. 1, pp. 14-24, March 2012.

8. J. Marek, “MEMS for automotive and consumer electronics,” *IEEE International Solid-State Circuits Conference Digest of Technical Papers (ISSCC)*, pp. 9-17, February 2010.

9. A. Burg, A. Meruani, B. Sandheinrich, and M. Wickmann, “MEMS gyroscopes and their applications,” *Introduction to Microelectromechanical System, Northwestern University*, 2011.

10. S. Nasiri, M. Lim, and M. Housholder, “A critical review of the market status and industry challenges of producing consumer grade MEMS gyroscopes”, *http://invensensecom/mems/gyro/documents/whitepapers.html*

11. Nasiri, S., “A critical review of MEMS Gyroscope Technology and Commercialization Status,” *3150A Coronado Drive, Santa Clara, California US, http://invensense.com/mems/gyro/documents/whitepapers.html*

12. R. Waters, C. Tally, B. Dick, H. Jazo, M. Fralick, M. Kerber and A. Wang, “Design and analysis of a novel electro-optical MEMS gyroscope for navigation applications,” *IEEE Sensors*, pp. 1690-1695, November 2010.

13. D. Keymeulen, C. Peay, K. Yee, and D.L. Li, “Effect of Temperature on MEMS Vibratory Rate Gyroscope," *IEEE Aerospace Conference*, pp. 1-6, March 2005.

14. J-W. Joo and S-H. Choa, “Deformation Behavior of MEMS Gyroscope Sensor Package Subjected to Temperature Change,” *IEEE Transactions on Components and Packaging Technologies*, vol. 30, no. 2, pp. 346-354, June 2007.

15. D. Xia, S. Chen, S. Wang and H. Li, “Microgyroscope temperature effects and compensation-control methods,” *International Journal of Sensors 9*, no. 10, pp. 8349-8376, 2009.

16. C. Patel, P. McCluskey and D. Lemus, “Performance and reliability of MEMS gyroscopes at high temperatures,” *12th IEEE Intersociety Conference on Thermal and Thermomechanical Phenomena in Electronic Systems (ITherm),* pp.1-5, June 2010.

17. J. K. Shiau, C. X. Huang, and M. Y. Chang, “Noise characteristics of MEMS gyro’s null drift and temperature compensation,” *Journal of Applied Science and Engineering*, vol. 15, no. 3, pp. 239-246, 2012.

18. I. P. Prikhodko, A. A. Trusov, and A. M. Shkel, “Compensation of drifts in high-Q MEMS gyroscopes using temperature self-sensing,” *Sensors and Actuators A: Physical 201*, pp. 517-524, 2013.

19. S. Feng, G. Qiufen, G. Yuansheng and L. Junshan, “Research on Thermal Characteristic in Slow-Small Temperature Changing for MEMS Linear Vibration Gyroscope,” *Proceedings of 2006 IEEE Conference on Mechatronics and Automation,* pp. 475-479, June 2006.

20. Z. Hou, D. Xiao, X. Wu, P. Dong, Z. Niu, Z. Zhou and X. Zhang, “Effect of parasitic resistance on a MEMS vibratory gyroscopes due to temperature fluctuations,” *IEEE International Conference on Nano/Micro Engineered and Molecular Systems (NEMS),* pp. 293-296, February 2011.

21. K. Shcheglov, C. Evans, R. Gutierrez and T. K. Tang, “Temperature dependent characteristics of the JPL silicon MEMS gyroscope,” *IEEE Aerospace Conference Proceedings,* vol. 1, pp. 403-411, 2000.

22. F. Jiancheng and L. Jianli, “Integrated Model and Compensation of Thermal Errors of Silicon Microelectromechanical Gyroscope,” *IEEE Transactions on Instrumentation and Measurement*, vol. 58, no. 9, pp. 2923-2930, September 2009.

23. J. B. Bancroft and G. Lachapelle, “Estimating MEMS gyroscope g-sensitivity errors in foot mounted navigation,” *Ubiquitous Positioning, Indoor Navigation, and Location Based Service (UPINLBS)*, pp. 1-6, October 2012.

24. R. Feng, J. Bahari, J. D. Jones, and A. M. Leung, “MEMS Thermal gyroscope with self-compensation of the linear acceleration effect,” *Sensors and Actuators A: Physical 203*, pp. 413-420, 2013.

25. A. Walther, C. Le Blanc, N. Delorme, Y. Deimerly, R. Anciant, and J. Willemin, “Bias Contributions in a MEMS Tuning Fork Gyroscope,” *Journal of Microelectromechanical Systems*, vol. 22, no. 2, pp. 303-308, April 2013.

26. X. Wu, L. Duan and W. Chen, “A Kalman filter approach based on random drift data of Fiber Optic Gyro,” *6th IEEE Conference on Industrial Electronics and Applications (ICIEA)*, pp.1933-1937, June 2011.

27. D. Xia, S. Chen, S. Wang, and H. Li, “Microgyroscope temperature effects and compensation-control methods”. *International Journal of Sensors 9*, no. 10, pp. 8349-8376, 2009.

28. V. Kaajakari, “Theory and analysis of MEMS resonators,” *Validation Technologies Incorporated*, 2011. *http://www.ieee-uffc.org/frequency-control/learning/pdf/Kaajakari-MEMS_Resonators_v2b.pdf*

29. X. Ji, S. Wang,Y. Xu, Q. Shi and D. Xia, “Application of the Digital Signal Procession in the MEMS Gyroscope De-drift,” *1st IEEE International Conference on Nano/Micro Engineered and Molecular Systems, NEMS '06*, pp. 218-221, January 2006.

30. Q. Zhang, Z. Tan and L. Guo, “Compensation of Temperature Drift of MEMS Gyroscope Using BP Neural Network,” *International Conference on Information Engineering and Computer Science, ICIECS 2009*, pp. 1-4, December 2009.

31. J. K. Bekkeng, “Calibration of a Novel MEMS Inertial Reference Unit,” *IEEE Transactions on Instrumentation and Measurement*, vol. 58, no. 6, pp. 1967-1974, June 2009.

32. C. Zhang, Q. Wu, T. Yin and H. Yang, “A MEMS gyroscope readout circuit with temperature compensation,” *5th IEEE International Conference on Nano/Micro Engineered and Molecular Systems (NEMS)*, pp. 458-462, January 2010.

33. H. Sun, K. Jia, X. Liu, G. Yan, Yu. Hsu, R. M. Fox, and H. Xie, “A CMOS-MEMS Gyroscope Interface Circuit Design With High Gain and Low Temperature Dependence,” *IEEE International Sensors Journal*, vol. 11, no. 11, pp. 2740-2748, November 2011.

34. T. Yin, H. Wu, Q. Wu, H. Yang and J. Jiao, “A TIA-based readout circuit with temperature compensation for MEMS capacitive gyroscope,” *IEEE International Conference on Nano/Micro Engineered and Molecular Systems (NEMS)*, pp. 401-405, February 2011

35. S-R. Chiu, C-Y. Sue, C-H. Lin, L-T. Teng, L-P. Liao, Y-W. Hsu and Y-K. Su, "Active thermal compensation of MEMS based gyroscope," *2012 IEEE Sensors*, pp.1-4, October 2012

36. I. P. Prikhodko, S. A. Zotov, A. A. Trusov and A. M. Shkel, “Thermal Calibration of Silicon MEMS Gyroscopes,” *IMAPS International Conference and Exhibition on MEMS packaging, Fountain Hills AZ US*, March 2012.

37. K. Wang, L. Yong and R. Chris, “The effect of the temperature-correlated error of inertial MEMS sensors on the integration of GPS/INS,” *Proceedings of International Global Navigational Satellite Systems (IGNSS 2009) Symposium*, 2009.

APPENDIX A

MATLAB PROGRAMING FOR DIFFERENT METHODS

A.1 Routine for Temperature Compensation Using CF Method

```
function data = calc_CF ( T , rawData , Eq );

% calc_F = Routine to compensate temperature effects
% The function is used only fot Temperature compensation
% T  = Input TEMPERATURE
% rawData  = Input GYROSCOPE RATE DATA
% Eq = EQUATION for Temperature Compensation by CF method
% data = Temperature COMPENSATED DATA

dl = length(T);
%dl = the lenght of data for which code will run

data = 1:dl; % initializing 'data' with dummy values

for i=1:dl   % loop for complete data set

   error = polyval(Eq , T(i));
   % calculating error based upon temperature input

   data(i) = rawData(i) - error ;
   % subtracting error from RAW data

end

smt = 4096;
% Moving Average Filter averaging factor

s_D = smooth(rawData,smt);
% applying moving average filter to RAW Data for plots

s_data = smooth(data,smt);
% applying moving average filter to compensated Data for plots


%%%%%%%% Saving the RAW data for further use %%%%%%

fileID = fopen('C:\\MATLAB\\RAW.txt','w');
fprintf(fileID,'%20.17f \n',rawData);
```

```
fclose(fileID);

%%%%%%%%% Saving Compensated data for further use %%%%%%

fileID = fopen('C:\\MATLAB\\COMPENSATED.txt','w');
fprintf(fileID,'%20.17f \n',data);
fclose(fileID);

% end of routine
```

A.2 Routine for Temperature/Acceleration Compensation Using NN Method

```
function data = calc_bpp( net ,T , rawData );

% calc_bpp = function to compensate using Neural networks
% The function valid for both Temperature and acceleration
% data = COMPENSATED DATA
% T = Temperature Input
% rawData = RAW Gyro Data with drift in it
% net = Trained Network for temperature or acceleration

l = length(rawData);
% l = length for which code will run

data = 1:l;
% Initializing the matrix with dummy data

for i=1:l
   % loop for complete data length

   if(mod(i,100) == 1)
   % updating error at every 100th sample

   error = sim(net , T(: , i ) );
   %error calulation based upon temperature input

   end

   data(i) = D(i) - error;
   % subtraction of error from RAW data

end

 %%%%%%%%% Saving the RAW data for further use %%%%%%
fileID = fopen('C:\\MATLAB\\RAW','w');
fprintf(fileID,'%20.17f \n',rawData);
fclose(fileID);
```

```
%%%%%%%%% Saving Compensated data for further use %%%%%%%
fileID = fopen('C:MATLAB\\NN_Data.txt','w');
fprintf(fileID,'%20.17f \n',data);
fclose(fileID);

% end of routine
```

A.3 Routine for Acceleration Compensation Using CF Method

```
function data = calc_CFA (Ax, Ay, Az, Graw , EqX, EqY, EqZ)

% calc_CFA = routine to calculate commpensation effects
%           using the CF method
% Ax = acceleration input from x-axis
% Ay = acceleration input from y-axis
% Az = acceleration input from z-axis
% Graw  = gyroscope data to be compensated
% EqX= Equation to compensate effect of x-axis accelerometer
% EqY= Equation to compensate effect of y-axis accelerometer
% EqZ= Equation to compensate effect of z-axis accelerometer
% data = output of the routine with compensated G data

bias = mean(Graw(1:49200));
% mean value of first 49200 samples
% 49200 is the minimum error value

l = length(Graw);
% length of the data samples

data = Graw;
% dummy initialization of the output matrix

Gbfree = Graw-bias;
% removing ON bias offset by subtracting from RAW data

for i=1:l    %duration of processing

   error = polyval(EqY,Ay(i))  - polyval(EqX,Ax(i)) +  polyval(EqZ,Az(i));
   % calculationg error resulting from each of the three axes

   data(i) = Gbfree(i) - error;
   % subtracting the error from RAW data to get compensated data

end      % end of routine
```

A.4 Routine for Hysteresis Compensation Using CF Method

```
function data = removeHys( T , rawData , EqH );

% removeHyst = routine to remove hysteresis from the data
% data = output of the routine with compensated data
% T = Temperature input from the sensor
% rawData = raw data with hysteresis in it
% EqH = Equation that relation hysteresis and temperature difference

dl = length(T);
% length of the data for calculations

to = T(1);
% defines the corner point of temperature
% the point at which the slope of temperature changes
% in this case it is the first sample of the data

data = 1:dl;
% dummy initialization of the output data

for i=1:dl   % defining the loop length

   error = polyval(EqH , abs(to-T(i)));
   % calculate the difference between corner point and current temperature
   % take absolute of that value
   % compensation based on the difference of temperatures

   data(i) = rawData(i) - error ;
   % the hysteresis error is subtracted from the RAW data

end

% end of routine
```

APPENDIX B

SCREEN SHOTS FROM DIFFERENT SOFTWARES

B.1 Interface for ADIS16488 and ADIS16136

Figure B.1 shows screen shot of interface software for data acquisition from ADIS16488 and ADIS13163 sensors. The real time values of acceleration and gyroscope can also be seen in the figure.

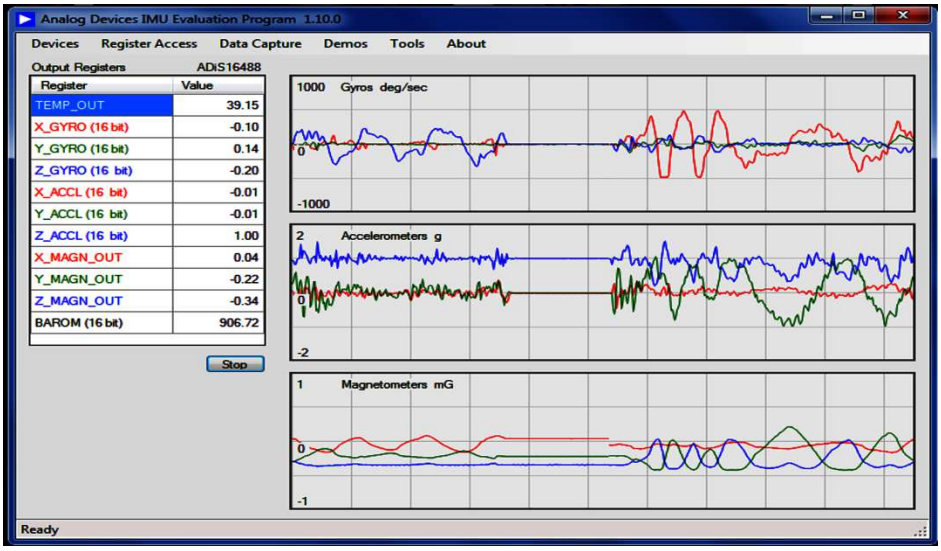

Figure B.1: Screenshot of the interface software, giving real time values of all the sensors in the ADIS16488 IMU. This feature is very important for leveling of the sensor to get acceleration data.

Figure B.2 shows different options which are available to the user for data recording. The sampling rate and other features can be adjusted from this screen of the software. Figure B.3 shows the menu where any sensor can be selected from the software. The communication protocol is adjusted according to the type of sensor.

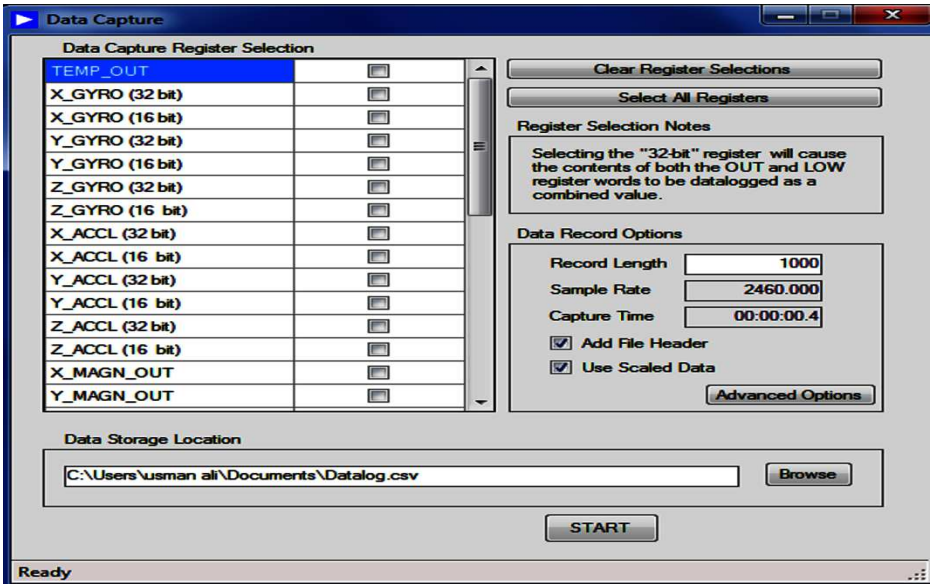

Figure B.2: Screenshot of data recording options. Any sensor data can be recorded and the data rate is variable and program controlled.

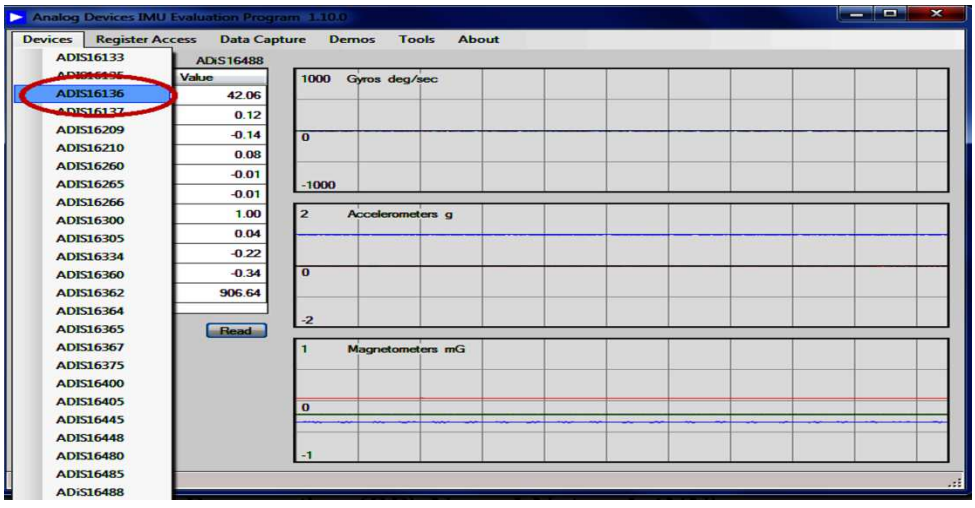

Figure B.3: Screenshot showing the sensor selection from the interface software. All the sensors shown in the list are compatible with the evaluation board of ADIS16488.

B.2 Interface software for ADXRS450

Figure B.4 shows the interface software for ADXRS450. The real time values for gyroscope are shown in the interface software. The software provides recording and viewing options at different sampling rates. The encircled areas show real time data and its graphical plot. The selection between viewing and recording is also encircles.

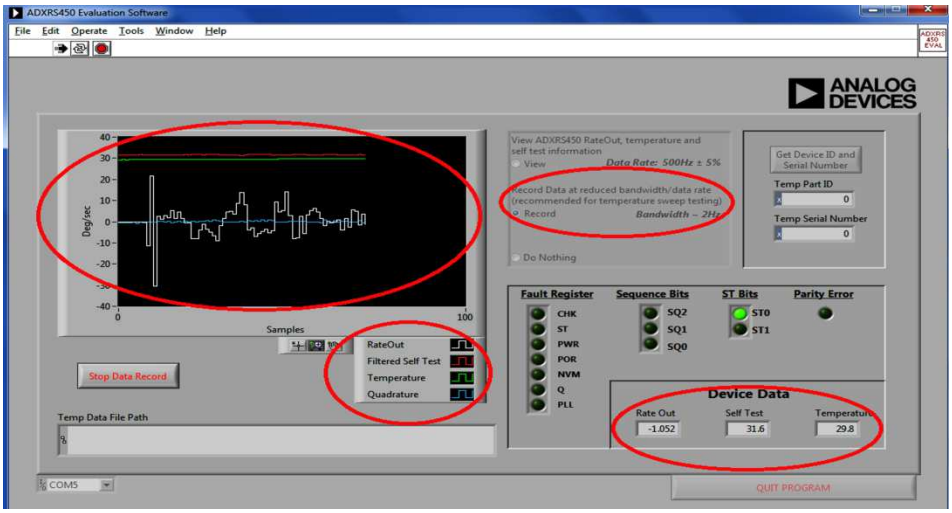

Figure B.4: The interface software of ADXRS450 is shown with important parameters encircled in red color.

B.3 Interface software for XSENSE MTi-10

Figure B.5 shows the interface software for XSENSE sensor. The screen shot shows the recording process in real time. The values of acceleration, gyroscope and magnetometers are displayed. Temperature for individual sensors is also recorded by the interface software but not shown in the interface.

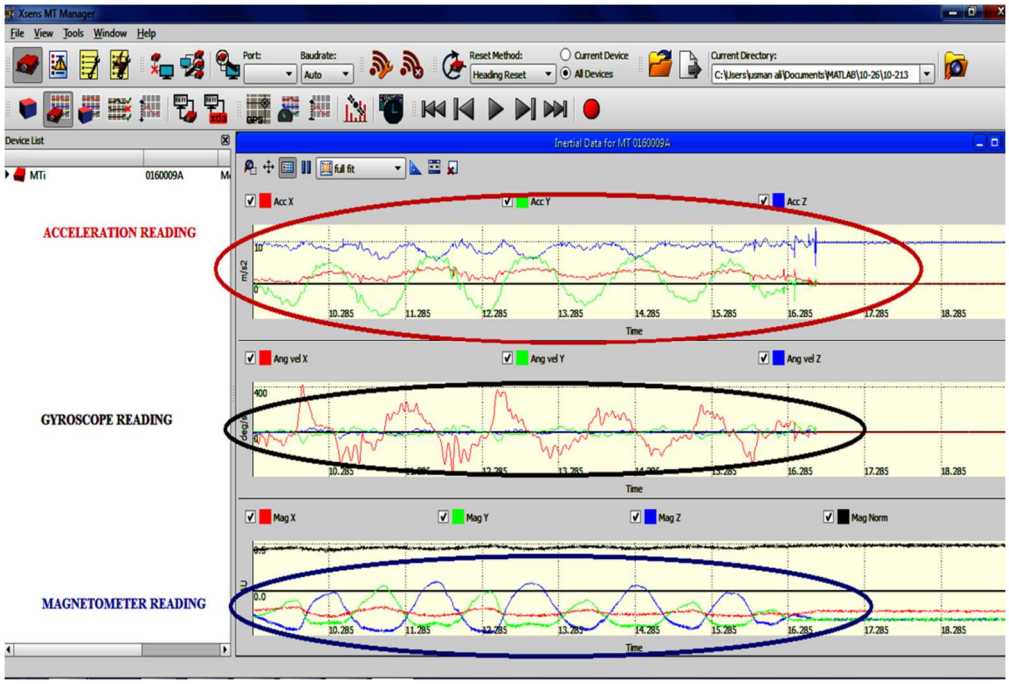

Figure B.5: The figure is a screenshot of the interface software while data is captured from the sensor. The 3 axes of acceleration and 3 axes of gyroscope data can be seen very clearly. Temperature data is also recorded but not shown in the interface.

APPENDIX C

SCREEN SHOT FOR NEURAL NETWORK TOOL

C.1 Performance parameters for neural network training

Figure C.1 shows the screen shot from the MATLAB toolbox used for training neural networks. Blue circle shows the main windows that commands any training of data. Red circle is showing the network shape of current data. Green is showing the performance parameters of currently trained data.

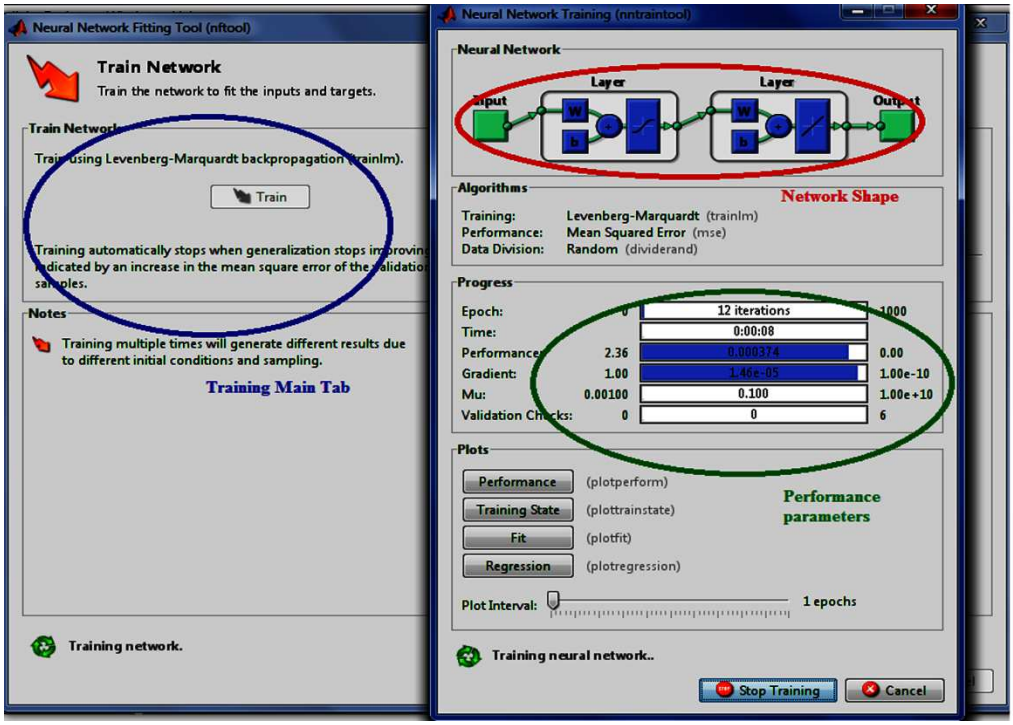

Figure C.1: Figure shows the toolbox provided by MATLAB for neural network construction and optimization. The network shape and performance parameters can be seen in the figure.